

STRUCTURAL CONTROLS ON THE SEISMIC
SEQUENCE STRATIGRAPHY OF THE BEN NEVIS,
AVALON, AND EASTERN SHOALS FORMATIONS,
TERRA NOVA FIELD, JEANNE D'ARC BASIN,
OFFSHORE NEWFOUNDLAND

CENTRE FOR NEWFOUNDLAND STUDIES

**TOTAL OF 10 PAGES ONLY
MAY BE XEROXED**

(Without Author's Permission)

ALISON GOLLOP

**STRUCTURAL CONTROLS ON THE SEISMIC SEQUENCE
STRATIGRAPHY OF THE BEN NEVIS, AVALON, AND EASTERN
SHOALS FORMATIONS, TERRA NOVA FIELD,
JEANNE D'ARC BASIN, OFFSHORE NEWFOUNDLAND**

by

Alison Gollop

A thesis submitted to the
School of Graduate Studies
in partial fulfilment of the
requirements for the degree of
Master of Science



Department of Earth Sciences
Memorial University of Newfoundland

April 2003

St. John's

Newfoundland

ABSTRACT

The structural controls on the seismic sequence stratigraphy of the lower Cretaceous succession in the Terra Nova oil field, Grand Banks of Newfoundland, is studied using a digital 3-D seismic database and wireline log data from 11 offshore wells.

Three seismic sequences (Units A, B, and C) were mapped in the Terra Nova area, roughly corresponding to the Eastern Shoals, Avalon, and Ben Nevis formations, respectively. Each sequence is bounded by distinct unconformities. The development of these sequences and their boundaries was controlled by an interplay of sediment input, changes in sea level, tectonism, accommodation space, and climate. However, tectonism (i.e., fault-block subsidence and rotation) is interpreted to be the principal cause for the sedimentary patterns and development of the major unconformities in the Terra Nova field; global eustatic sea-level variations had only a minor influence on unconformity generation.

The N-S-trending fault system in the Terra Nova field was active during the Tithonian to mid-Valanginian, as evidenced by fault growth within the Hibernia and Rankin formations. The E-W-trending fault system was previously interpreted to have been formed during mid-Aptian to Albian extensional phases; however, growth-strata patterns within the Eastern Shoals Formation suggest instead that the E-W-trending fault system in the Terra Nova field was initiated by at least the late Barremian and was active until late Albian. Also, the N-S-trending fault system in the Terra Nova field was reactivated at this time. This fault system terminates upward against the Albian unconformity, so that by late Albian the active rifting in the Terra Nova field is

interpreted to have ceased.

A “pop-up” feature immediately west of the Voyager Fault in the Terra Nova field has been previously interpreted to have formed by transpressional stresses induced by oblique-slip movement. However, geometries similar to those presented in the model of Jackson and Vendeville (1992 and 1994) suggest that a large salt diapir may lie in the footwall of the Voyager Fault. Therefore, an alternative interpretation is proposed for this “pop-up” feature, as a localized contractional feature related to diapirism.

The lower Cretaceous succession in the Terra Nova field does not contain hydrocarbons, but forms reservoirs in other oil fields such as Hibernia and White Rose. It is proposed that the reservoir facies represented by the Ben Nevis and Avalon formations in the Terra Nova field were charged with hydrocarbons at some point but were subsequently breached, allowing oil to escape from the traps. This scenario is consistent with published fluid-inclusion studies.

ACKNOWLEDGEMENTS

I would like to sincerely thank my supervisors: Ali Aksu, whose guidance, support, and charismatic nature are a constant inspiration to me; and Rick Hiscott, for his kind supervision and friendship, and whose thoroughness was much appreciated at the end of the day. I would like to thank Petro-Canada (Terra Nova Alliance) in St. John's for supplying high quality data, and especially would like to acknowledge Nicholle Carter, John Katay, and Ian Delong, for their guidance and technical support. I also wish to thank Hugh Wishart for the project idea and Amit Mehra for facilitating financial support on behalf of Petro-Canada Limited. I would like to express my appreciation to Landmark Graphics for the software grant awarded to Memorial University that greatly facilitated the interpretation of my data on workstations in the Department of Earth Sciences at MUN. I would like to thank the Natural Sciences and Engineering Research Council of Canada for support in the form of an Industrial Postgraduate Scholarship; the Government of Newfoundland and Labrador for funding through an Atlantic Accord Career Development Graduate Award; and the School of Graduate Studies for financial support. I gratefully acknowledge Tom Calon for the fruitful structural discussions and for his editorial reviews. I am especially thankful to Tony Kocurko, who was instrumental in allowing me to load my dataset on workstations at MUN and whose computer expertise will forever amaze me. I am also grateful to all my colleagues and friends in the Department of Earth Sciences at Memorial University for their companionship and constant support. Special thanks to my officemate and friend Dianne and to my family for their unfailing encouragement and support.

TABLE OF CONTENTS

Abstract.....	ii
Acknowledgements.....	iv
List of Tables.....	vii
List of Figures.....	viii
1. Introduction.....	1
1.1 Definition of Problem and Objectives.....	1
1.2 Regional Geological Setting.....	2
1.3 Regional Tectonic Evolution.....	8
1.4 Regional Structure.....	15
1.5 Regional Stratigraphy and Tectono-Stratigraphic Evolution.....	20
1.6 The Terra Nova Oil Field.....	24
1.6.1 Introduction.....	24
1.6.2 Terra Nova stratigraphy.....	27
1.6.3 Terra Nova structure.....	29
1.6.4 Ben Nevis, Avalon, and Eastern Shoals formations.....	32
1.6.5 Biostratigraphy.....	36
2. Data and Methods.....	41
2.1 Terra Nova 3-D Seismic Dataset.....	41
2.2 Seismic Data Acquisition.....	41
2.3 Well Data.....	44
2.4 Programs Used.....	44
2.4.1 OpenWorks TM	44
2.4.2 SeisWorks/3D TM	47
2.4.3 StratWorks TM	48
2.4.4 SynTool TM	48
2.5 Methodology.....	49
2.5.1 Horizon mapping.....	49
2.5.2 Fault mapping.....	50
2.5.3 Map generation.....	50
2.5.4 Seismic sequence stratigraphy.....	50
3. Results.....	56
3.1 Seismic Markers.....	56
3.2 Data Analysis.....	60
3.3 Description of Seismic Packages.....	64

3.3.1	Unit A.....	65
3.3.2	Unit B.....	69
3.3.3	Unit C.....	81
3.3.4	Unit Ci.....	87
3.4	Synthetics.....	92
4.	Discussion.....	98
4.1	Overview of Stratal Architecture and Structure.....	98
4.2	Origin of Unconformities.....	104
4.2.1	<i>Tectonic controls on stratigraphic sequence development</i>	104
4.2.2	<i>Eustatic controls on stratigraphic sequence development</i>	110
4.3	Development of Structures in the Terra Nova Field Area.....	113
4.3.1	<i>Fault systems</i>	113
4.3.2	<i>Terra Nova Anticline</i>	115
4.3.3	<i>Transpressional structures</i>	118
4.3.4	<i>Salt structures</i>	119
4.4	Implications for Hydrocarbon Occurrences.....	124
4.	Conclusions.....	129
	References.....	132

LIST OF TABLES

Chapter 1

Table 1.1	Principal hydrocarbon reservoirs in the Jeanne d'Arc Basin.....	15
Table 1.2	Geologic tops and thicknesses of the Ben Nevis, Avalon, and Eastern Shoals formations.....	33
Table 1.3	Biostratigraphic column for the Terra Nova K-07 well.....	37
Table 1.4	Biostratigraphic column for the Terra Nova K-08 well.....	38

Chapter 2

Table 2.1	Instrumentation and Recording Parameters, 1997 Terra Nova 3-D Survey.....	43
Table 2.2	Well header information for Terra Nova and other relevant wells.....	45
Table 2.3	Drill Stem Test (DST) and Repeat Formation Sample (FRS) results in the Ben Nevis Formation for the Terra Nova K-17 and King's Cove A-26 wells.....	46
Table 2.4	Cored intervals in the Ben Nevis Formation in the North Trinity H-71 well.....	47

LIST OF FIGURES

Chapter 1

Figure 1.1	Sedimentary basins offshore eastern Canada.....	3
Figure 1.2	Bathymetric map of the Newfoundland and Labrador offshore area.....	4
Figure 1.3	Significant discoveries offshore Grand Banks.....	5
Figure 1.4	Map of the Jeanne d'Arc Basin.....	7
Figure 1.5	Lithostratigraphy of the Jeanne d'Arc Basin.....	11
Figure 1.6	Principal tectonic elements of the Grand Banks and Orphan Basin.....	17
Figure 1.7	Formal lithostratigraphy of the Terra Nova field area.....	21
Figure 1.8	Map of the Terra Nova field area showing the major fault trends.....	26
Figure 1.9	Structure map and cross-section of the Terra Nova oil field.....	30

Chapter 2

Figure 2.1	Seismic grid for the 1997 Terra Nova survey.....	42
Figure 2.2	Seismic stratigraphic reflection terminations within an idealized seismic sequence.....	52

Chapter 3

Figure 3.1	Location of seismic lines used in thesis.....	57
Figure 3.2	Seismic section showing seven events mapped in the study area.....	59
Figure 3.3	Attribute classification based on post-stack seismic data.....	61
Figure 3.4	Time-structure map of the event defining the top of the Eastern Shoals Formation.....	66
Figure 3.5	Azimuth map of the event defining the top of the Eastern Shoals Formation.....	67
Figure 3.6	Amplitude map of the event defining the top of the Eastern Shoals Formation.....	68
Figure 3.7	Gamma-ray/sonic log for the Terra Nova K-18 well.....	70
Figure 3.8	Interpreted line showing parallel reflections within Unit A.....	71
Figure 3.9	Thickened sections of Units A and C.....	72
Figure 3.10	Interpreted line showing angular subcrop of seismic reflections below the Barremian unconformity.....	73
Figure 3.11	Time-structure map of the event defining the top of the Avalon Formation.....	75
Figure 3.12	Amplitude map of the event defining the top of the Avalon Formation.....	76
Figure 3.13	Gamma-ray/sonic log for the Ben Nevis I-45 well.....	77
Figure 3.14	Gamma-ray/sonic log for the Terra Nova H-99 well.....	78

Figure 3.15	Interpreted trace showing onlap onto the mid-Aptian unconformity.....	79
Figure 3.16	Interpreted line showing onlap onto the mid-Aptian unconformity.....	80
Figure 3.17	Gamma-ray/sonic log for the North Trinity H-71 well.....	82
Figure 3.18	Time-structure map of the event defining the top of the Ben Nevis Formation.....	83
Figure 3.19	Combined dip/azimuth map of the event defining the top of the Ben Nevis Formation.....	84
Figure 3.20	Amplitude map of the event defining the top of the Ben Nevis Formation.....	85
Figure 3.21	Interpreted sections showing (A) angular subcrop of reflections beneath the Albian unconformity and (B) onlap onto the Albian unconformity.....	88
Figure 3.22	Interpreted seismic section showing the structure of the Terra Nova Anticline.....	89
Figure 3.23	Schematic cross-section from Terra Nova K-17 to North Trinity H-71.....	90
Figure 3.24	Gamma-ray/sonic log for the Terra Nova K-17 well.....	93
Figure 3.25	Interpreted seismic sections showing the paleovalley incised on the mid-Aptian unconformity.....	94
Figure 3.26	Synthetic seismogram for Terra Nova C-09.....	96
Figure 3.27	Synthetic seismogram for North Trinity H-71.....	97

Chapter 4

Figure 4.1	Summary diagram showing Mesozoic sea-level curve, inferred times of fault activity and the strata architecture of depositional sequences.....	100
Figure 4.2	Schematic cross-section from Terra Nova K-17 to I-97.....	102
Figure 4.3	Seismic sections showing the location of the Terra Nova Anticline and the keystone graben.....	121
Figure 4.4	Seismic sections showing the approximate outline of a salt diapir.....	122
Figure 4.5	Petroleum Systems Events Chart.....	126

CHAPTER ONE: INTRODUCTION

1.1 Definition of Problem and Objectives

The Ben Nevis, Avalon, and Eastern Shoals formations represent one of the most important petroleum reservoirs in the Jeanne d'Arc Basin. Although this system does not contain hydrocarbon reserves in the Terra Nova field, it is economically significant in other oil fields such as Hibernia and White Rose. A complete assessment of the key geological and geophysical aspects in the project area will explain why the succession is not hydrocarbon-bearing at Terra Nova, but contains hydrocarbons at other fields in the Jeanne d'Arc Basin. Knowing why hydrocarbons are trapped in some areas and not in others will assist oil companies in assessing the viability of future and existing oil and gas fields and will have a positive impact on future exploration initiatives.

The intent of this M.Sc. thesis is to develop a thorough understanding of the structural controls on the seismic and sequence stratigraphy of the lower Cretaceous late-rift succession in the Terra Nova oil field, Grand Banks of Newfoundland.

Specific objectives of the proposed thesis research are:

- to use a 3-D seismic dataset to map prominent reflections, sequence boundaries, faults and facies attributes in the Terra Nova oil field, using workstation software - *Landmark*;
- To interpret and understand phases of structural development and the impact of these events on stratigraphy and sedimentation;

- To attempt to explain hydrocarbon charge within the lower Cretaceous interval so as to clarify why the Ben Nevis and Avalon formations are water-saturated in the Terra Nova oil field.

1.2 Regional Geological Setting

The basins offshore eastern Canada (Figure 1.1) formed about 200 million years ago as North America separated from Europe and Africa. This separation resulted in the formation of the present-day Atlantic Ocean, through the processes of lithospheric extension along the margins and seafloor spreading. Prior to this, near the end of the Paleozoic Era, the area now known as the continental margin of Newfoundland was at the centre of the Pangea supercontinent, surrounded to the south, east, and north by areas that would later become northwest Africa, Iberia, and the British Isles, respectively (McAlpine, 1990). Subsequent fragmentation during the Mesozoic led to the present-day position of the Grand Banks, off the eastern margin of North America.

The Newfoundland and Labrador offshore areas (Figure 1.2) comprise approximately 1.6 million km² (Department of Mines and Energy, 2000). Within this offshore area, twenty sedimentary basins and sub-basins, ranging in age from Early Paleozoic to Late Cretaceous, and 18 fields (Figure 1.3), have been identified (Department of Mines and Energy, 2000). The Grand Banks is a broad continental shelf that extends to the south and east of the Island of Newfoundland and reaches 450 km seaward. To the south, the Grand Banks of Newfoundland is separated from the Scotian shelf by the Laurentian Channel and to the east is separated from the Flemish Cap by the

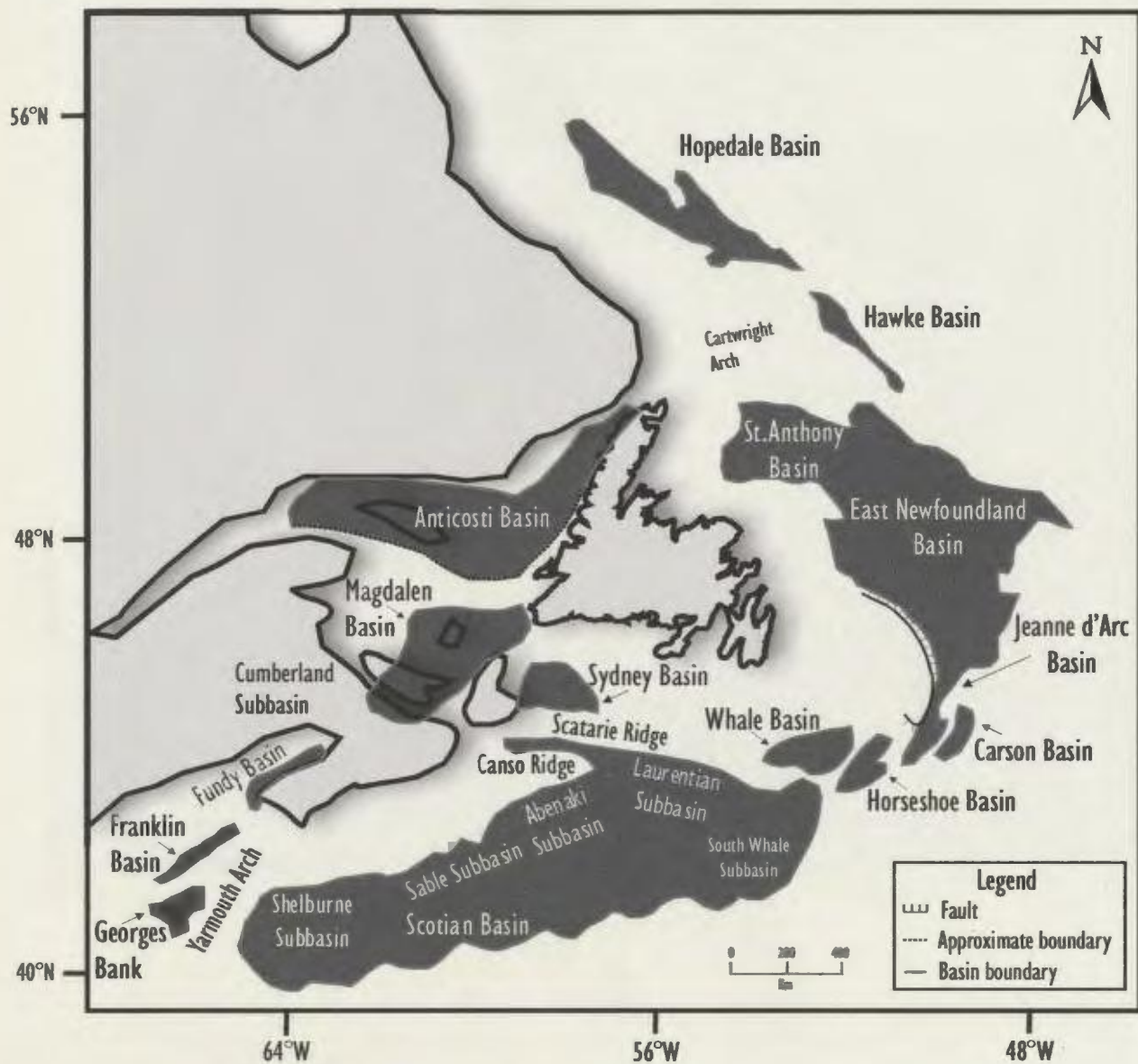


Figure 1.1 Sedimentary basins offshore Eastern Canada (after Keen et al., 1990)

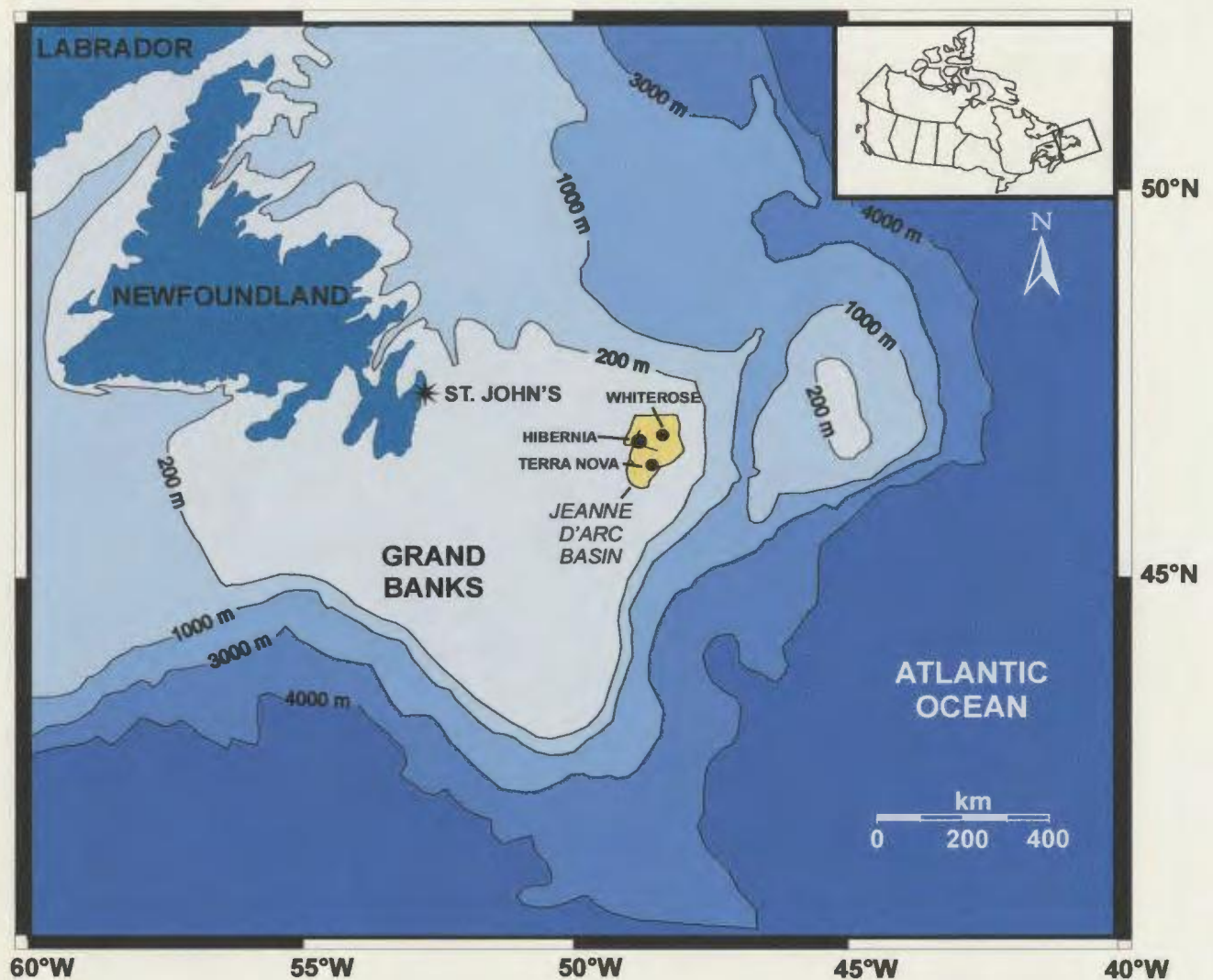


Figure 1.2 Bathymetric map of the Newfoundland and Labrador offshore area, only showing the 200, 1000, 3000, and 4000 m isobaths (modified from Canadian Hydrographic Services, 1990). The Jeanne d'Arc Basin is highlighted in yellow.

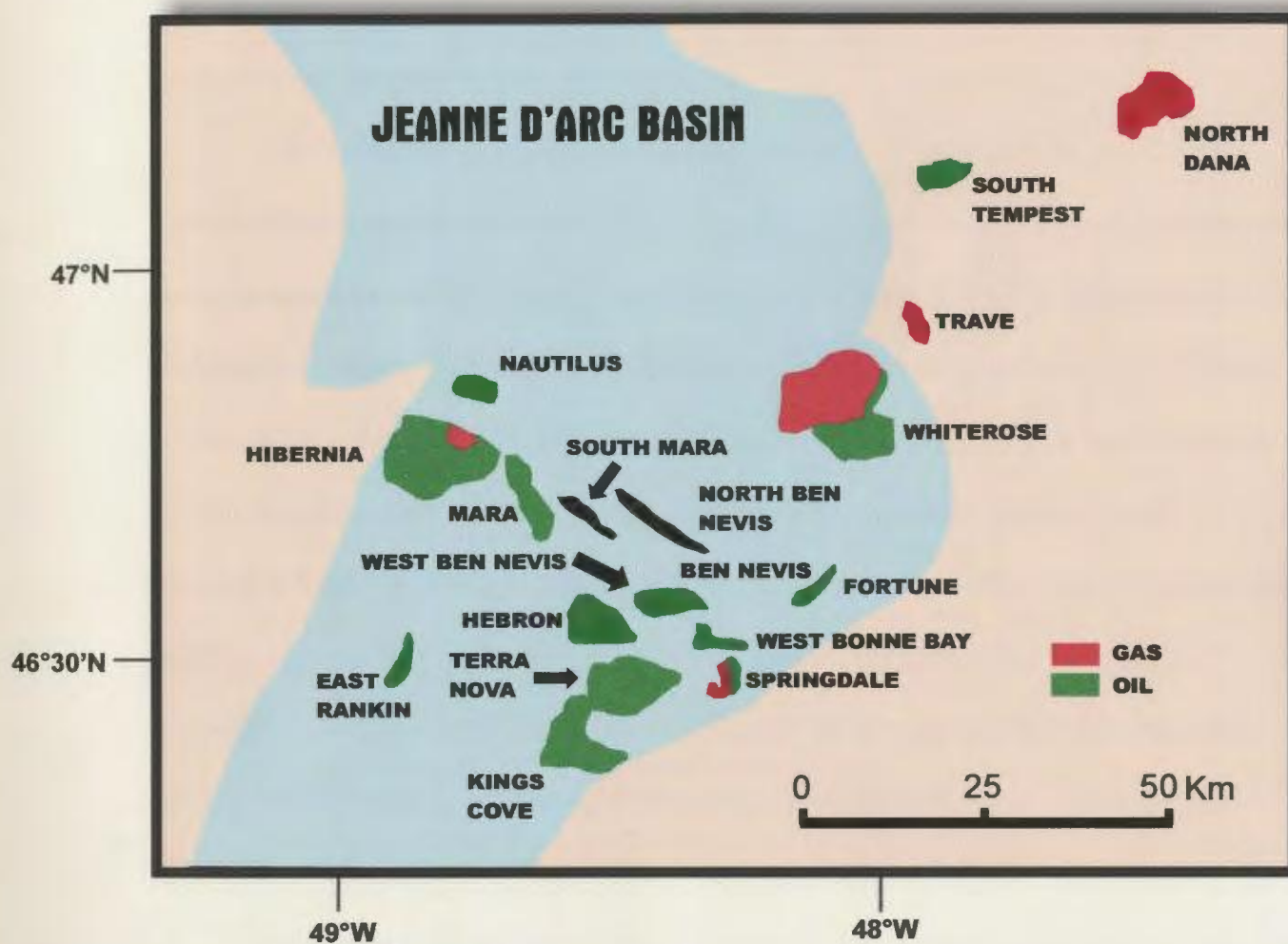


Figure 1.3 Significant discoveries offshore Grand Banks (after C-NOPB, 2002b). The location of the Jeanne d'Arc Basin is shown in Figure 1.2.

Flemish Pass. The Grand Banks is bounded to the north by the Northeast Newfoundland shelf and slope (Canadian Hydrographic Services, 1990). Except in the south where the shelf is cut by several deep channels, water depths are generally less than 200 m (Canadian Hydrographic Services, 1990).

The Grand Banks of Newfoundland is underlain by continental crust from the Appalachian Orogen consisting of upper Precambrian and Lower Paleozoic sedimentary and igneous rocks of the Avalon Zone (Grant et al., 1986). These Appalachian rocks are overlain by a series Mesozoic rift basins that includes the Jeanne d'Arc, South Jeanne d'Arc, Whale, South Whale, Orphan, and Flemish Pass Basins. These basins formed in response to extension related to the opening of the present-day Atlantic Ocean. Extension began in the Late Triassic and, as the ocean opened sequentially from south to north, a series of rift basins formed along the eastern margin of North America. Subsequent to continental break-up, the rift successions were buried beneath passive-margin drift sequences consisting of Mesozoic and Cenozoic strata. These deposits extend over the modern continental slope and rise.

The Jeanne d'Arc Basin (Figure 1.4) is one of the larger Mesozoic rift basins on the Grand Banks of Newfoundland. Situated on the northeastern margin of the Grand Banks, the sedimentary basin trends northeast and covers an area greater than 10,000 km². It is the deepest basin, comprising a Mesozoic-Cenozoic sedimentary succession as much as 20 km thick, 14 km of which are syn-rift sediments (Tankard et al., 1989; Driscoll and Hogg, 1995), and has the most complete stratigraphic record (Keen et al., 1987). This fault-bounded basin has a half-graben geometry and plunges to the northeast.

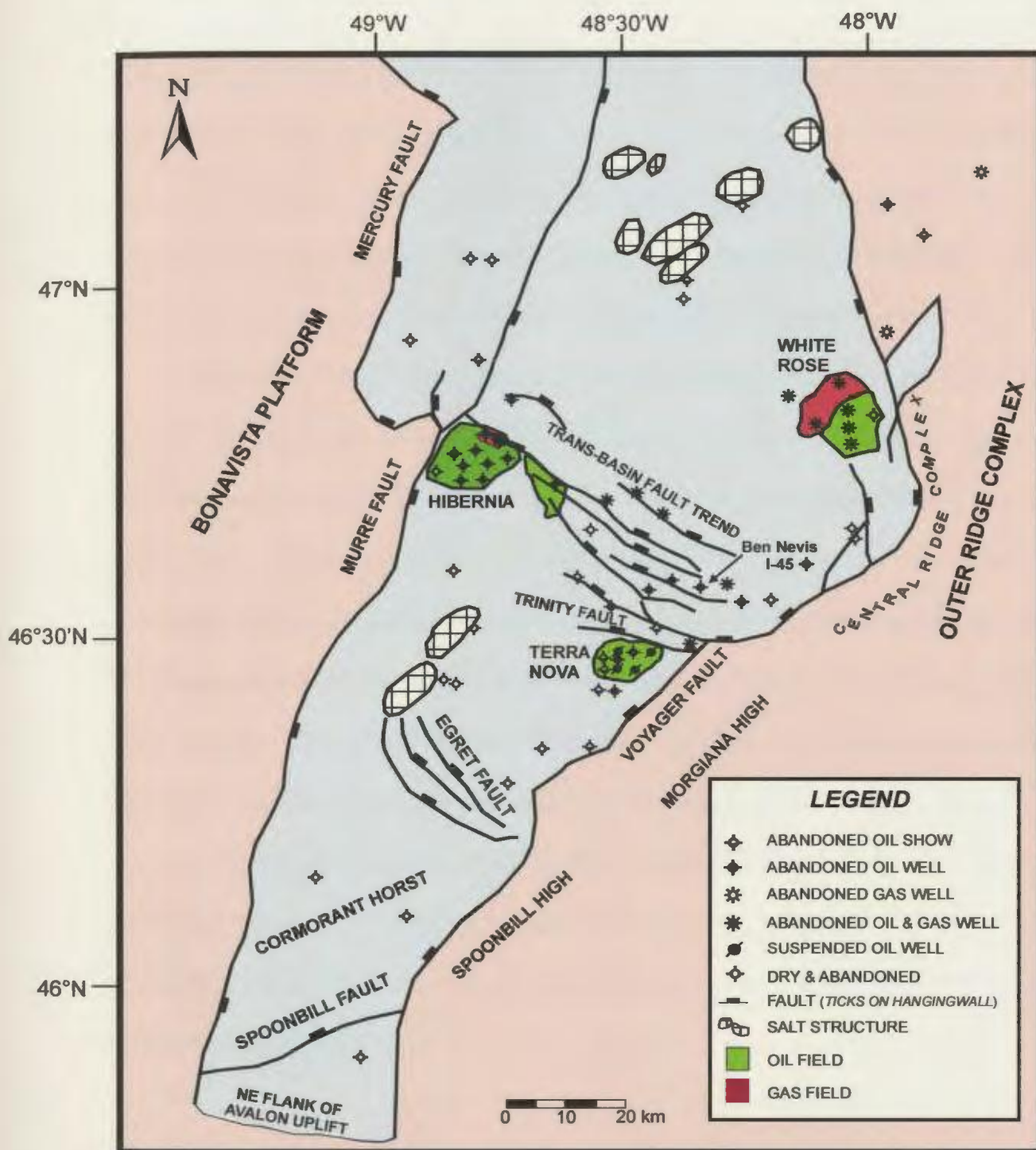


Figure 1.4 Map of the Jeanne d'Arc Basin, showing well locations, major structural elements, and areas of hydrocarbon exploration (including the Terra Nova, Hibernia, and White Rose oil fields). To the west, the basin is bounded by the Bonavista Platform, the Murre Fault, and the Mercury Fault; to the east by the Voyager Fault and the Outer Ridge Complex (which includes the Morgiana High, the Central Ridge Complex, and the Spoonbill High); and to the south by the Avalon Uplift (modified from McAlpine, 1990)

In the north, the basin is 100 km wide, but narrows to 42 km across in the south (Arthur et al., 1982). Bordering the basin to the west is a large basement platform called the Bonavista Platform; to the east is a series of basement ridges referred to as the Outer Ridge Complex and, to the south, the Avalon Uplift. To the north, the Jeanne d'Arc Basin opens into the East Newfoundland and Orphan Basins (Petro-Canada, 1996).

The Jeanne d'Arc Basin is the only oil-prone basin on the Grand Banks of Newfoundland (Enachescu et al., 1997). Drilling in the Jeanne d'Arc Basin began in 1971, but interest peaked in 1979 with the discovery of the Hibernia oil field (i.e. P-15 well). Since then, nearly 2 billion barrels (318 million m³) of recoverable reserves have been discovered, including the Hibernia and Terra Nova fields, as well as the Hebron-Ben Nevis series of pools and the White Rose, Nautilus, Mara, and South Tempest fields. Two gas discoveries (Trave and North Dana) and one oil discovery (South Tempest) are located on the adjacent Outer Ridge Complex (Department of Mines and Energy, 2000). Geologically, the eastern Newfoundland offshore area is the best known and most extensively explored region of the northern Atlantic continental margin of North America. In fact, it is the only North American east coast area that contains world-class oil fields (Enachescu, 1993).

1.3 Regional Tectonic Evolution

The Mesozoic basins off eastern Canada formed in response to multiple rifting and spreading events associated with the break-up of the supercontinent Pangea and the formation of the present-day North Atlantic Ocean and the Labrador Sea (Sinclair, 1993;

McAlpine, 1990). In particular, the North Atlantic Ocean formed as a result of the separation of the European and North American plates (Arthur et al., 1982). Thick depositional sequences in the Grand Banks rift basins record the complex tectonic history of the breakup of Pangea and the formation of the present-day Atlantic Ocean (Sinclair, 1988).

During the Late Triassic through Early Cretaceous (Albian), three distinct rifting episodes affected the Jeanne d'Arc Basin, each preceded by a period of broad regional warping or arching, and each followed by a period of passive subsidence (Sinclair, 1988). There is broad agreement regarding the rifting events that affected the Jeanne d'Arc Basin during Triassic and Early Jurassic; however, there are significant contrasts in the interpretations of the timing, type, and range of the third tectonic event, during Late Jurassic through Early Cretaceous (Sinclair, 1993; Figure 1.5). Several authors have recognized two Mesozoic rift phases that affected the Grand Banks (Jansa and Wade, 1975; Wade, 1978; Hubbard et al., 1985; Hubbard, 1988; Tankard and Welsink, 1987, 1988; Tankard et al., 1989; and McAlpine, 1990). However, Sinclair (1988), Enachescu (1986, 1987), Hiscott et al. (1990), Driscoll and Hogg (1995), and Driscoll et al. (1995) have identified three distinct rift phases that affected the Grand Banks during the Mesozoic. In addition, Sinclair (1988) recognized "onset warp stages" occurring prior to the latter two rift phases in the Jeanne d'Arc Basin. The majority of the tectonic interpretations for the timing, type and duration of the third tectonic event in the Jeanne d'Arc Basin are summarized in a publication by Sinclair (1993; Figure 1.5).

The first Mesozoic rifting episode occurred in the Late Triassic through Early

A. Jansa and Wade (1975) and Wade (1978)
B. Hubbard et al. (1985) and Hubbard (1988)
C. Driscoll and Hogg (1995) and Driscoll et al. (1995)
D. Enachescu (1986, 1987)
E. Tankard and Welsink (1987, 1988) and Tankard et al. (1989)
F. Sinclair (1988)
G. Hiscott et al. (1990)
H. McAlpine (1990)

R = rift
P = passive, thermal anomaly decay
T = transitional
OW = onset warp
R2T = a transitional phase of early extension before brittle deformation of the upper crust
R2C = classic rifting with 20 My of fault-dominated subsidence
R2D = a decaying rift phase with an increasing degree of regional thermal subsidence anticipating an interpreted Aptian breakup event

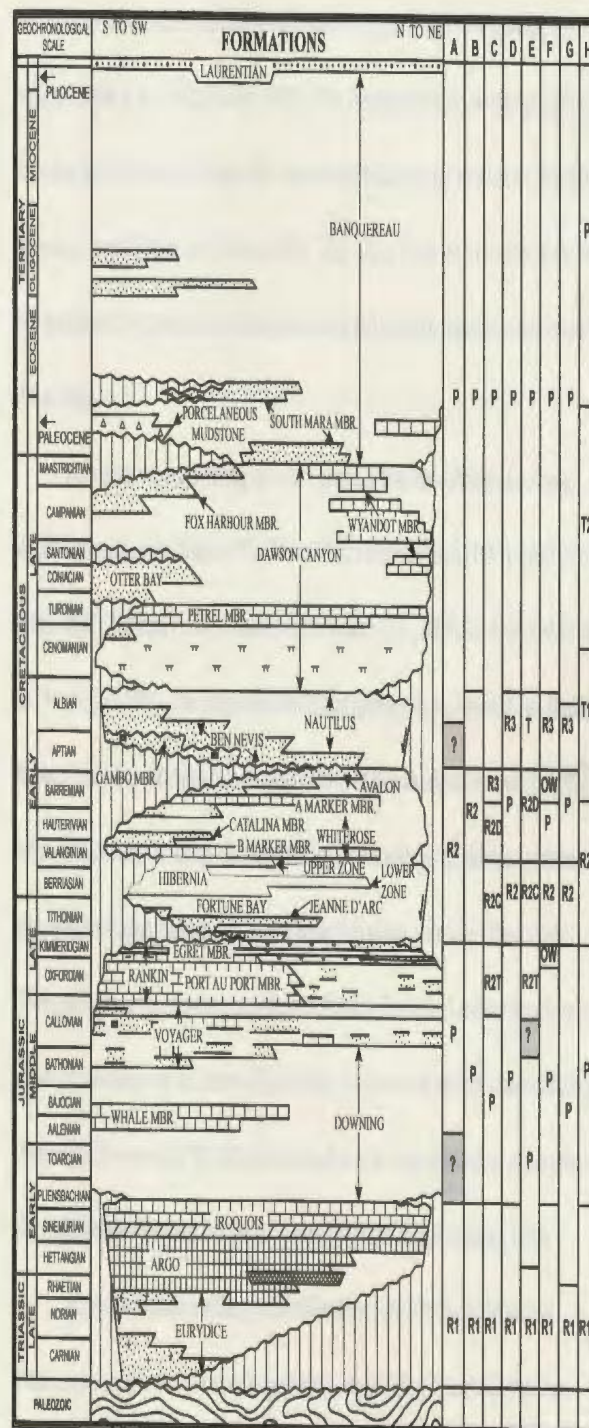


Figure 1.5 Lithostratigraphy of the Jeanne d'Arc Basin, showing the major differences in the interpretations for the timing, type and duration of the third tectonic event (after Sinclair, 1993)

Jurassic. Deformation began during the Triassic with NW-SE tensional stresses and synchronous sedimentation and the development of a series of NE-SW-trending rift valleys (Arthur et al., 1982; Sinclair, 1988). The Triassic extension laid the groundwork for subsequent breakup of Pangea, but was not significant enough to allow the formation of oceanic crust (Hiscott and Wilson, 1987). This rifting led to the formation of the large NE-trending half-graben that underlies the central and southern portions of the Jeanne d'Arc Basin.

Following the initial rifting episode a period of regional subsidence occurred. According to Jansa and Wade (1975), Wade (1978), Hubbard et al. (1985), Enachescu (1986, 1987), Hubbard (1988), Tankard and Welsink (1987, 1988), Tankard et al. (1989), and McAlpine (1990), who interpreted two rifting episodes in the Jeanne d'Arc Basin, the Rankin Formation corresponds to the later portion of the subsidence episode that followed Late Jurassic rifting. Towards the end of this stage of subsidence, a marine transgression occurred which deposited organic-rich shales across the Grand Banks. These shales are known as the Egret Member (Rankin Formation) and are the primary source of oil and gas in the Jeanne d'Arc Basin. By the end of the first phase of rifting, the tectonic framework of the Grand Banks had been developed and most of the present-day sedimentary basins and troughs had formed (Enachescu and Dunning, 1994).

A second episode of rifting occurred from the Late Jurassic to the earliest Cretaceous (i.e. Tithonian to early Valanginian). Its initiation is marked by the base-Tithonian unconformity. At this time, after substantial separation of the North American and African plates further to the south (Arthur et al., 1982), the locus of greatest

extension stepped to the east of the Grand Banks, initiating the separation of the eastern Grand Banks from Iberia (Wade, 1978). This rifting episode, which consisted of mainly NW-SE and E-W tensional stresses and synchronous sedimentation, resulted in the development of a series of mainly NE-SW- and N-S-trending faults (Enachescu, 1988; Sinclair 1993, 1994).

Several hypotheses are proposed for the development of the Avalon Uplift. Kerr (1985) suggested that the continental crust beneath the Grand Banks arched upwards at this time, perhaps in isostatic response to the changed rift pattern, resulting in the uplift of the southern end of the Jeanne d'Arc Basin (Figure 1.4). Alternatively, the Avalon Uplift could have resulted from thermal expansion due to heat leakage northward from the central Atlantic Mid-Ocean Ridge (MOR), resulting in a thermal dome that would have migrated eastward through the continental crust of the Grand Banks as the MOR passed along the transform margin (Todd and Keen, 1989). Yet another possibility is that the Avalon Uplift reflects the passage of a plume, which added igneous material to the base of the crust and caused it to rise buoyantly (Keen et al, 1994). In either case, this uplift, running southeast from the Avalon Peninsula, resulted in extensive erosion of older Jurassic sediments along the arch and separated the evolving basins of the northeast Grand Banks from those in the southwest (Department of Mines and Energy, 2000).

The second period of rifting was followed by the break-up of Iberia and the Grand Banks, possibly as early as mid-Valanginian (Enachescu 1986 and 1987; Sinclair, 1988), or as late as mid-Aptian (Jansa and Wade, 1975; Wade, 1978; Hubbard et al., 1985; Hubbard, 1988; Tankard and Welsink, 1987 and 1988; Tankard et al., 1989; Hiscott et al.,

1990; McAlpine, 1990; and Driscoll et al., 1995). It was during the second episode of rifting (Late Jurassic to earliest Cretaceous) that the main hydrocarbon-bearing reservoir rocks in the Terra Nova field (Jeanne d'Arc Formation sandstones) were deposited (Petro-Canada, 1996). Table 1.1 provides a listing of the main reservoirs in the Jeanne d'Arc Basin, as well as their period of deposition. Some discrepancy exists with regards to the timing of deposition of the Avalon Formation; it has been interpreted to have formed during the onset phase of the third (and final) rifting episode by Sinclair (1993, 1994), but Driscoll (1992) and Driscoll and Hogg (1995) have interpreted the Avalon Formation as syn-rift deposits.

A third rifting episode possibly took place in the mid-Aptian to late Albian (Enachescu 1986, 1987; Sinclair, 1988). This period consisted of NE-SW extension and the growth of NW-SE-trending ("trans-basin") normal faults in the Jeanne d'Arc Basin (Enachescu, 1988; Sinclair 1993, 1994). Rifting propagated northeast and then northwest to the Labrador Sea by the end of the Cretaceous (Sinclair, 1988; Department of Mines and Energy, 2000). The continental margins were first stretched, followed by the separation of the Labrador margin from Greenland in the Campanian (Srivastava, 1978). At this time, Greenland remained attached to Europe. It was not until early in the Cenozoic that seafloor spreading began between Greenland and Europe.

By Late Cretaceous, regional thermal subsidence due to lithospheric crustal cooling occurred in the Grand Banks. Since the Late Cretaceous, the Grand Banks area, including the Jeanne d'Arc Basin, has formed part of a passive continental margin.

Table 1.1 Principal hydrocarbon reservoirs in the Jeanne d'Arc Basin and the rifting period during which they formed.

Reservoir	Age	Rifting Event	Field
Ben Nevis Formation	Early Cretaceous (late Aptian to Albian)	Third (mid-Aptian to late Albian)	Hibernia Whiterose Hebron/Ben Nevis/West Ben Nevis Complex North Ben Nevis Springdale Nautilus King's Cove
Avalon Formation	Early Cretaceous (Aptian)	Third (mid-Aptian to late Albian)	
Hibernia Formation	Early Cretaceous (Berriasian to Valanginian)	Second (Tithonian to early Valanginian)	Hibernia Whiterose Hebron West Bonne Bay Ben Nevis
Jeanne d'Arc Formation	Late Jurassic (Kimmeridgian to Tithonian)	Second (Tithonian to early Valanginian)	Terra Nova Hebron

Understanding the complex tectonic evolution of the Grand Banks area is crucial, since it is intimately linked to the structural development of the area (Section 1.4) and has controlled many factors necessary for stratigraphic sequence generation (Section 1.5).

1.4 Regional Structure

The eastern Newfoundland offshore area, which encompasses the Grand Banks, is bounded to the north by the Charlie Gibbs Fracture Zone and to the southwest by the South Newfoundland Transform Margin, which separate the Grand Banks from the

Labrador and Scotian shelves, respectively (Figure 1.6). The J-Anomaly Ridge bounds the Grand Banks to the southeast (Sullivan and Keen, 1978; Enachescu, 1993).

Internally, the Grand Banks is divided into southern, central, and northern provinces by major strike-slip faults (Tankard and Welsink, 1988).

The Jeanne d'Arc Basin is a half-graben located on the Grand Banks of Newfoundland. The main structural elements of the basin are summarized in Figure 1.4. The NE-trending half-graben, which dominates the structure of the southern and central portions of the basin, was developed during the first tectonic episode (Late Triassic to Early Jurassic). Situated to the west, the Bonavista Platform is a stable shelf consisting of Paleozoic rocks overlain by Tertiary and Upper Cretaceous strata (Sinclair et al., 1992). A basin-bounding fault zone, consisting of the NE-trending Murre and Mercury faults (also formed during the first tectonic episode), separates the Bonavista Platform from the Jeanne d'Arc Basin to the east. To the south, the basin is bounded by the Avalon Uplift, which was formed during the second rifting episode (Sinclair et al., 1992).

The Outer Ridge Complex bounds the basin to the east and is a structural high composed of north- and northeast-trending basement ridges. Highly deformed Triassic and Jurassic rocks overlay this complex, which consists of a number of structural elements (Figure 1.4), including the Spoonbill High, the Morgiana High, and the Central Ridge. The Spoonbill and Morgiana Highs separate the southern and central portions of the Jeanne d'Arc Basin from the Carson Basin to the south (Enachescu, 1987). The Central Ridge borders the northern regions of the Jeanne d'Arc Basin. This ridge is separated from the Jeanne d'Arc Basin to the west by the Voyager Fault, which formed a significant

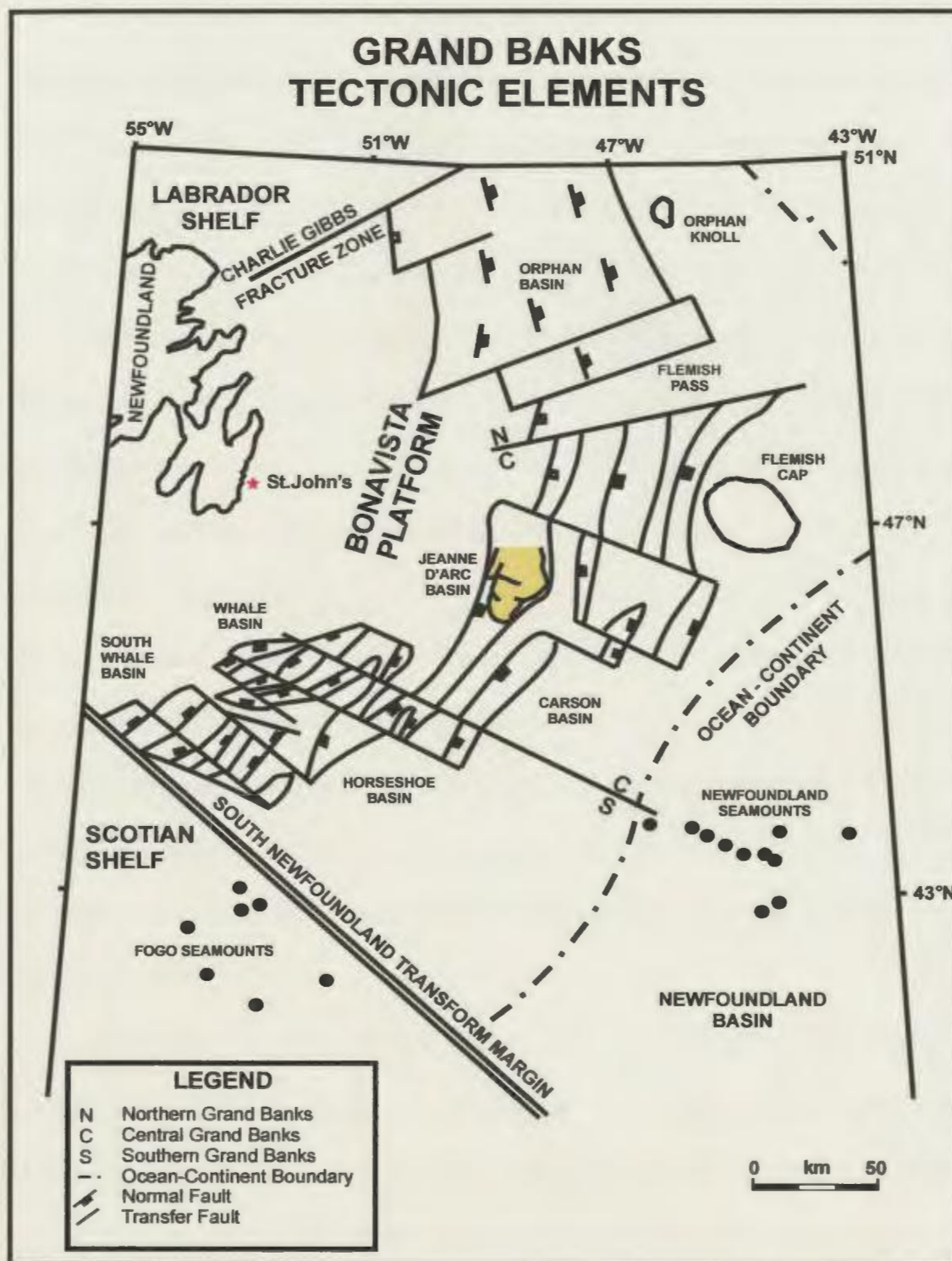


Figure 1.6 Map showing the principal structural elements of the Grand Banks and Orphan Basin (after Tankard and Welksink, 1988; and Welsink et al., 1989). The Grand Banks is separated from the Scotian and Labrador shelves by the South Newfoundland Transform Margin and the Charlie Gibbs Fracture Zone, respectively. Internally, major strike-slip faults divide the area into southern (S), central (C), and northern (N) provinces.

Cretaceous basin-bounding fault along the eastern margin of the Jeanne d'Arc Basin (Enachescu, 1987). Scarcely mentioned in literature is the Cormorant Horst. Located in the southernmost region of the Jeanne d'Arc Basin, it is bounded to the north by the Egret Fault (Enachescu, 1987) and to the south by the Spoonbill Fault.

Three main sets of faults dominate the structural framework of the Jeanne d'Arc Basin: NE-SW- and N-S-trending listric faults parallel to the basin margins; high-angle normal faults parallel to the basin margins; and a series of NW-SE- and E-W-trending trans-basin faults (the Trans-Basin Fault Trend) perpendicular to the other two sets (Enachescu, 1987; McAlpine, 1990). The development of NE-SW- and N-S-oriented faults took place during the second rifting episode, under NW-SE and E-W extension, respectively (Enachescu, 1988; Sinclair 1993, 1994). The formation of the "trans-basin fault trend" may be associated with the formation of NW-SE-trending listric normal faults in response to NE-SW tension associated with the third rifting episode (mid-Aptian to Albian), which led to the separation of North America from Europe (Jayashinghe, 1988).

The "trans-basin fault trend" divides the Jeanne d'Arc Basin into three structural-stratigraphic segments. Firstly, south of the Egret Fault, erosion and depositional thinning have removed most of the upper Jurassic and lower Cretaceous successions. Secondly, between the Egret Fault and the Hibernia to Ben Nevis "trans-basin fault trend", the uppermost Jurassic to Lower Cretaceous succession thickens dramatically. Lastly, north of the "trans-basin fault trend", a thickened middle Cretaceous succession has been preserved (McAlpine, 1990).

In certain areas, the Jeanne d'Arc Basin is underlain by salt. Salt has played a role in the structural development of the sedimentary fill. Movement and subsequent withdrawal of the salt has affected faulting in the Jeanne d'Arc Basin (McAlpine, 1990). To the north, near the Adolphus wells, there are diapiric structures, some of which reach nearly 10 km in diameter. The Egret salt wall is located in the central portion of the Jeanne d'Arc Basin (near the Egret Fault) and trends roughly NNE. Salt accumulation and subsequent movement are intimately linked to extensional tectonics. The faults associated with the evaporitic deposits, in combination with the tectonically generated extensional faults which define the basin, created traps into which hydrocarbons could migrate (Sinclair et al., 1992). Some of the major faults in the basin, such as the Trinity, Egret, Spoonbill, and Murre Faults, were reactivated in the Late Cretaceous and Early Tertiary.

In summary, the structural framework of the Jeanne d'Arc Basin was formed during three successive rifting episodes that affected the basin. The main basin-bounding Murre and Mercury Faults, which are responsible for the asymmetric half-graben geometry of the basin, were formed during the first rifting episode (Late Triassic to Early Jurassic) and trend NE-SW. N-S-trending faults, which characterize the central Jeanne d'Arc Basin, and NE-SW-oriented faults in the basin were formed during the second rifting episode (Late Jurassic to Early Cretaceous). The third episode of rifting was responsible for the formation of the NW-SE-trending trans-basin normal faults that, in combination with the other faults, define the asymmetric, funnel-shaped geometry of the basin.

1.5 Regional Stratigraphy and Tectono-Stratigraphic Evolution

Formal stratigraphic nomenclature for the Jeanne d'Arc Basin (Figure 1.7) has been presented and revised by Jansa and Wade (1975), Sinclair (1988), Tankard and Welsink (1988, 1989), Grant and McAlpine (1990), and McAlpine (1990), among others. The stratigraphic nomenclature developed in response to an understanding of the tectonic and structural development of the Grand Banks (Tankard and Welsink, 1988; Grant and McAlpine, 1990; McAlpine, 1990). Megacycles of rift and post-rift subsidence have been identified by Enachescu (1986, 1987), Tankard and Welsink (1987, 1988), Sinclair (1988), Tankard et al. (1989), McAlpine (1990), and Hiscott et al. (1990). They can be matched at the large scale with unconformity-bound sequences. On a smaller scale, depositional sequences, bounded by second-order unconformities, document the complex interaction of tectonic subsidence (Tankard and Welsink, 1987), eustatic sea-level changes, sediment supply and climate (Vail et al., 1977; Vail 1987; Posamentier et al., 1988; Van Wagoner et al., 1988).

The Eurydice Formation was deposited during initial extension of the Grand Banks and marks the base of the Mesozoic section in the Jeanne d'Arc Basin and consists of continental redbeds (Grant and McAlpine, 1990). It is overlain by the Argo and Iroquois formations, representing restricted-marine evaporite and shallow marine limestone deposition in the Jeanne d'Arc Basin (McAlpine, 1990).

During the first thermal sag phase, from mid-Pliensbachian to Kimmeridgian, a broad epicontinental sea occupied the Grand Banks and a thick post-rift succession, consisting of the Downing, Voyager, and Rankin formations, was deposited. This

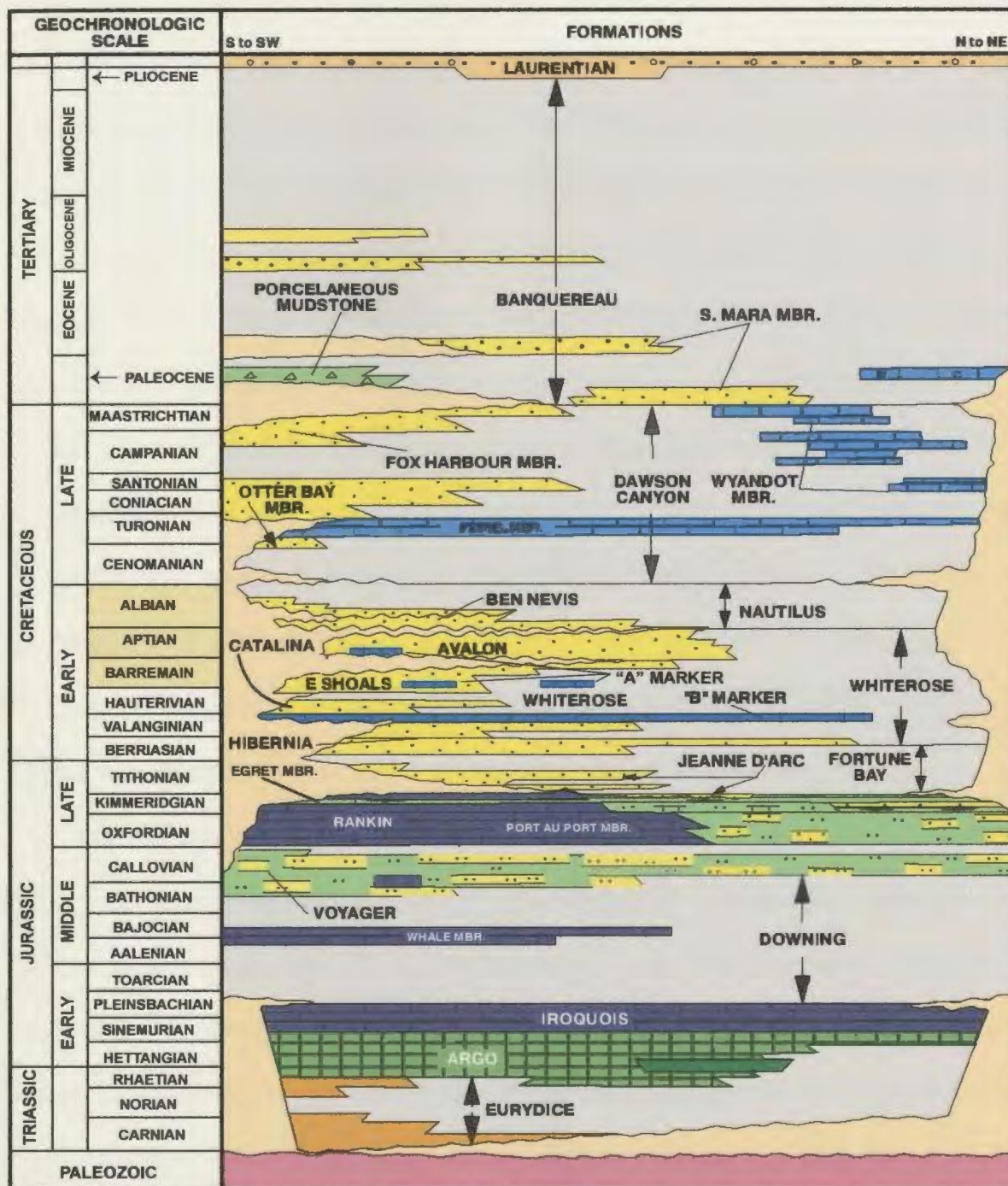


Figure 1.7 Formal stratigraphy of the Jeanne d'Arc Basin, with particular reference to Terra Nova stratigraphy. The highlighted region shows the position of the upper Barremian to lower Aptian Eastern Shoals Formation, the Aptian Avalon Formation, and the upper Aptian to Albian Ben Nevis Formation (after C-NOPB, 2002 a & b; Petro-Canada, 1996)

succession is made up of deep-water marine shales and limestones. This period of sag marks a break in the extension of the continental lithosphere, between the initial rifting event and Late Jurassic reactivation of the system. According to those authors who interpreted only two rifting episodes in the, the upper Callovian to Kimmeridgian Rankin Formation, which consists of organic-rich shales, limestones, and marlstones, represents the end of the post-rift sequence. Of particular interest is the Kimmeridgian Egret Member of the Rankin Formation, which is an organic-rich shale, regarded as the principal hydrocarbon source rock in the Jeanne d'Arc Basin (Swift and Williams, 1980; Powell, 1985; Creaney and Allison, 1987; McAlpine, 1990). The Egret Member is interpreted by Sinclair (1988) as the "onset warp" phase of the second episode of extension in the basin, a phase during which there is differential subsidence but insignificant faulting.

Together, the Jeanne d'Arc, Fortune Bay, and Hibernia formations represent a syn-rift succession (Figure 1.7). The near-base Tithonian unconformity marks the renewal of extension in the basin, with the Jeanne d'Arc Formation representing the beginning of the second rifting episode. Fluvial sandstones and conglomerates of the Jeanne d'Arc Formation (Kimmeridgian to Tithonian) grade basinward into the shales of the Fortune Bay Formation (Tithonian). The overlying sandstones of the Hibernia Formation (Berriasian to Valanginian) were deposited in a prograding fluvial-deltaic setting (M.J. Bidgood, pers. comm., 2002). This syn-rift package, consisting of the Jeanne d'Arc, Fortune Bay, and Hibernia formations, is characterized by syn-tectonic structures related to continued extension, salt diapirism, and sedimentary faulting.

Post-rift subsidence and deepening in the Jeanne d'Arc Basin are represented by the deposition of the B-marker limestones, Eastern Shoals sandstones, and marine sandstones of the Catalina Formation, including the distally equivalent shales of the Whiterose Formation (Figure 1.7). Both the B-marker limestones and the top of the Eastern Shoals Formation (also known as the Barremian unconformity or the A-seismic marker) are excellent regional stratigraphic and seismic markers in the basin. In particular, the B-marker limestone indicates the initiation of a second period of stability within the basin, referred to as the second thermal sag period (Sinclair, 1988).

In the western and northern portions of the basin (e.g., at the Hibernia and Whiterose oil fields), a limestone known as the A-marker limestone was deposited directly above the Whiterose shales (Figure 1.7). However, in the central and southern portions of the basin, a thick accumulation of calcareous sandstones and oolitic limestones was deposited in a shallow- to marginal-marine setting. This succession is designated as the Eastern Shoals Formation by McAlpine (1990). Sinclair (1988) instead designated this succession as the A-marker Member of the Avalon Formation. Thus, Sinclair's (1988) A-Marker Member of the Avalon Formation (or lower Avalon Member, as used in Terra Nova well history reports) is a synonym for part or all of the Eastern Shoals Formation. The Eastern Shoals Formation will be used in this study.

The Aptian Avalon Formation unconformably overlies the Eastern Shoals Formation and is an upward coarsening marine sandstone succession. The upper Aptian to Albian Ben Nevis Formation unconformably overlies the Avalon Formation and consists of shallow- to marginal-marine sandstones. Together, the Avalon and Ben Nevis

formations create one of the most important petroleum reservoirs in the Jeanne d'Arc Basin. The stratigraphy of this succession will be discussed in more detail later as it is critical to the geology of the Terra Nova oil field (Section 1.6.4).

The Ben Nevis Formation is overlain by the Nautilus Formation. Extensive marine shales make up the Nautilus Formation, which was deposited in the deepest portions of the Jeanne d'Arc Basin. Since Late Cretaceous, the Jeanne d'Arc Basin has undergone thermal subsidence, resulting in the deposition of the post-rift Dawson Canyon Formation (Cenomanian to Maastrichtian). This formation includes the chalky Petrel Limestone Member, the Otter Bay and Fox Harbour deltaic members, and the Wyandot Member. The deposition of the Dawson Canyon Formation marked the initiation of the most recent (and final) thermal sag period to affect the Grand Banks region.

The base Tertiary unconformity marks the upper boundary of the upper Cretaceous succession and represents a relative sea-level drop at this time. The South Mara Member of the Banquereau Formation was deposited directly above this unconformity. The Banquereau Formation (McAlpine, 1990) comprises the Tertiary section in the Jeanne d'Arc Basin. There has been little sediment supply to the Jeanne d'Arc Basin since Eocene time and the basin now forms part of a stable passive continental margin.

1.6 The Terra Nova Oil Field

1.6.1 Introduction

The Terra Nova oil field is situated on the southeastern flank of the Jeanne d'Arc

Basin (Figure 1.2), approximately 350 km east-southeast of St. John's, Newfoundland, and 35 km southeast of the Hibernia oil field. Located in 95 m of water, it is the second largest oil field discovered on the Grand Banks, after Hibernia, and covers an area of 67 km². Geologically, the field can be divided into four structural fault blocks (Figure 1.8): West Flank, Graben, East Flank, and Far East. The main reservoir is the upper Jurassic Jeanne d'Arc Formation. Terra Nova was discovered in mid-1984 with the drilling and testing of the Petro-Canada et al. Terra Nova K-08 wildcat well, which flowed oil on tests from three separate sandstone zones (Petro-Canada, 1984). Following the discovery well, five delineation wells (K-07, C-09, I-97, H-99, and E-79) drilled into the Graben and East Flank identified five major and two minor oil-bearing sandstone intervals within the structure. Three 3-D seismic surveys have been conducted over the Terra Nova field, the most recent during the summer of 1997.

A consortium led by Petro-Canada (including ExxonMobil Canada Properties., Husky Energy Operations Ltd., Norsk Hydro Canada Oil and Gas, Murphy Oil Company Ltd., Mosbacher Operating Ltd., and Chevron Canada Resources) is producing oil from the field at an average rate of 18,250 cubic meters per day (115,000 barrels a day) over 6 years. The field contains over one billion barrels (160 million m³) of oil in place and has up to a 17-year expected production life, compared with 20 years or more for the Hibernia oil field. Development began in the East Flank and will continue to the Graben. Recoverable oil reserves are estimated at 370-400 million barrels (58 – 63 million m³) from the Graben and East Flank with the possibility of an additional 100 million barrels (16 million m³) being produced from the Far East Flank. Recoverable natural gas and

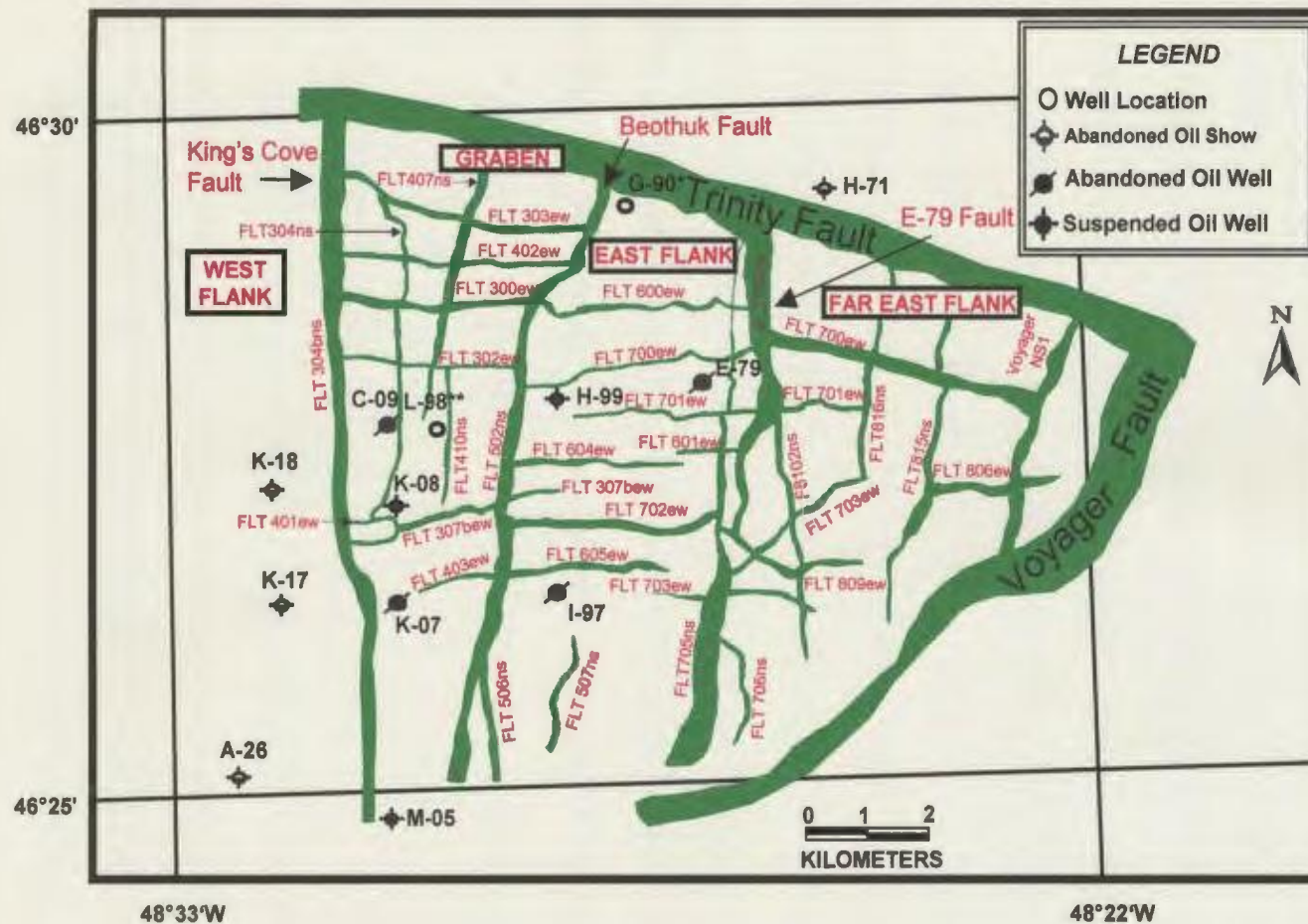


Figure 1.8 Map of the Terra Nova oil field showing the major fault trends and the location of various wells (N. Carter, pers. comm., 2002). Note that well locations G-90* and L-98** include the following development wells respectively: G-90 1, G-90 2, G-90 3, G-90 2Z, G-90 2Y, G-90 2X, and G-90 2W; and L-98 1, L-98 1Z, L-98 2, and L-98 3.

natural gas liquids (NGL) reserves are estimated at 0.269 trillion cubic feet (76 trillion m³) and 14 million barrels (2 million m³), respectively (C-NOPB, 2002b). The West Flank has little potential for commercial oil production; the two wells that were drilled in that fault block encountered water-saturated sandstones. The oil in the Terra Nova field is a light crude, similar to that encountered at the Hibernia oil field, and is located at depths between 3200 and 3700 m below the seafloor (Petro-Canada, 1996).

A Floating, Production, Storage, and Offloading (FPSO) vessel is being used for the development of the Terra Nova oil field, rather than a gravity-based structure (GBS), which is being used to develop the Hibernia oil field. This is due to the greater water depth and smaller recoverable oil reserves at the Terra Nova field compared to the Hibernia field. Subsea equipment has been installed into "glory holes" excavated on the seafloor, to protect it from iceberg scour. A total of 26 wells are planned for the Graben and East Flank, including 15 producers, 8 water injectors, and 3 gas injectors. A total of 10 wells are foreseen for the Far East structural block (5 producers and 5 water injectors).

1.6.2 Terra Nova stratigraphy

Wells in the Terra Nova field only drilled to depths of upper Jurassic to lower Cretaceous rocks; hence, only these successions will be discussed. All other stratigraphic successions were described earlier in the Regional Stratigraphy section (Section 1.5).

The marine shales and siltstones of the Voyager Formation are the oldest rocks penetrated in the Terra Nova oil field; the upper portion of the formation was encountered in the K-08 discovery well. The overlying Rankin Formation includes the Egret Member,

the primary source rock in the Jeanne d'Arc Basin. The Jeanne d'Arc Formation, which unconformably overlies the Rankin Formation, forms the reservoir in the Terra Nova oil field and consists of seven stacked sandstone successions. The overlying Fortune Bay Formation consists of marine shales, which form an adequate top seal for this reservoir. Hibernia Formation sandstones, which overlie the Fortune Bay Formation, have the same reservoir qualities as Jeanne d'Arc sandstones, but are water-saturated within the field.

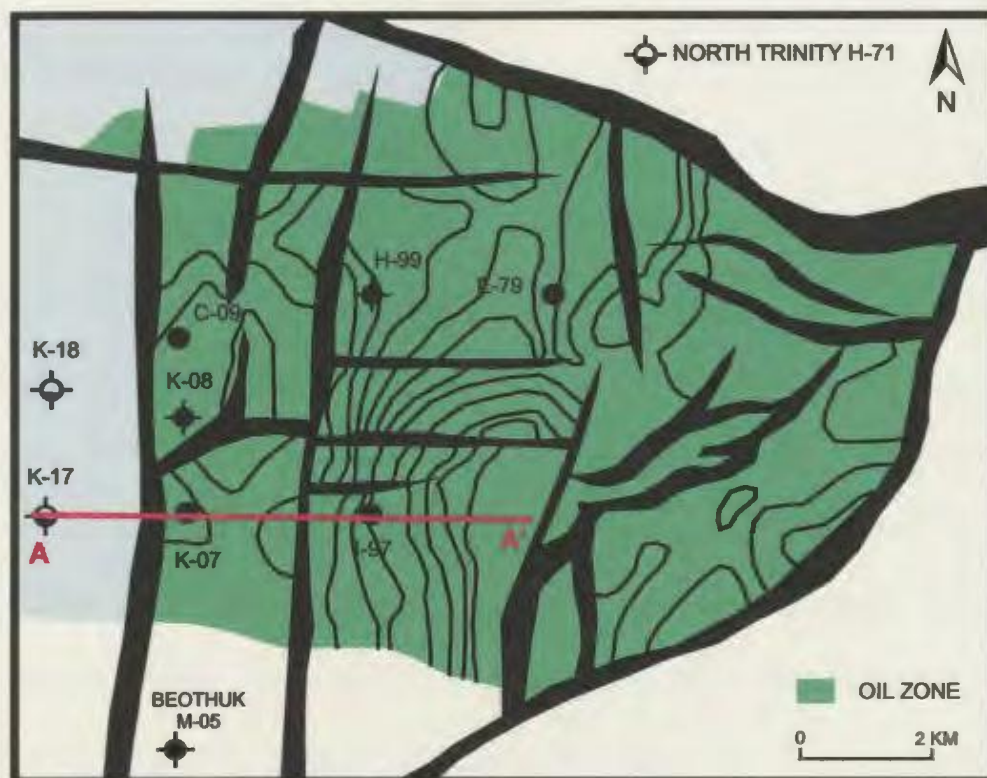
Although the B-marker limestone unconformably overlies the Hibernia Formation across the majority of the Jeanne d'Arc Basin, the contact is conformable at the Terra Nova field (D.E. Noseworthy, pers. comm., 2002). The B-marker is composed of oolitic limestones and fine- to medium-grained calcareous sandstones. The Catalina Formation, and the distally equivalent Whiterose Formation shales, overlies the B-marker limestone. Within the Terra Nova oil field, the Whiterose shales were deposited during a period of subsidence following the second rifting episode. The Eastern Shoals Formation conformably overlies the Whiterose Formation, which in turn is overlain by the Avalon and Ben Nevis formations. This lower Cretaceous succession is further discussed below (see Subsection 1.6.4).

The Nautilus Formation, which consists of marine shales, overlies the Ben Nevis Formation at the Terra Nova oil field. The Dawson Canyon Formation unconformably overlies the Nautilus Formation and is a dominantly marine-shale succession. It is in turn overlain by a thick sequence of marine shales of the Banquereau Formation, the youngest rocks in the Terra Nova oil field.

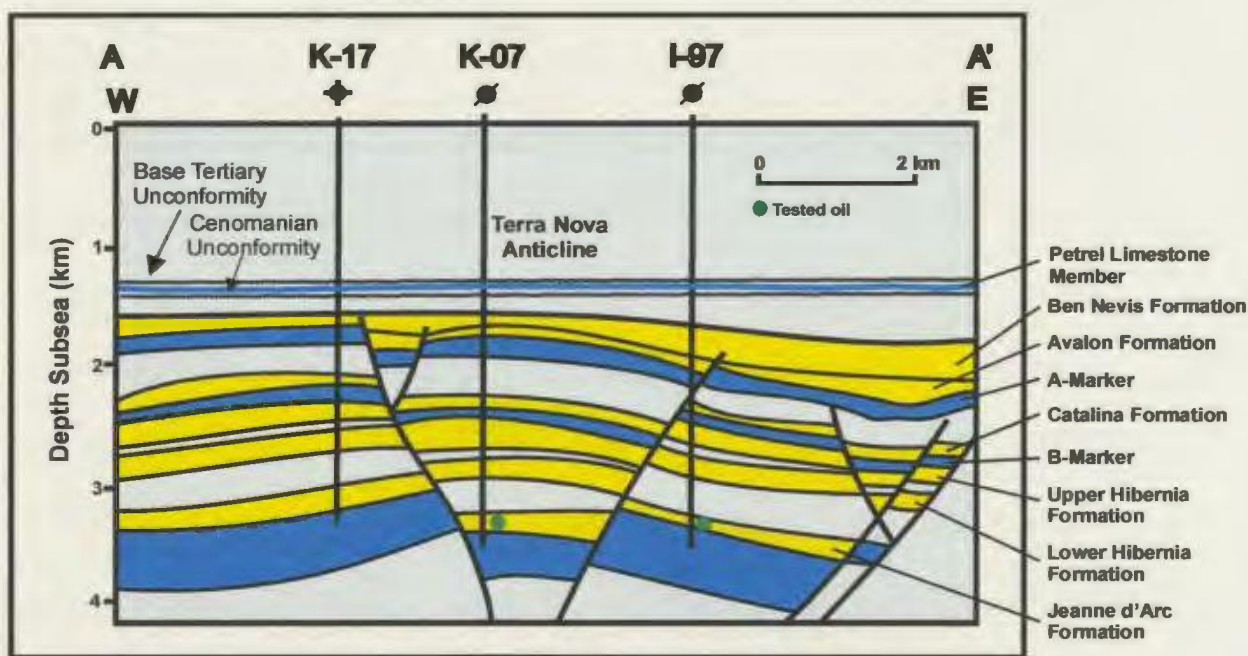
1.6.3 Terra Nova structure

The Terra Nova oil field can be divided geologically into three main fault blocks bounded by major N-S-trending faults. These fault blocks are further subdivided into smaller compartments by E-W-trending faults (Figure 1.8). Major N-S-trending faults bound the field to the east and west. Sinclair et al. (1992) have described the Terra Nova structure (Figure 1.9) as a northward-plunging, salt-cored anticline (hereafter referred to as the Terra Nova Anticline) with a significant graben at the crest. This north-plunging anticlinal nose covers an area of approximately 200 km². According to Enachescu et al. (1997), the Terra Nova structure was formed and presently sits in an elbow of the Voyager Fault. Closure at Terra Nova is both stratigraphically and structurally controlled. It is controlled to the west by the graben-bounding fault (called the King's Cove Fault), to the north and east by the flanks of the plunging anticlinal nose, and to the south by the pinchout of the Jeanne d'Arc sandstone (Sinclair et al., 1992). The large NW-SE-trending Trinity Fault also controls the closure to the north. Thus, the reservoir trap at Terra Nova is a multi-sided, fault-controlled, depositional wedge (Enachescu et al., 1997).

The three major fault blocks have been tested by numerous wells. The central keystone Graben fault block has been tested by the K-07, C-09, and the K-08 discovery wells. The East Flank fault block has been tested by the I-97, H-99, and E-79 wells, and has been found to contain the main oil-bearing portions in the field. The Far East Flank has only been penetrated by one well (2001-2002) and is estimated to contain additional hydrocarbons, which may increase the resource estimates of the field. The minor West



A



B

Figure 1.9

A. Structure map of the reservoir sands (Jeanne d'Arc sandstone) at Terra Nova. The oil zone is outlined in green. B. Geological cross-section of the Terra Nova oil field, showing major faults, reservoir zones, and the Terra Nova Anticline (after Department of Mines and Energy, 2000; C-NOPB, 2002b)

Flank fault block has been investigated by two wells, K-17 and K-18. However, these wells encountered water-saturated sandstones within the principal reservoir horizons.

According to Enachescu et al. (1997), the faults at Terra Nova are parts of two intersecting extensional listric fault systems (N-S- and E-W-trending faults) that compartmentalize the basin. The roughly N-S-trending Voyager Fault forms the main antithetic fault to the Murre Fault (Enachescu, 1987) and bounds the Jeanne d'Arc Basin to the east. It consists of several antithetic and synthetic N-S-trending faults that divide the Terra Nova area into the four fault blocks as described above. Growth strata are recorded in the hanging walls of these faults, indicating that the faults were active during the main rifting episodes in the basin. In fact, Enachescu (1987) and Sinclair (1988) have interpreted the N-S-trending faults to have developed during the "onset warp" phase of the second rifting episode in the basin (Late Jurassic to Early Cretaceous). However, these faults might also represent reactivation of older faults related to NW-SE extension in the Late Triassic to Early Jurassic.

According to the Terra Nova Development Plan Application (1996), the N-S-trending fault system dips between 40° and 50° and consist of two sets: an easterly-dipping set and a westerly-dipping set. At reservoir level, the dip separation is between 100 and 450 m. The Voyager Fault dips approximately 58° to the northwest and has a dip separation of up to 1600 m at the Rankin Formation level. Most of the N-S-trending faults in the field are interpreted as sealing faults, based on well test data and dip separations. On the other hand, the E-W-trending fault system at Terra Nova consists of non-sealing faults with smaller vertical separations than the N-S-trending system

(Enachescu et al., 1997). This fault system, including the “trans-basin fault trend” to the north, was initiated in response to NE-SW-oriented extension in the mid-Cretaceous, during the third tectonic episode to have affected the Jeanne d’Arc Basin (Sinclair 1993, 1994). The Ben Nevis Formation was deposited during this mid-Aptian to late Albian stage of extension.

1.6.4 Ben Nevis, Avalon, and Eastern Shoals formations

The Ben Nevis, Avalon, and Eastern Shoals formations together form one of the most important hydrocarbon reservoirs in the Jeanne d’Arc Basin. They constitute a sedimentary package deposited in a shallow- to marginal-marine environment during the final stages of rift development in the basin.

The late Barremian to early Aptian Eastern Shoals Formation is recognized as a lowstand prograding wedge that terminated with lagoonal red mudstones (Hassan, 1990). It conformably overlies the Whiterose Formation and consists of a 100 - 130 m succession of dominantly shallow- to marginal-marine calcareous sandstones and oolitic limestones (Table 1.2; McAlpine, 1990).

The Eastern Shoals Formation is unconformably overlain by the Avalon Formation. Together, the Eastern Shoals and Avalon formations possibly represent the “onset warp” phase of the third (and final) rifting episode and are therefore termed “pre-rift” sediments (Sinclair 1993, 1994; Enachescu 1986, 1987). However, Driscoll (1992), Driscoll and Hogg (1995), Driscoll et al. (1990, 1995), Tankard and Welsink (1987, 1988), and Tankard et al. (1989) have interpreted the Avalon Formation as being syn-rift

Table 1.2 Geologic tops and thicknesses of the Ben Nevis, Avalon, and Eastern Shoals formations in Terra Nova and other relevant wells (C-NOPB, 2002a; Petro-Canada 1984; 1985; 1986a, 1986b, 1986c, 1988a, 1988b, 1988c, 1990; Canterra 1985, 1987). See Figure 1.8 for well locations. Depths are in MD (measured depth). The Avalon Formation is missing in the Terra Nova K-17, the North Trinity H-71, and the Avondale A-26 wells; their thicknesses are indicated by N/A = not applicable. The Ben Nevis thicknesses include the Gambo Member.

FORMATION/ MEMBER	BEN NEVIS		GAMBO		AVALON		EASTERN SHOALS	
	Top (m)	Thickness (m)	Top (m)	Thickness (m)	Top (m)	Thickness (m)	Top (m)	Thickness (m)
WELL								
Terra Nova C-09	1583	112	1676	19	1695	75	1770	120
Terra Nova E-79	1789	153	1908	34	1942	64	2006	130
Terra Nova H-99	1676	141	1783	34	1817	27	1844	17
Terra Nova I-97	1692	181	1847	26	1873	81	1954	117
Terra Nova K-07	1579	134	1680	33	1713	35	1748	119
Terra Nova K-08	1582	135	1685	32	1717	57	1774	121
Terra Nova K-17	1542	156	1633	65	Eroded	N/A	1698	37
Terra Nova K-18	1590	143	1697	36	1733	67	1800	128
North Trinity H-71	1921	264	2161	24	Eroded	N/A	2185	87
Beothuk M-05	1510	253	1700	63	1763	41	1804	106
Avondale A-26	1506	157	1654	9	Eroded	N/A	1663	87
RANGE OF THICKNESS	112 – 264 m		9 – 65 m		27 – 81 m		17 – 130 m	
AVERAGE THICKNESS	166 m		34 m		55 m		97 m	

deposits and have noted fault growth within the Avalon succession.

The Aptian Avalon Formation is an upward coarsening succession of marine sandstones. It is recognized as a regressive sequence deposited, unconformably overlain at a sequence boundary by the upper Aptian to Albian Ben Nevis sequence. The latter consists of a stacked succession of marine to marginal-marine calcareous sandstone, bioclastic limestone, and minor shale, with varying thickness across the basin (Petro-Canada, 1996). At the Terra Nova field, the Avalon Formation has a thickness of 30 - 80 m (Table 1.2). It is composed of lagoonal and tidal flat mudstones and fine-grained estuarine sandstones (McAlpine, 1990) and represents a regressive phase of basin infilling, possibly a "forced regression" in response to renewed tectonic uplift in the southern portion of the basin.

Sediment of the Avalon Formation was likely sourced from a delta that occupied the Jeanne d'Arc Basin to the south, with minor sediment contributions from the east and west perimeter highs. Storm waves and tidal currents dispersed sediments of the Avalon Formation northward, resulting in thinly bedded clean sands with interbedded silty beds (Hassan, 1990). Near the end of the deposition of the Avalon Formation, abrupt sea-level fall resulted in incision of fluvial/estuarine channels (Hassan, 1990), represented by the mid-Aptian unconformity.

The Ben Nevis Formation was deposited during the third and final episode of rifting that affected the Jeanne d'Arc Basin during the Aptian-Albian. This rifting period created considerable accommodation space and increased the sedimentary input to the basin. Hence, it had a dramatic influence on stratigraphic stacking patterns in the basin.

Therefore, the “forced regression” that coincided with deposition of the Avalon Formation was terminated and a period of transgression was initiated. Sedimentation leading to the development of the Ben Nevis Formation took place in a shallow, open to restricted shelf environment.

The Ben Nevis Formation consists of a 110 - 180 m thick upward fining succession (Table 1.2) of shoreface sandstones and back-barrier facies, which were reworked predominantly along the “trans-basin fault trend”, resulting in reservoir quality sandstones with high porosity of 24%, as well as high permeability (McAlpine, 1990). During the deposition of these sandstones, landward retreat of the shoreline occurred (due to rising relative sea level), and resulted in the aggradation of fluvial/estuarine channels and the reworking of coastal sands (Hassan, 1990). These thick accumulations of sandstones are attributed to a high rate of sediment supply, which almost kept up with continued subsidence during transgression (Hassan, 1990). The Ben Nevis Formation is interpreted as syn-rift sediments by Sinclair (1993, 1994) and McAlpine (1990) and post-rift sediments by Driscoll (1992) and Driscoll and Hogg (1995).

The lower Cretaceous succession at Terra Nova consists of excellent reservoir rocks, but they are mostly water-saturated and hence do not contain hydrocarbons. There is a heavy oil accumulation within the Ben Nevis Formation. Several wells have penetrated the lower Cretaceous succession in the Terra Nova field. The continuing development of the field allows for real-time validation of stratigraphic models, presented in Chapter 4. The Ben Nevis Formation is extensively cored at North Trinity H-71, which will permit the ground truthing of the lithological interpretation of acoustic facies,

which will be discussed in Chapters 3 and 4.

1.6.5 Biostratigraphy

Biostratigraphic reports for two Terra Nova wells, K-07 (Awai-Thorne et al., 1986) and K-08 (La Borde and de Gasparis, 1984), are used in the following discussion. Last occurrence and/or high occurrence of foraminifera, ostracods, radiolaria, dinoflagellates, pollen, and spores species provide a constraint for the age of the lower Cretaceous succession in the Terra Nova field (Table 1.3 and 1.4).

The upper boundary of the Eastern Shoals Formation occurs at approximately 1749 m true vertical depth sub-sea (TVDSS), equivalent to 1774 m measured depth (MD) in the Terra Nova K-08 well. The formation has a thickness of 121 m with the lower boundary occurring at 1895 m MD (Table 1.2). The top of the Eastern Shoals Formation is characterized by the last occurrence of the arenaceous benthic foraminifera *Trocholina infragranulata* at 1775 m MD in the Terra Nova K-08 well, designating the top as Aptian (Ascoli 1976, 1990), or late Barremian to early Aptian (Williamson, 1987). Other microfossils present in the K-08 well at the Eastern Shoals stratigraphic interval include *Lenticulina rotulata* and *L. humilis* (the highest occurrence present at 1810 m MD).

In the Terra Nova K-07 well, the age of the Eastern Shoals Formation is characterized by the foraminifera *Trocholina infragranulata* and by an abundance of the foraminifera *Choffatella decipiens*, both of either Aptian age (Ascoli 1976, 1990) or late Barremian to early Aptian age (Williamson, 1987). Other microfossils present include *Protocythere triplicata* (late Barremian: Ascoli, 1990), *Pseudoceratium pelliiferum*

Table 1.3 Biostratigraphic column for the Terra Nova K-07 well (modified from Awai-Thorne et al., 1986)

GEOCHRONOLOGICAL SCALE			FAUNA	Youngest reported age of microfossil occurrence	FORMATION	
MESOZOIC	CRETACEOUS	ALBIAN	<i>Verneuillina cf. subfiliformis</i>	early-middle Albian (Bartenstein and Bettenstaedt, 1962); early Albian (Ascoli, 1976 and 1990)	BEN NEVIS (including Gambo Member)	
		APTIAN	No biostratigraphy available for this interval			AVALON
		LATE BARREMIAN–EARLY APTIAN	<i>Trocholina infragranulata</i>	Aptian (Ascoli, 1976 and 1990); late Barremian or early Aptian (Williamson, 1987)	EASTERN SHOALS	
			<i>Choffatella decipiens</i>	Aptian (Ascoli, 1976 and 1990); late Barremian or early Aptian (Williamson, 1987)		
			<i>Protocythere triplicata</i>	Barremian (Ascoli, 1990)		
			<i>Pseudoceratium pelliferum</i>	Barremian (Millioud, 1969; Williams, 1974; Bujak and Williams, 1978); late Barremian (Davey, 1979)		
			<i>Mudergonia staurota</i>	Barremian (Millioud, 1969); late Barremian (Davey, 1974)		
		<i>Kleithriasphaeridium simplicispinum</i>	late Barremian (Davey and Williams, 1966; Sargeant, 1966; Davey, 1974); late Aptian (Duxbury, 1978)			

Table 1.4 Biostratigraphic column for the Terra Nova K-08 well (modified from La Borde and de Gasparis, 1984)

GEOCHRONOLOGICAL SCALE			FAUNA	Youngest reported age of microfossil occurrence	FORMATION	
MESOZOIC	CRETACEOUS	ALBIAN	<i>Verneuillina cf. subfiliformis</i>	early-middle Albian (Bartenstein and Bettenstaedt, 1962); early Albian (Ascoli, 1976 and 1990)	BEN NEVIS (including Gambo Member)	
			<i>Epistomina polypoides</i>	late Albian (Williamson, 1987)		
			<i>Epistomina carpenteri</i>	middle or late Albian (Williamson, 1987)		
			<i>Epistomina cretosa</i>	middle or late Albian (Williamson, 1987); Albian (Ascoli, 1990)		
			<i>Lenticulina gaultina</i>	middle or late Albian (Ascoli, 1990)		
			<i>Protocythere cf. speetonensis</i>	late Albian (Ascoli, 1990)		
		LATE APTIAN	<i>Orbitolina sp.</i>	Aptian (Williamson, 1987)	BEN NEVIS	
		APTIAN	No biostratigraphy available for this interval			AVALON
		LATE BARREMIAN- EARLY APTIAN	<i>Trocholina infragramulata</i>	Aptian (Ascoli, 1976 and 1990); late Barremian to early Aptian (Williamson, 1987)	EASTERN SHOALS	

(Barremian: Millioud, 1969; Williams, 1974; Bujak and Williams, 1978; late Barremian: Davey, 1979), *Mudergonia staurota* (Barremian: Millioud, 1969; late Barremian: Davey, 1974) from 1790 – 1820 m MD, and *Kleithriasphaeridium simplicispinum* (late Barremian: Davey and Williams, 1966; Sargeant, 1966; Davey 1974; late Aptian: Duxbury, 1978). Thus, the biostratigraphic studies of both these wells indicate that the Eastern Shoals Formation in the Terra Nova field is an upper Barremian to lower Aptian succession (La Borde and de Gasparis, 1984; Awai-Thorne et al, 1986).

The Avalon Formation occurs between 1713 and 1748 m MD in the Terra Nova K-07 well and between 1717 and 1774 m MD in the Terra Nova K-08 well (Table 1.2). No good biostratigraphic indicators were discussed in these intervals. However, because the sandstones in the Avalon Formation occur stratigraphically between the Eastern Shoals and Ben Nevis formations, it is postulated that the Avalon Formation is of early to middle Aptian in age.

The Ben Nevis Formation occurs between 1579 and 1713 m MD in the Terra Nova K-07 well and between 1582 and 1717 m MD in the Terra Nova K-08 well. The last occurrence of the arenaceous benthic foraminifera *Verneuillina cf. subfiliformis* in this interval (in the K-07 well) suggests an early to middle Albian age (Bartenstein and Bettenstaedt, 1962) or an early Albian age (Ascoli 1976, 1990). In the Terra Nova K-08 well, abundant microfossils include the foraminifera *Epistomina polypoides* (late Albian: Williamson, 1987), *E. carpenteri* (middle to late Albian: Williamson, 1987), *E. cretosa* (middle to late Albian: Williamson, 1987; Albian: Ascoli, 1990), *Lenticulina gaultina* (middle to late Albian: Ascoli, 1990) and the ostracod *Protocythere cf. speetonensis* (late

Albian: Ascoli, 1990). In contrast to the Albian ages given above, the highest occurrence of *Orbitolina sp.* at 1665 m MD suggests an Aptian age (Williamson, 1987).

Collectively, the occurrences of all the above microfossils indicate that the Ben Nevis Formation, including the Gambo Member, is of late Aptian to Albian age (La Borde and de Gasparis, 1984; Awai-Thorne et al., 1986).

CHAPTER TWO: DATA AND METHODS

2.1 Terra Nova 3-D Seismic Dataset

The 3-D seismic survey used in this study (Figure 2.1) was acquired during the summer of 1997 by PGS Exploration and consists of high quality, fully-migrated digital seismic reflection lines. These digital data have been provided by the Terra Nova consortium of companies (Petro-Canada, ExxonMobil Canada Properties, Husky Energy Operations Ltd., Norsk Hydro Canada Oil and Gas, Murphy Oil Company Ltd., Mosbacher Operating Ltd., and Chevron Canada Resources) for use on SGI (Silicon Graphics Incorporated) platforms equipped with *Landmark* workstation software at Memorial University of Newfoundland. In addition, the consortium provided an integrated digital well-log database and lithological and biostratigraphic data from offshore wells.

2.2 Seismic Data Acquisition

PGS Exploration shot the 1997 Terra Nova seismic survey in July 1997 for Petro-Canada and Husky Oil. The primary navigation system was DGPS STARFIX; the secondary, DGPS WADS. It was shot using a 3-D single vessel, with two sources and eight streamers.

The survey consists of 587 east-west-oriented shotlines and 1220 north-south-oriented traces and covers approximately 27 km x 14 km (380 km²). The survey was done with eight, 4050 m digital streamers, separated by 100 m, resulting in 41-fold data. Acquisition parameters are shown in Table 2.1.

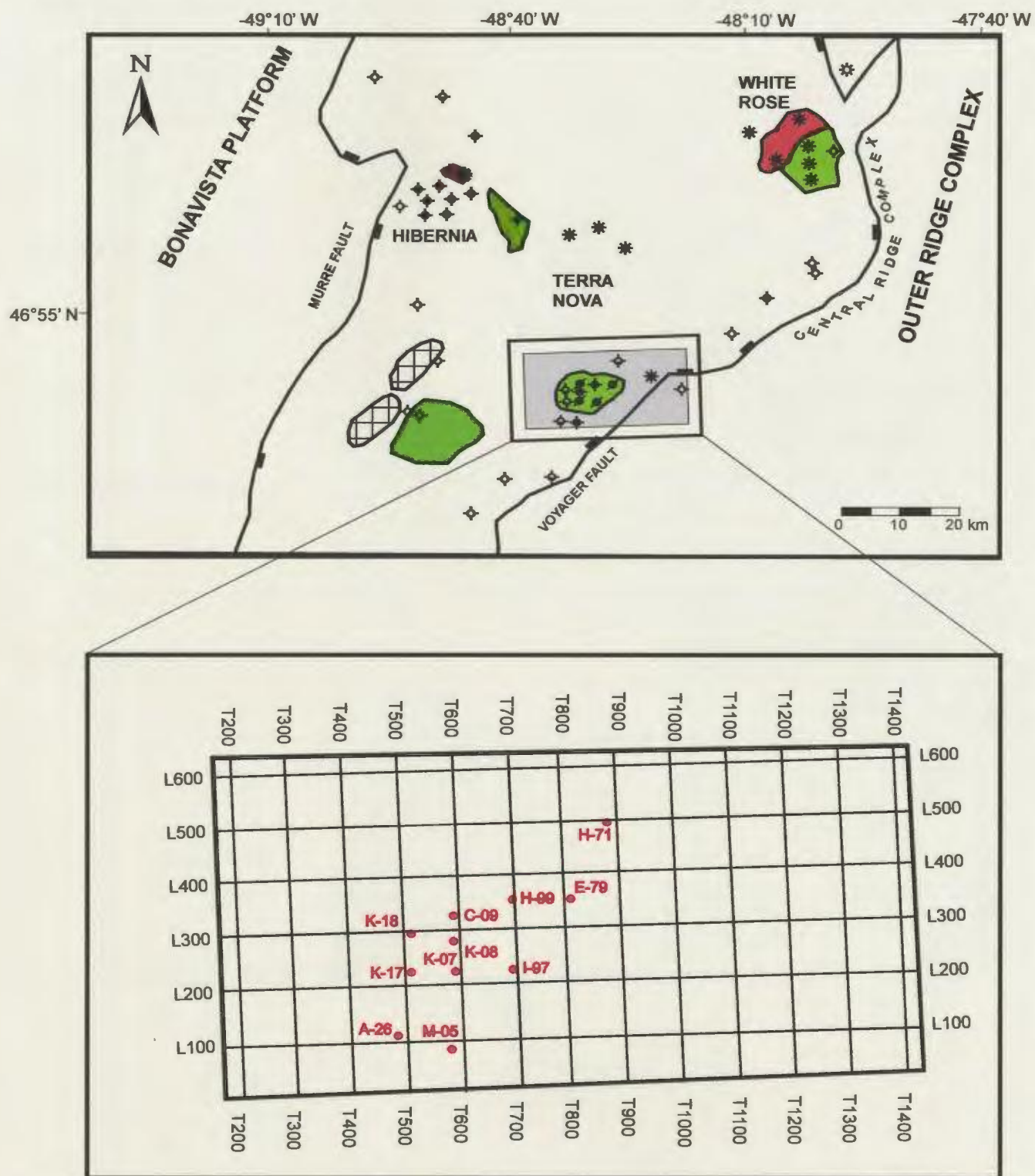


Figure 2.1 Seismic grid for the 1997 Terra Nova survey, southern Jeanne d'Arc Basin. The grey shaded area shows the region of readable seismic data.

Table 2.1 Instrumentation and Recording Parameters, 1997 Terra Nova 3-D Survey

Parameter		Value
Field Parameters	Shot By	PGS Exploration
	Shot For	Petro-Canada/Husky Oil
	Date Shot	April 1997
	Navigation System	Primary – DGPS STARFIX Secondary – DGPS WADS
	General Survey Details	3-D Single Vessel Two Sources Eight Streamers
Source Parameters	Energy Source	Airgun Array
	Number of Sources	2 – Alternate Shooting
	Source Separation	50 m
	Operating Pressure	$1.724 \times 10^7 \text{ N/m}^2$
	Volume of Array	50600 cm^3
	Source Depth	7.5 m
	SP Interval	25 m
Recording Parameters	Format	SEGD 8036 (3 BYTE)
	Filter	3(6) – 206(276) Hz (DBOCT)
	Sample Rate	2 ms
	Record Length	7 s
Streamer Parameters	Number of Streamers	8
	Streamer Interval	100 m
	Number of Groups	1296 (62 x 8)
	Group Interval	25 m
	SP-Near Group	270 m
	Cable Length	4050 m
	Cable Depth	8 m (± 1 m)
	Fold	41

2.3 Well Data

A complete digital well-log database, in addition to lithological and biostratigraphic data from offshore wells, was provided by the Terra Nova consortium of companies. Once the data was loaded onto workstations at Memorial University of Newfoundland, it was necessary to tie the wells to the 1997 seismic data, based on geological tops determined by the C-NOPB and by geoscientists at Petro-Canada. It was also necessary to generate synthetic seismograms for each well, which further enabled the lithological data to be tied to the seismic data. Well history reports provided description of cores, samples, and cuttings; drill stem test (DST) and reverse formation sampler (RFS) results; porosity and permeability data, and facies descriptions. Table 2.2 gives well header information for the Terra Nova wells used in this study, as well as information for other relevant wells in the study area. DST and RFS tests were performed on only two wells in the study area; Terra Nova K-17 and King's Cove A-26. The results of these tests are given in Table 2.3. Only the North Trinity H-71 well was cored in the study area, where it penetrated sandstones of the Ben Nevis Formation (Table 2.4). Sandstones of the Avalon and Eastern Shoals formations were not cored in any of the wells in and around the Terra Nova oil field.

2.4 Programs Used

2.4.1. *OpenWorks*TM

*OpenWorks*TM is a collection of software that provides a data and system-management framework for the integration of seismic, geological, and petrophysical

Table 2.2 Well header information for the Terra Nova and other relevant wells, southeastern Jeanne d'Arc Basin, Grand Banks. See Figure 1.8 for well locations. (C-NOPB, 2002 a and b)

Well Number	Type	Location (NAD83)	Datum (KB)	Total Depth	Year Drilled
Terra Nova Wells					
Terra Nova K-08	Discovery	46° 27' 31.28" N; 48° 30' 55.72" W	24.7 m	4499.8 m	1984
Terra Nova K-18	Delineation	46° 27' 43.73" N; 48° 32' 27.70" W	24.4 m	3925.6 m	1984
Terra Nova K-07	Delineation	46° 26' 43.25" N; 48° 30' 53.88" W	23.0 m	3550 m	1985
Terra Nova K-17	Exploratory	46° 26' 43.19" N; 48° 32' 27.79" W	24.0 m	3250 m	1985
Terra Nova I-97	Delineation	46° 26' 42.36" N; 48° 28' 45.55" W	23.3 m	3465 m	1986
Terra Nova H-99	Delineation	46° 28' 29.07" N; 48° 28' 46.12" W	23.6 m	1562 m <i>Re-Entry:</i> 3510 m	1987
Terra Nova C-09	Delineation	46° 28' 09.26" N; 48° 30' 54.91" W	24.1 m	3640 m	1988
Terra Nova E-79	Delineation	46° 28' 28.56" N; 48° 26' 44.40" W	24.0 m	2622 m <i>Re-Entry:</i> 3605 m	1988
Other Relevant Wells					
North Trinity H-71	Delineation	46° 30' 23.35" N; 48° 25' 31.62" W	23.2 m	4758 m	1985
Beothuk M-05	Exploratory	46° 24' 48.23" N; 48° 31' 10.17" W	23.8 m	3779 m	1985
King's Cove A-26	Exploratory	46° 25' 08.64" N; 48° 33' 01.98" W	23.8 m	3092 m	1990

Table 2.3 Drill Stem Test (DST) and Repeat Formation Sample (RFS) results in the Ben Nevis Formation for the Terra Nova K-17 and King's Cove A-26 wells, Terra Nova field area (see Figure 1.8 for well locations). (C-NOPB, 2002 a and b). NPTS = No flow to surface.

Well Number	RFS/DST #	Depth (m)	Formation	Results
Terra Nova K-17	RFS #1	1548.5	Ben Nevis	Recovered 0.009 m ³ gas, trace heavy oil (14.2° API) and 9.8 litres mud filtrate
	DST #1	1542.9 1562.1	Ben Nevis	Misrun
	DST #2	1542.9 1562.4	Ben Nevis	NPTS; Reverse circulated cushion, mud and formation fluid (90% max. oil, 14.6° API and water, 7500 ppm Cl ⁻)
King's Cove A-26	RFS #1	1528.7	Ben Nevis	Recovered 0.08 litres water (16500 ppm Cl ⁻)
	RFS #2	1557.4	Ben Nevis	Recovered 0.5 litres water (7500 ppm Cl ⁻)
	RFS #3	1559.0	Ben Nevis	Recovered 0.1 litres oil (12.1° API) and 12.1 litres mud filtrate
	DST #2	1540.0 - 1550.0 1555.0 1560.0	Ben Nevis	Misrun
	DST #3	1540.0 - 1550.0; 1555.0 - 1560.0	Ben Nevis	Oil @7.51 m ³ /d initially (13.3 - 18° API) with high water cut using downhole pump. Oil declined to a trace after 3 hours. Water (33000 ppm Cl ⁻) no rates available. Choke 12.7 mm.

Table 2.4 Cored intervals within the Ben Nevis Formation in the North Trinity H-71 well, adjacent to the Terra Nova oil field, Jeanne d'Arc Basin (see Figure 1.8 for well location). (C-NOPB, 2002 a and b). These cores are described in detail in Section 3.3.3.

Well Number	Core #	Depth (m)	Formation	Recovery (%)
North Trinity H-71	1	1997.0 - 2015.3	Ben Nevis Formation	100
North Trinity H-71	2	2015.3 - 2033.6	Ben Nevis Formation	100
North Trinity H-71	3	2033.6 - 2051.9	Ben Nevis Formation	100
North Trinity H-71	4	2088.2 - 2098.4	Ben Nevis Formation	84
North Trinity H-71	5	2164.7 - 2168.9	Ben Nevis Formation	74

applications and their data. It incorporates a comprehensive suite of geoscience applications, including 3-D and 2-D seismic interpretation, well-log analysis, geologic interpretation, mapping, and data management. These applications operate together in an integrated environment, which means one can run several applications concurrently and share data between them.

2.4.2 *SeisWorks/3DTM*

SeisWorks/3DTM is a comprehensive software package for 3-D seismic interpretation and analysis. It displays 3-D seismic data, interprets faults and horizons, and generates and annotates maps and contours. It also supports seismic interpretation in either time or depth. Data in *SeisWorks/3DTM* are stored in the *OpenWorksTM* database, so information can be interpreted and exported for use with other software packages.

2.4.3 *StratWorks*TM

*StratWorks*TM is a 2D geological interpretation package for well-log correlation, cross-section construction, surface and fault modeling, and map generation. Built upon the *OpenWorks*TM project data-management system, it allows close integration with other geological and geophysical software. For example, through integration with *SeisWorks*TM, ties between depth and seismic-time can be easily performed. *StratWorks*TM also permits geological interpretation in a production or exploration environment using the most commonly available well types and data.

2.4.4 *SynTool*TM

*SynTool*TM is an integrated interpretation tool that allows seismic data to be accurately tied with well depths, formation tops, and lithologies. It allows the creation of accurate synthetic seismograms, while its detailed log editing and processing capabilities aid in correcting for log-recording problems (e.g. tool sticking) and hole problems. Using *SynTool*TM, seismic wavelets can be calculated, displayed, and used to derive synthetics.

Ideally, sonic and density logs are used to generate synthetic seismograms. The standard sonic log is corrected using data from a vertical seismic profile (VSP) check-shot survey and the interval velocities are calculated. From this, acoustic impedance is determined. The bulk density log is then used in conjunction with the interval velocity data to calculate reflection coefficients. However, where density logs are not available or are of poor quality, the Gardner Equation (Gardner et al., 1974; Sheriff, 1991) can be used in conjunction with the sonic log to generate the synthetic seismogram. Finally, the reflection coefficients are convolved with a digital filter and displayed on the section.

2.5 Methodology

2.5.1 Horizon mapping

Preliminary horizon mapping was carried out with workstation software by using pull-down menu methods such as *interpolation*, *autotracking*, and *zapping* to track key seismic reflections. Based on the velocity survey for each well, lithostratigraphic horizons as interpreted in well logs were converted to two-way travel time and matched with (or “tied” to) their corresponding reflections on seismic profiles. Once the lithostratigraphic horizons were tied to the seismic data, the reflections were traced away from the reference well. ZAP!TM is an automatic horizon-tracking package within the *Landmark* environment that allows highly accurate interpretations in areas of complex geology (such as highly-faulted areas) or low data quality. Even though *interpolation* allows the generation of quick, generalized maps, ZAP!TM is a preferred method since it takes seismic amplitude into account in the interpretations.

Subsequently, the key horizons were tracked on intersecting traces, using *tie-ticks* as guides. The auto-picked horizons were re-examined and difficult areas were resolved through further manual interpretation. The initial interpretations were also refined by using *correlation polygons*, analyzing *horizon slices*, creating *time slices*, and displaying *arbitrary lines*. *Loop displays* were also helpful in horizon interpretation as a sequence of lines and traces could be selected to intersect the loop and improve the initial interpretation. Where faults were encountered, the horizon was not interpreted across them, as a gap in the horizon is essential in creating a *fault polygon basemap*. While a blue and white colour display was judged best for stratigraphic interpretations on seismic

profiles, a black and white display was preferred for structural analysis.

2.5.2 Fault mapping

Fault mapping was accomplished during and after horizon mapping, following an initial reconnaissance of the 3-D survey volume to determine general fault trends. Faults were picked on a network of lines, working in the direction of the dip of the fault. Correlation of faults was constantly verified in map and perspective views within SeisWorksTM, enabling the insertion of fault planes into the OpenWorksTM database. The fault planes were then triangulated so that faults could be projected and seen on uninterpreted lines and displayed in perspective view. Gaps in the horizon maps (described above) are essential in creating and correlating fault segments and ultimately in generating fault polygon maps.

2.5.3 Map generation

Mapping methods based on key horizons allow rapid assessment of large seismic surveys. Examples of maps created from selected horizons in the study area include time-structure, amplitude, and continuity. Other examples of subsurface mapping used in this study include isochron and isopach mapping, which allow determination of thickening and thinning patterns within stratigraphic units.

2.5.4 Seismic sequence stratigraphy

Seismic stratigraphy is the “geological approach to the stratigraphic interpretation of seismic data” (Vail and Mitchum, 1977). It involves the recognition, mapping and study of regional and global sedimentary sequences and their bounding unconformities in

seismic data. The origin of seismic sequences is most commonly ascribed to relative sea-level fluctuations.

The first step in seismic stratigraphic studies is to divide the seismic data into distinct stratigraphic packages or depositional units that correspond to seismic sequences and systems tracts. The bounding unconformities are identified on the basis of reflection termination patterns and their continuity (Figure 2.2).

Below an unconformity, *toplap* is the termination of strata against an overlying surface, representing depositional bypass and/or minor erosion; *truncation* implies the deposition of strata and their subsequent tilting and removal along an unconformity surface. Above a discontinuity, *onlap* is a base-discordant relationship in which initially horizontal strata progressively terminate against an initially inclined surface, or in which initially inclined strata terminate progressively updip against a surface of greater initial inclination; *downlap* is a relationship in which seismic reflections of inclined strata terminate downdip against a more gently inclined or horizontal surface. If onlap cannot be distinguished from downlap because of subsequent deformation, the term *baselap* is used.

Sequence stratigraphy is a subdiscipline of stratigraphy where sedimentary basin fills are subdivided into genetic packages bounded by unconformities and their correlative unconformities (Emery and Myers, 1996). The sequence stratigraphy proposed by Vail and Mitchum (e.g. 1977) and Van Wagoner et al. (e.g. 1988) divides strata into genetically-related deposits based on sea-level changes and analyzes strata in a chronostratigraphic framework.

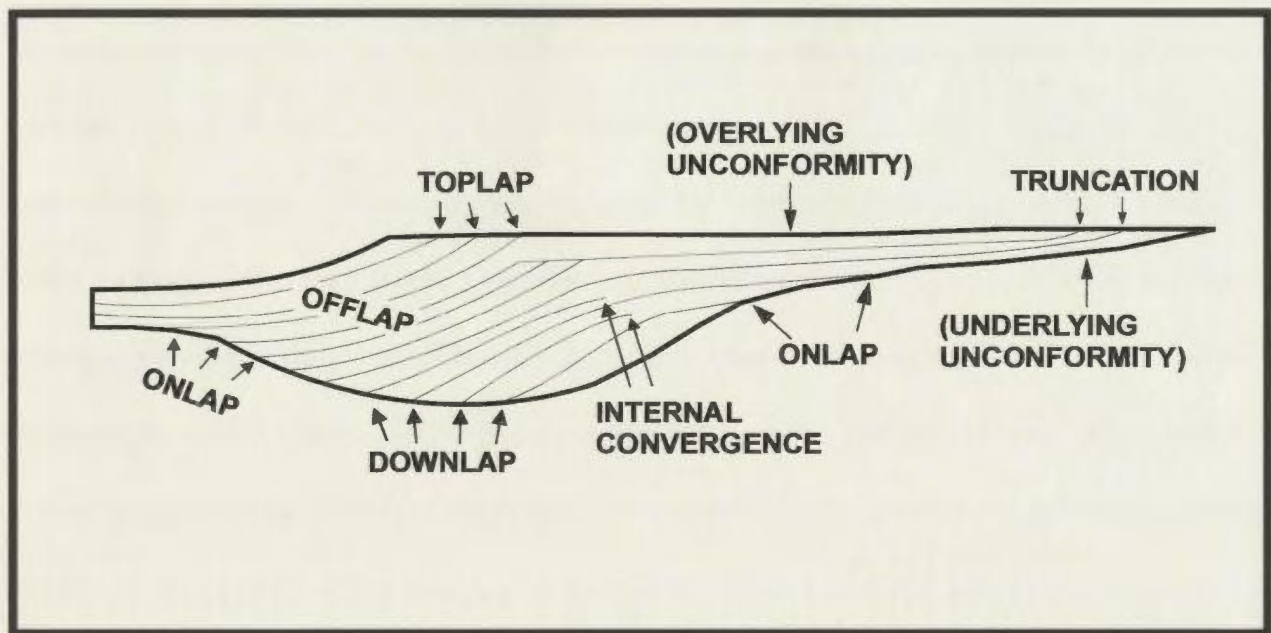


Figure 2.2 Seismic stratigraphic reflection terminations within idealized seismic sequence (after Mitchum et al., 1977)

Sediment supply and the rate of creation of accommodation space are two important factors governing the stratigraphic geometry. Different geometric arrangements of strata form the basis for the division of a basin-fill succession. A fundamental unit of sequence stratigraphy is the *depositional sequence*, a stratigraphic unit deposited during a particular period in the basin history that is bounded at its top and bottom by unconformities or their correlative conformities (Mitchum, 1977). It represents a period of deposition between two episodes of significant relative sea-level fall. In a sequence stratigraphic framework, the surface created by sea-level fall is called a *sequence boundary*. It is an unconformity in the landward direction and its correlative conformity on the outer shelf or in the adjacent deep basin where there was no erosion (Van Wagoner et al., 1988). Depending on the position of the lowstand shoreline relative to the shelf edge (or offlap break), it is possible to differentiate between type 1 and type 2 sequence boundaries (Van Wagoner et al., 1988). Type 1 boundaries form when sea level falls below the shelf edge whereas type 2 boundaries are associated with a down-dip shoreline shift to some immediate point on the shelf.

Between events of relative sea-level fall that create the sequence boundaries, there are generally periods of relative sea-level rise. The sediments deposited during these periods will show patterns of transgression, aggradation, and progradation which reflect the changes in sea level. Different *systems tracts* can be recognized by the stratal patterns that can subsequently be related to stages in the cycle of sea-level rise and fall (Posamentier et al., 1988; Van Wagoner et al., 1988). Systems tracts are defined by the stacking patterns of *parasequence sets* and *parasequences*, which are relatively

conformable successions of genetically related beds or bedsets bounded by marine flooding surfaces, separating younger from older strata, across which there is evidence of an abrupt increase in water depth (Van Wagoner et al., 1988).

The *transgressive systems tract* (TST) is formed during the most rapid rise in sea level or when sediment supply is reduced during a time of constant sea-level rise. It is characterized by a general landward shift in facies belts (that is, shallow water facies overlain by deeper-water deposits). It is the middle systems tract of both type 1 and type 2 sequences and can also be referred to as a retrogradational parasequence set (Van Wagoner et al., 1988). The base of the transgressive systems tract is the *transgressive surface* at the top of the lowstand or shelf-margin systems tract, which marks the end of lowstand progradation and the onset of transgression. It is the first marine flooding surface across the shelf within a sequence (Van Wagoner et al., 1988). Parasequences within the TST onlap the sequence boundary in a landward direction and downlap the transgressive surface in a basinward direction. The rate of creation of accommodation space will be greater than the sediment influx, resulting in, for example, outer-shelf deep-water mudstone overlying inner-shelf shallow-marine sandstones.

The surface formed by subaerial erosion may be modified as sea level rises during transgression, being reworked by wave action on the beach and shoreface as the land is flooded. Such surfaces of marine reworking and erosion that form during transgression are called *ravinement surfaces* (Swift, 1975). This type of surface was first recognized by Stamp (1921). Reworking at the ravinement surface produces a transgressive sand sheet (Swift et al., 1971) consisting of *palimpsest* sediments, so named because their

texture is inherited from the initial depositional environment. The ravinement surface thus acts like a facies belt (Myers and Milton, 1996), moving shoreward with other coastal facies during transgression. It is therefore a diachronous surface. The ravinement surface forms a striking surface in logs, cores, and outcrops.

The top of the transgressive systems tract is the *downlap surface*, a marine-flooding surface onto which the toes of the prograding clinoforms in the overlying highstand systems tract downlap (Van Wagoner et al., 1988). It is termed the *surface of maximum flooding* and distinguishes the retrogradational sets below from the overlying aggradational to progradational parasequence set(s).

CHAPTER THREE: RESULTS

This chapter delineates the seismic stratigraphy and structural architecture of the lower Cretaceous succession in the Terra Nova oil field. Firstly, the seismic markers that were mapped over the study area are described, including the reflection character and areal distribution of the seismic events. Secondly, the depositional units are defined and their boundaries are described. Integration of formation lithologies with available well data provided ground truth for seismic facies and attributes. Thirdly, the interpretative steps carried out on the seismic data, including seismic amplitude studies and synthetic seismogram generation, are reviewed. Finally, the structural styles in the Terra Nova field area are presented and linked with (a) the stratigraphy in the field area, and (b) associated fault systems.

The seismic sections presented in this thesis consist of east-west-oriented shotlines and north-south-oriented traces (Figure 3.1). Most of the seismic sections illustrated in Figure 3.1 follow a straight line; the sections that do not follow a straight line are termed *arbitrary lines*, since they do not follow a particular east-west or north-south direction.

3.1 Seismic Markers

Eleven wells provide control points over the survey area for the interpretation of the lower Cretaceous reflectors (Figure 3.1). Formation tops and unconformities are largely based on picks provided by C-NOPB in the Schedule of Wells (2002a) and by McAlpine (1990). The ties between well synthetics and seismic data are satisfactory to

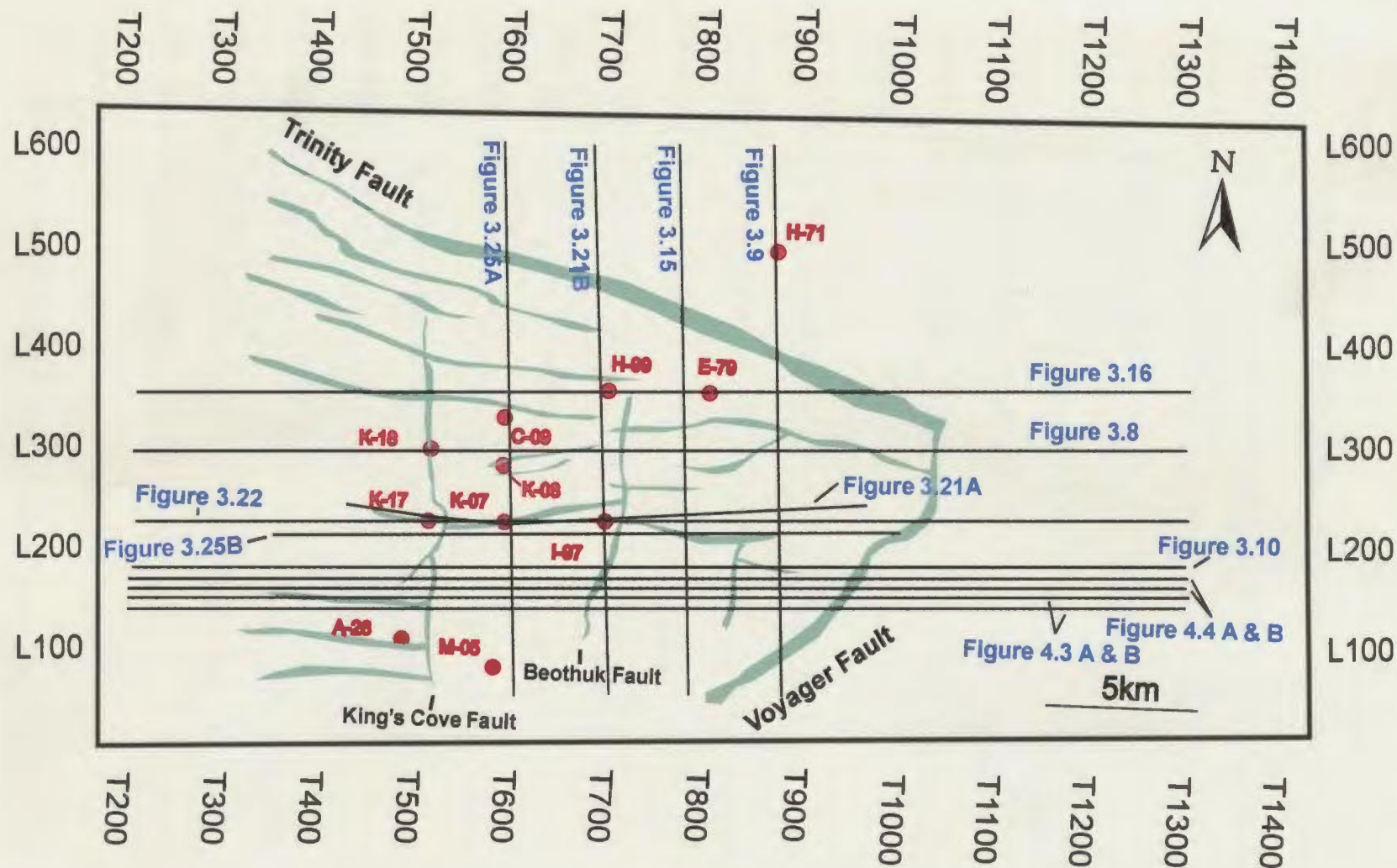


Figure 3.1 Location of the seismic lines used in Figures 3.8, 3.9, 3.10, 3.15, 3.16, 3.21, 3.22, 3.25, 4.3, and 4.4 in the Terra Nova oil field area. The faults shown are from the Avalon horizon structure map. See Figure 1.8 for the names of the smaller faults not labeled on this map.

excellent.

Seven prominent seismic markers (Figure 3.2) were correlated and mapped over the entire survey area: base Tertiary unconformity, Petrel Limestone Member, top Ben Nevis Formation, top Gambo Member, top Avalon Formation, top Eastern Shoals Formation, and top B-Marker limestone.

The base Tertiary marker is a high amplitude peak that is generally present and continuous throughout the entire basin. It forms a strong, coherent reflection caused by a positive impedance contrast. It is defined as the maximum value of a peak on a seismic display.

The Petrel Limestone Member marker is characterized by a positive impedance contrast, causing the corresponding seismic event to be coherent and high in amplitude. Near the centre of the field, the Petrel marker is a “doublet” that varies in amplitude. Amplitude variation is expected because the marker is an unconformity with different rocks juxtaposed in different places.

The event that defined the top of the Ben Nevis Formation is generally a low amplitude reflection over most of the study area, but has high amplitude in the Terra Nova Anticline area (Figure 1.9). It is characterized by a negative impedance contrast and is defined as the minimum value of a peak on a seismic display. It is often difficult to recognize the event marking the top of the Ben Nevis Formation because of imaging problems associated with a highly structured area, and facies variations within the Ben Nevis Formation.

The event marking the top of the Gambo Member is a moderately strong

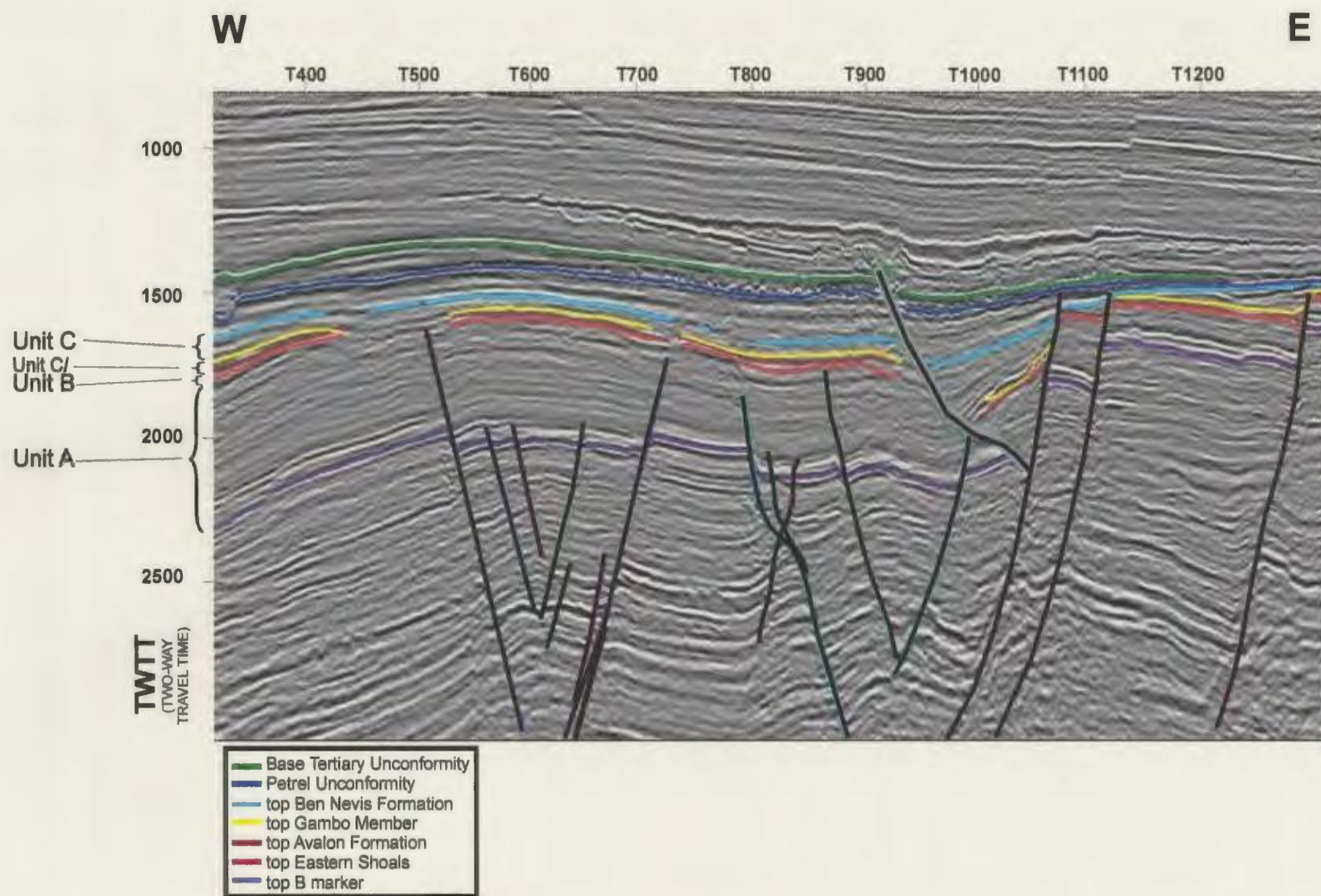


Figure 3.2 Interpreted seismic section showing the seven events mapped in the Terra Nova field area. The four seismic packages, Units A, B, C, and *Ci*, that are delineated in the study area are defined by their relationship to these markers, as described in Section 3.3.

reflection over most of the Terra Nova field area and is caused by a positive impedance contrast. It is defined as the maximum value of a peak on a seismic display.

The event marking the top of the Avalon Formation is generally a high amplitude reflection over most of the field area, but its amplitude is low in a few regions. It is characterized by a negative impedance contrast, resulting in a corresponding coherent seismic event, and is defined as the minimum value of a peak on a seismic display. The reflection consists of a “doublet” near the centre of the field.

The event marking the top of the Eastern Shoals Formation is commonly referred to as the “A-seismic marker”. It is seen on a seismic section as a prominent and widely correlatable reflection that results from a coherent and strong reflection associated with a positive impedance contrast. It is defined as the maximum value of a peak on a seismic display.

The top B-Marker event is a high amplitude, coherent reflection caused by a negative impedance contrast. On a seismic display, it is defined as the minimum value of a peak.

3.2 Data Analysis

Seismic attribute studies are used in an attempt to predict the rock properties away from existing well control. There are several seismic attributes representing numerical measures of various characteristics of the seismic data (Figure 3.3; Hart, 1999).

Amplitude attributes show how reflection amplitude and acoustic impedance differ within the 3-D seismic dataset, because of variations in such characteristics as lithology,

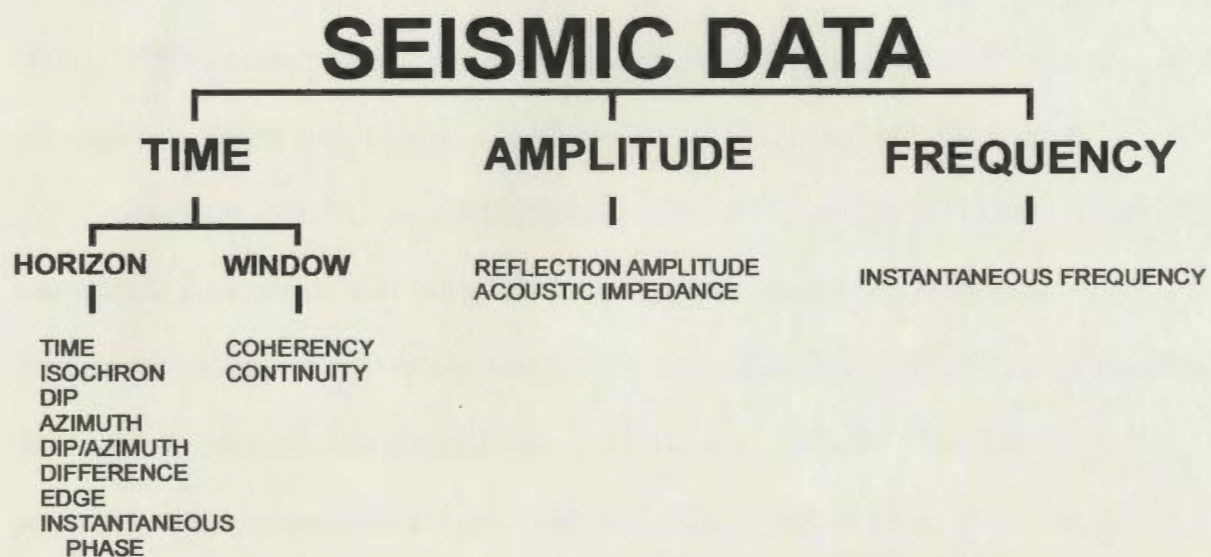


Figure 3.3 Attribute classification based on post-stack seismic data (modified after Brown, 1996; and Hart, 1999)

porosity, and bed thickness. Time-derived attributes that can be mapped comprise time structure, isochron, *difference*, *edge*, *dip*, *azimuth*, combined *dip/azimuth*, coherency, and continuity (items in italics are workstation terms for maps which can be generated within *Landmark*). Coherency and similar attributes relate individual traces to their neighbours (Hart, 1999). Instantaneous phase (time attribute) and instantaneous frequency (frequency attribute) are complex attributes that will not be used in this thesis.

According to Brown (1996), time-derived attributes give structural information and amplitude-derived attributes offer stratigraphic and reservoir information. Frequency-derived attributes are not yet well understood but it is anticipated that they will provide additional useful reservoir information. Attribute studies can be used to analyze horizon anomalies and other subtle features. Specifically, attributes such as *azimuth*, *edge*, *dip*, and *difference* can be used to reveal fault trends, lineations, and mispicks (a point not properly interpreted along a seismic reflection which causes a break in the inferred marker).

In addition to seismic attribute studies, horizons and time slices were analysed in order to better understand the geological and structural framework of the field area. Synthetic seismograms were generated for each of the wells in the study area and integrated with the seismic data to refine interpretations. Finally, biostratigraphy was reviewed to constrain the ages of the various depositional and structural events.

Time structure maps show the elevation of a particular horizon in TWT (two-way travel) time. Dip maps are coloured according to dip magnitude. Software calculates the dip in each bin and produces a map that can be used to determine structural framework in

the area. It shows exact changes in dip direction, true dip, and accounts for apparent dip direction in both the line and trace directions. It is very effective for detecting faults.

The azimuth map is closely related to the dip map. Azimuth maps are coloured according to the direction in which the events are dipping. They also show exact changes in true dip direction from 0 to 360 degrees. Software calculates the dip direction for each bin, producing a map that can be used to refine the structural understanding in the study area. Structures such as anticlines, synclines, rollovers, and graben are illuminated by changing the colour of an azimuth map using 'circular adjust' (a feature of the colour bar). This produces results similar to changing the illumination angle (sun angle) on a topographic map.

A combined dip/azimuth map is used to overcome the problem of the difference in detectability between one display and another (Hart, 1999). Often, features appear on one map that are omitted or not illuminated on the other. As a remedy, both dip and azimuth maps can be displayed in combination. The hue of the colour on a dip/azimuth map indicates the azimuth (i.e. north, south, east, or west), whereas the colour intensity indicates the dip angle. The pale colours represent shallow dips and the darker colours represent steep dips.

Difference maps show the difference in two-way travel (TWT) time between two adjacent traces in either the line or trace direction. It is similar to an isochron map, except that it deals with only one horizon, not two. The points on a difference map represent the differences in time between adjacent samples along a single horizon. Difference maps can detect small faults only a few traces wide, and can highlight

very subtle lineations and faults.

Edge detection highlights discontinuities in a mapped horizon. It detects differences in dip across a horizon and uses a different algorithm than that used in calculating a dip map, thus producing a map with different features than a dip map. Edge maps exaggerate sharp dip changes such as faults, steep horizon dips, or reef edges.

The combined study of amplitude and other seismic attributes results in a detailed structural and stratigraphic reconnaissance of the field. Amplitude is the strength or “loudness” of a seismic signal. The amplitude of a reflection is proportional to the reflection coefficient, although the character of the seismic wavelet and tuning phenomena often affect this relationship (Hart, 1999). Reflection coefficients can be negative or positive; thus, there exist both negative and positive amplitudes.

3.3 Description of Seismic Packages

On the basis of the seismic stratigraphy principle of Vail and Mitchum (1977), three seismic packages were delineated in the study area: Units A, B, and C (Figure 3.2). By studying unit thicknesses (Table 1.2), documenting the internal and bounding reflection patterns, and integrating the biostratigraphy and lithostratigraphy of the successions, it is possible to decipher the stratigraphic and structural evolution of the Lower Cretaceous sequence in the Terra Nova field area. Collectively, Units A, B, and C consist of a succession of sedimentary rocks which rests mostly conformably on the B-Marker limestone and is unconformably sealed at the top by shales overlying the Albian unconformity. Although the Ben Nevis and Avalon Formations generally form a

common reservoir in the Jeanne d'Arc Basin, each formation occurs within a separate sedimentary sequence.

3.3.1 Unit A

Unit A is the lowermost package within the lower Cretaceous sedimentary succession in the Terra Nova field area. Seismically, it consists of a moderately reflective package in which the reflectors have significant lateral continuity. The package is bounded at its base by the B-Marker limestone. The seismic top of Unit A is the coherent, strong, widely correlatable reflection at the top of the Eastern Shoals Formation (A-seismic marker, not to be confused with the A-Marker limestone, used by some authors, which is at a stratigraphically lower position in the section). Thus, Unit A encompasses the Eastern Shoals Formation, the White Rose Formation (including the B-Marker Member), and the Catalina Formation.

A time-structure map of the top of the Eastern Shoals Formation is presented in Figure 3.4. Notice that the horizon dips to the north and that the Terra Nova Anticline is clearly defined. An azimuth map for the same horizon is provided in Figure 3.5. Here, the structure of the marker defining the top of the Eastern Shoals Formation is clearly shown, and again, the Terra Nova Anticline is highlighted near the centre of the field. The strong, coherent character of the marker defining the top of the Eastern Shoals Formation is illustrated in the amplitude map in Figure 3.6.

The Eastern Shoals Formation is defined here as a unit of mainly sandstone and sandy limestone which overlies the shales of the White Rose Formation. In the study

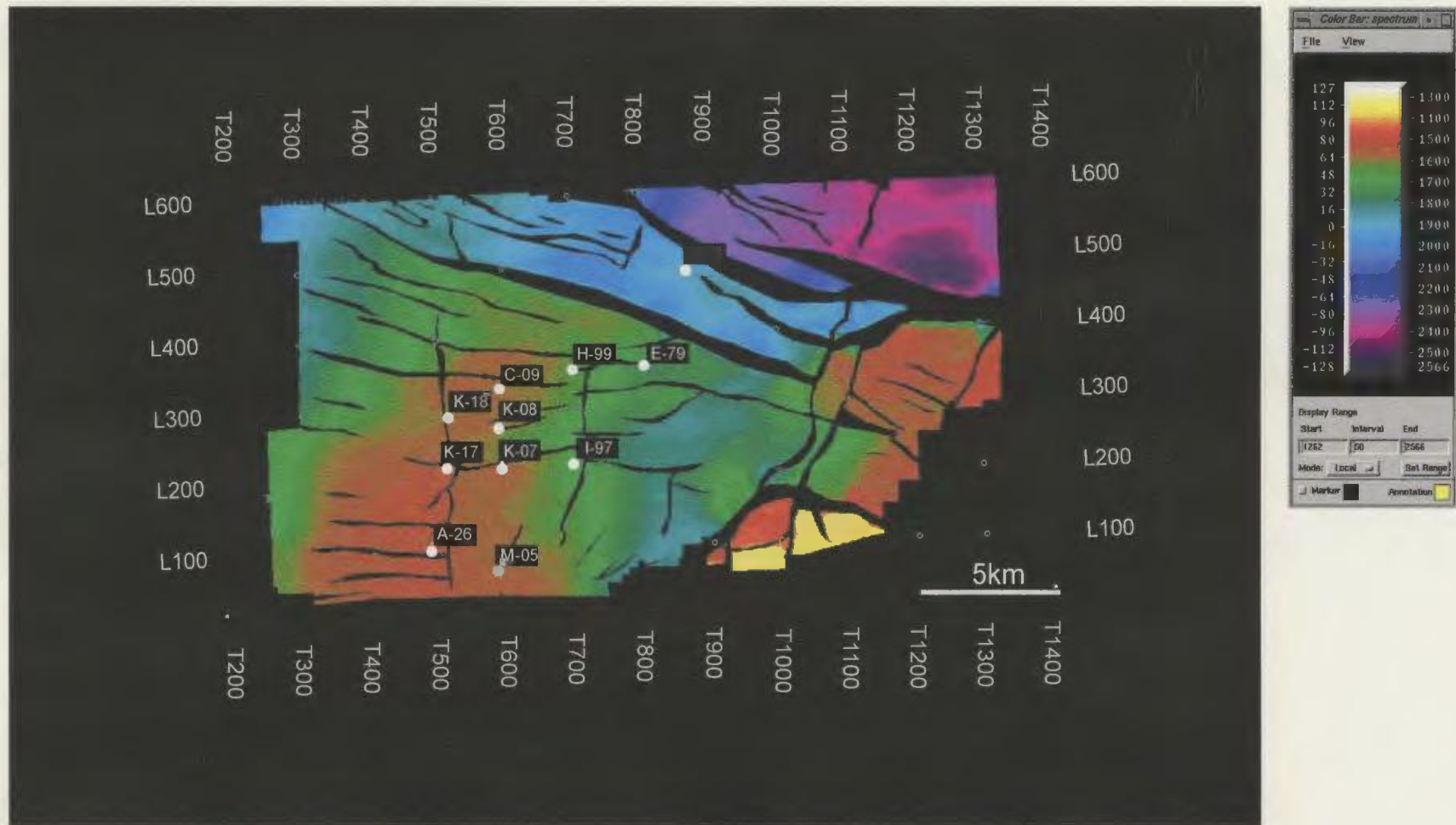


Figure 3.4 Time-structure map of the event defining the top of the Eastern Shoals Formation, Terra Nova oil field

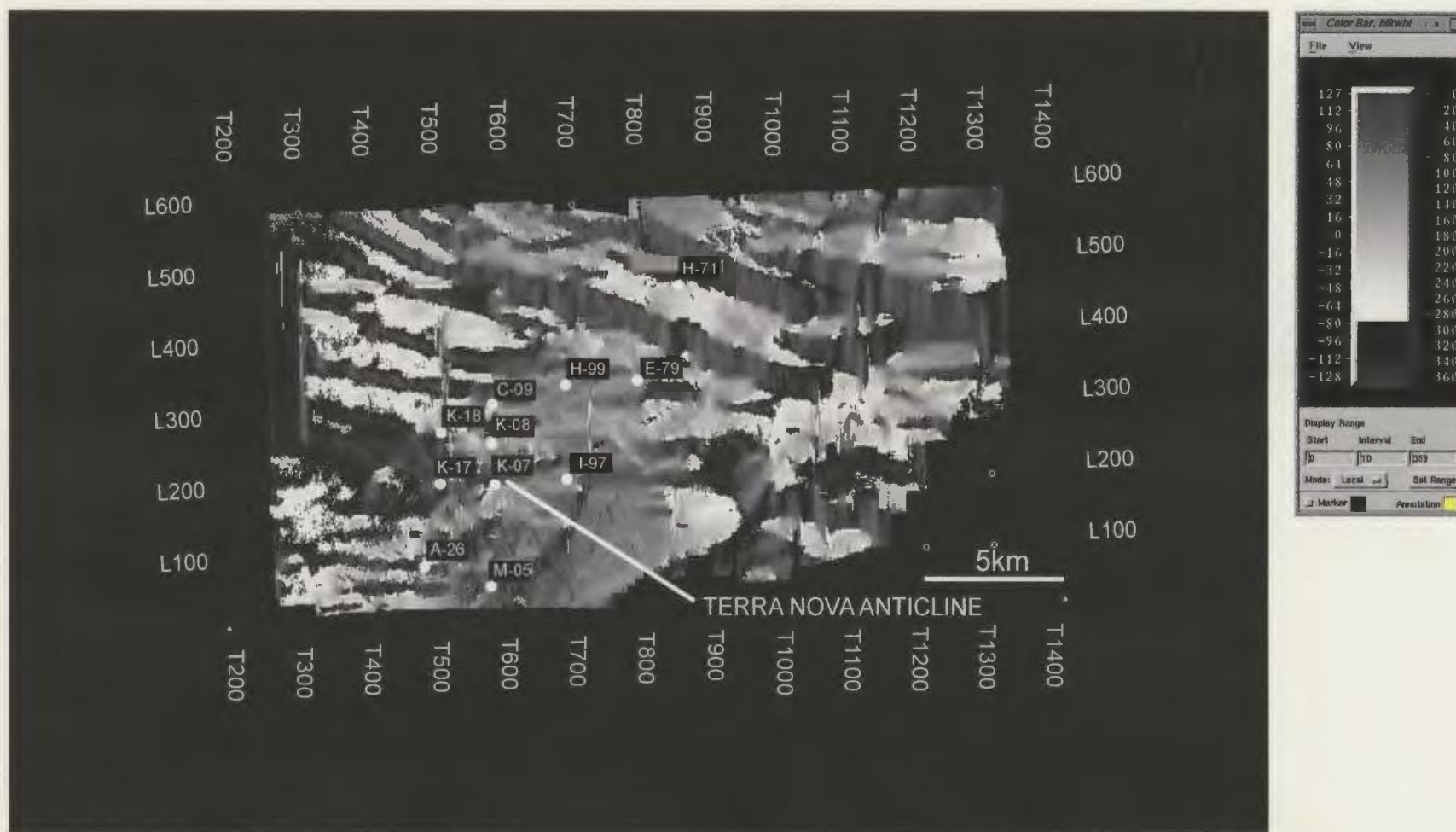


Figure 3.5 Azimuth map for the event defining the top of the Eastern Shoals Formation, Terra Nova oil field. The Terra Nova Anticline is located towards the centre of the field.

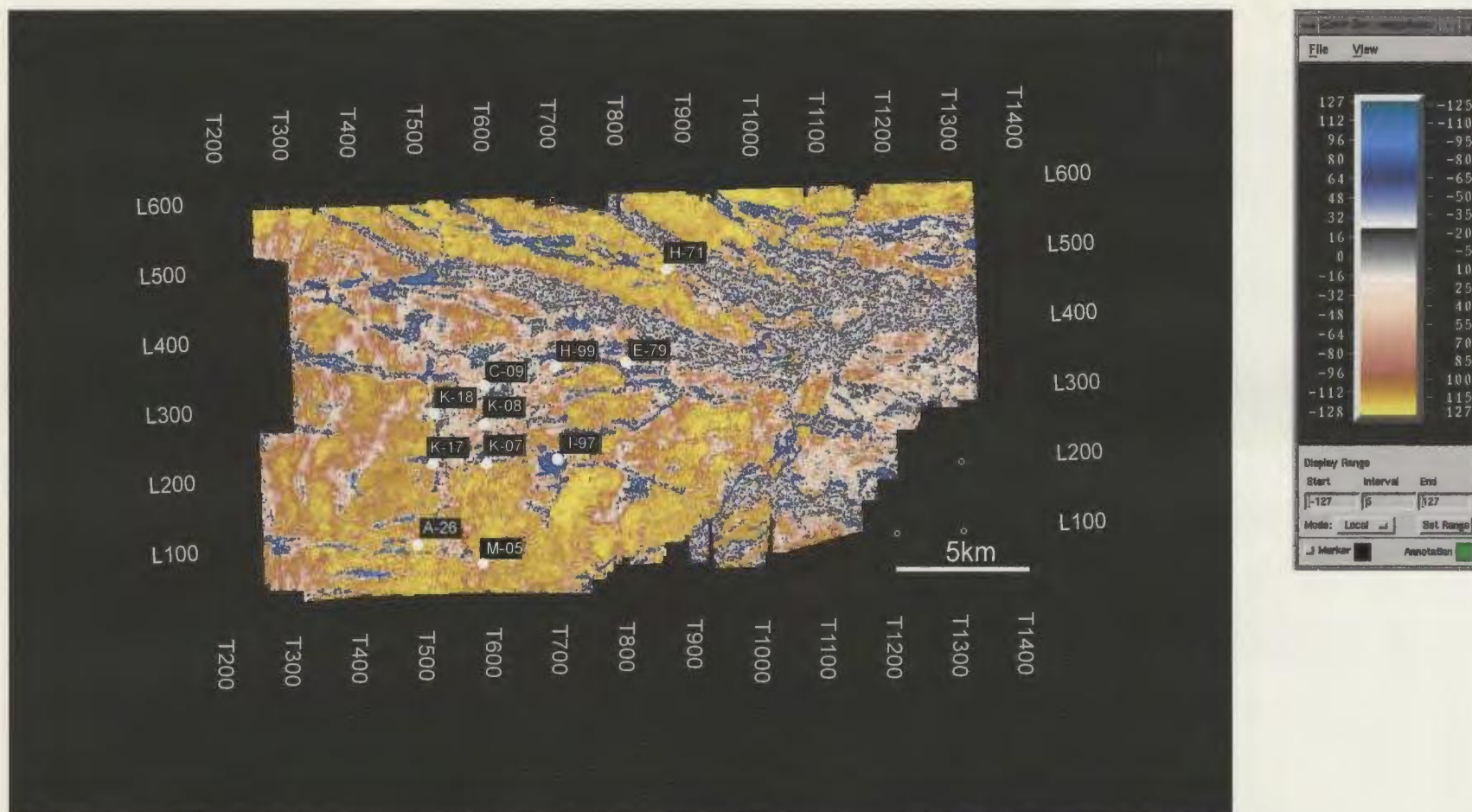


Figure 3.6 Amplitude map of the event defining the top of the Eastern Shoals Formation, Terra Nova field area. As is indicated by the color bar, this marker is a strong reflector over most of the field area and is characterized by a positive impedance contrast, resulting in a positive peak on a seismic section. Areas of low amplitude are indicative of faulting at the Eastern Shoals level.

area, the thickness of this formation ranges from 17 – 130 m with an average thickness of 97 m. Terra Nova K-17 penetrated an anomalous thickness of only 17 m. Two major lithofacies exist within the Eastern Shoals Formation: a massive calcareous sandstone and chalky/oolitic limestone sequence and a thick sequence of interbedded calcareous sandstone and argillaceous siltstone. In most of the Terra Nova wells the top of the Eastern Shoals Formation is picked where there is a noticeable increase in the gamma-ray response (Figure 3.7). This upper contact with the Avalon Formation is sharp and unconformable to disconformable, and is clearly marked on gamma-ray and sonic logs by breaks and lithological changes.

The thickness of Unit A does not vary significantly over the Terra Nova Anticline (Figure 3.8). However, there is a noticeable thickening of the unit northward across the Trinity Fault (Figure 3.9). Thinning and progressive angular subcrop of seismic reflections (Figure 3.10) is evident in the uppermost portions of Unit A (i.e. near the top of the marker which defines the top of the Eastern Shoals Formation). This truncation confirms that the A-seismic marker is an unconformity (known herein as the Barremian unconformity).

3.3.2 Unit B

Seismically, Unit B consists of moderately strong acoustic reflections that display good to very good lateral continuity (Figure 3.2). The package is bounded at its base by the event defining the top of the Eastern Shoals Formation (Figure 3.2), and at its top by a generally high amplitude, coherent reflection, known as the mid-Aptian unconformity

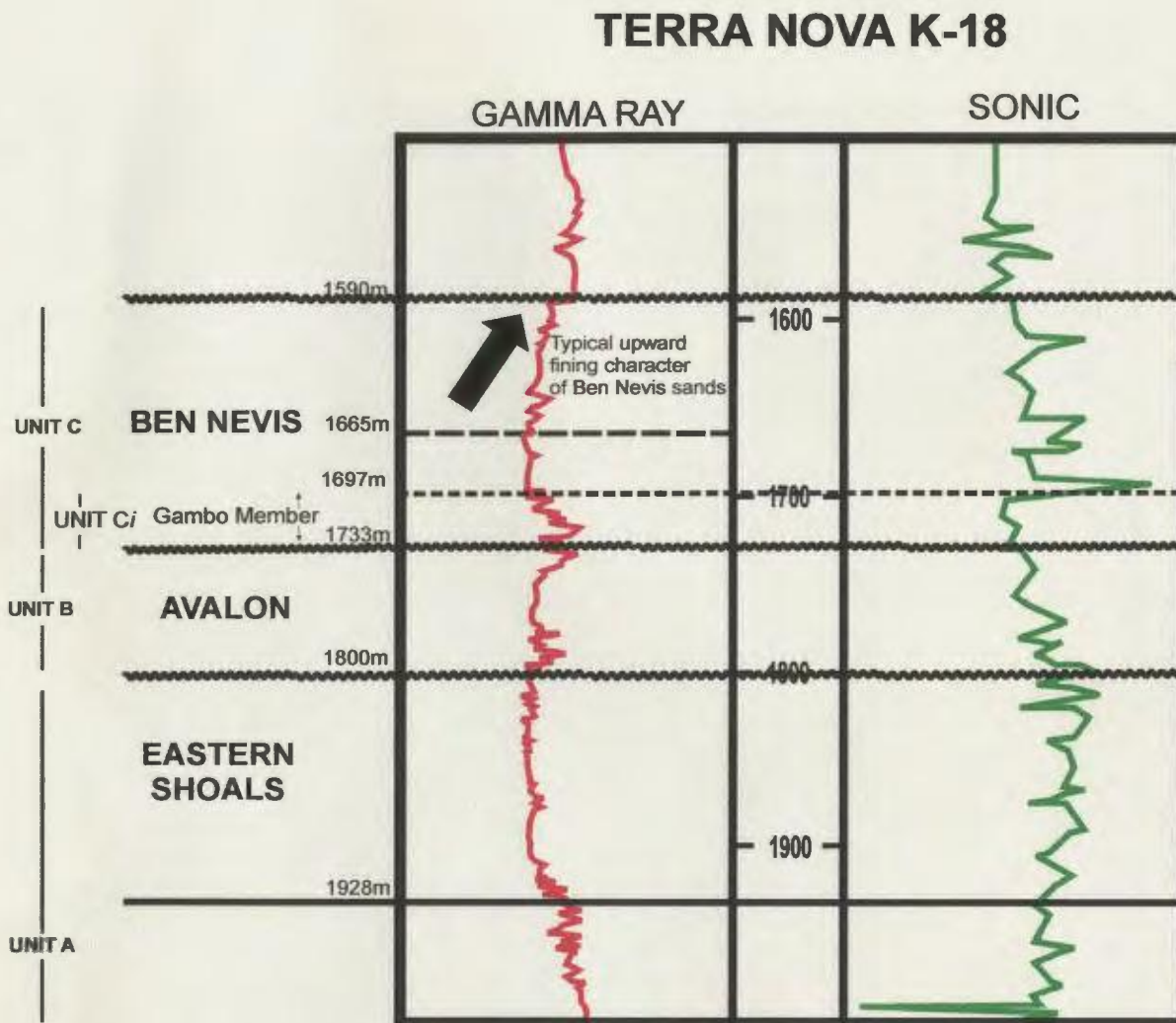


Figure 3.7 Gamma-ray/sonic log of the Terra Nova K-18 well. This well shows a typical upward fining section of the Ben Nevis Formation and typical log signatures of the contacts of members and formations. The mid-Aptian Unconformity is at the base of the Gambo Member of the Ben Nevis Formation. See Figure 1.8 for well location.

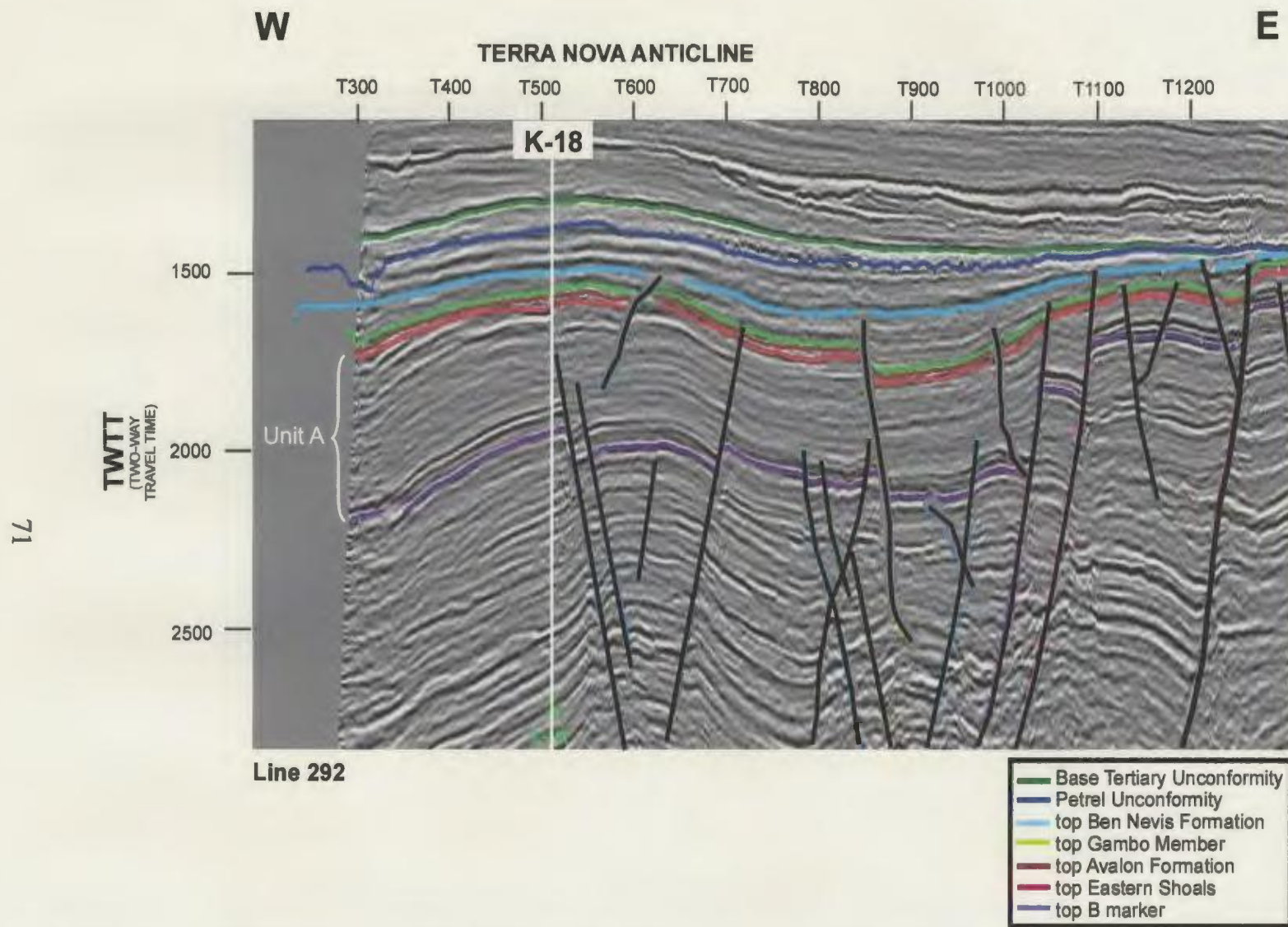


Figure 3.8 Interpreted line showing the parallel reflections within Unit A (Eastern Shoals Formation) and the location of the Terra Nova K-18 well. The thickness of the Eastern Shoals Formation does not vary significantly over the crest of the Terra Nova Anticline. See Figure 3.1 for well and seismic line location.

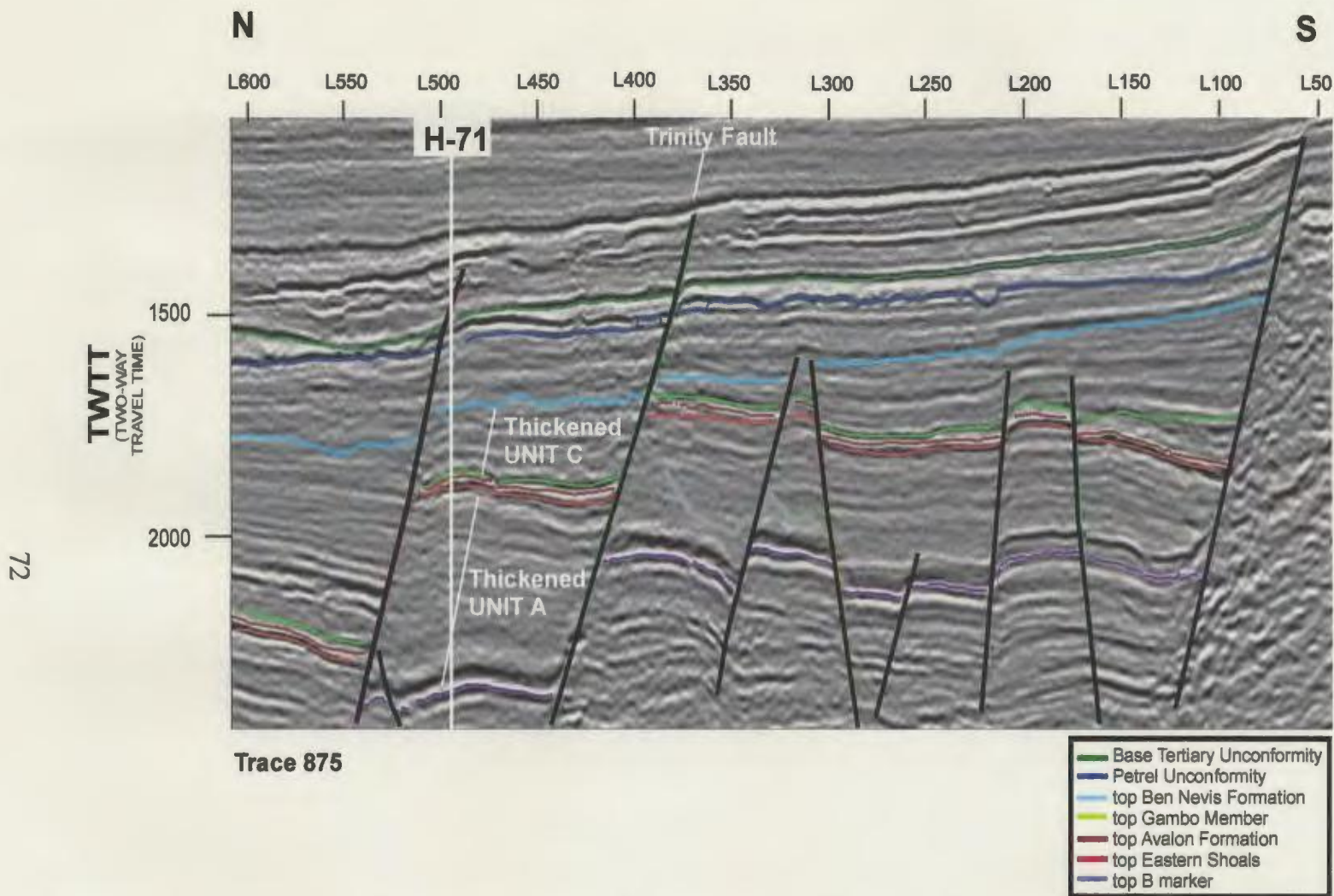


Figure 3.9

Thickened sections of Units A and C (incorporating the Eastern Shoals and Ben Nevis formations respectively) northward across Trinity Fault. Growth of Ben Nevis strata is clearly illustrated. Note the drag along the North Trinity Fault. The North Trinity H-71 well represents a typical section of the Ben Nevis Formation. See Figure 3.1 for well and seismic trace location.

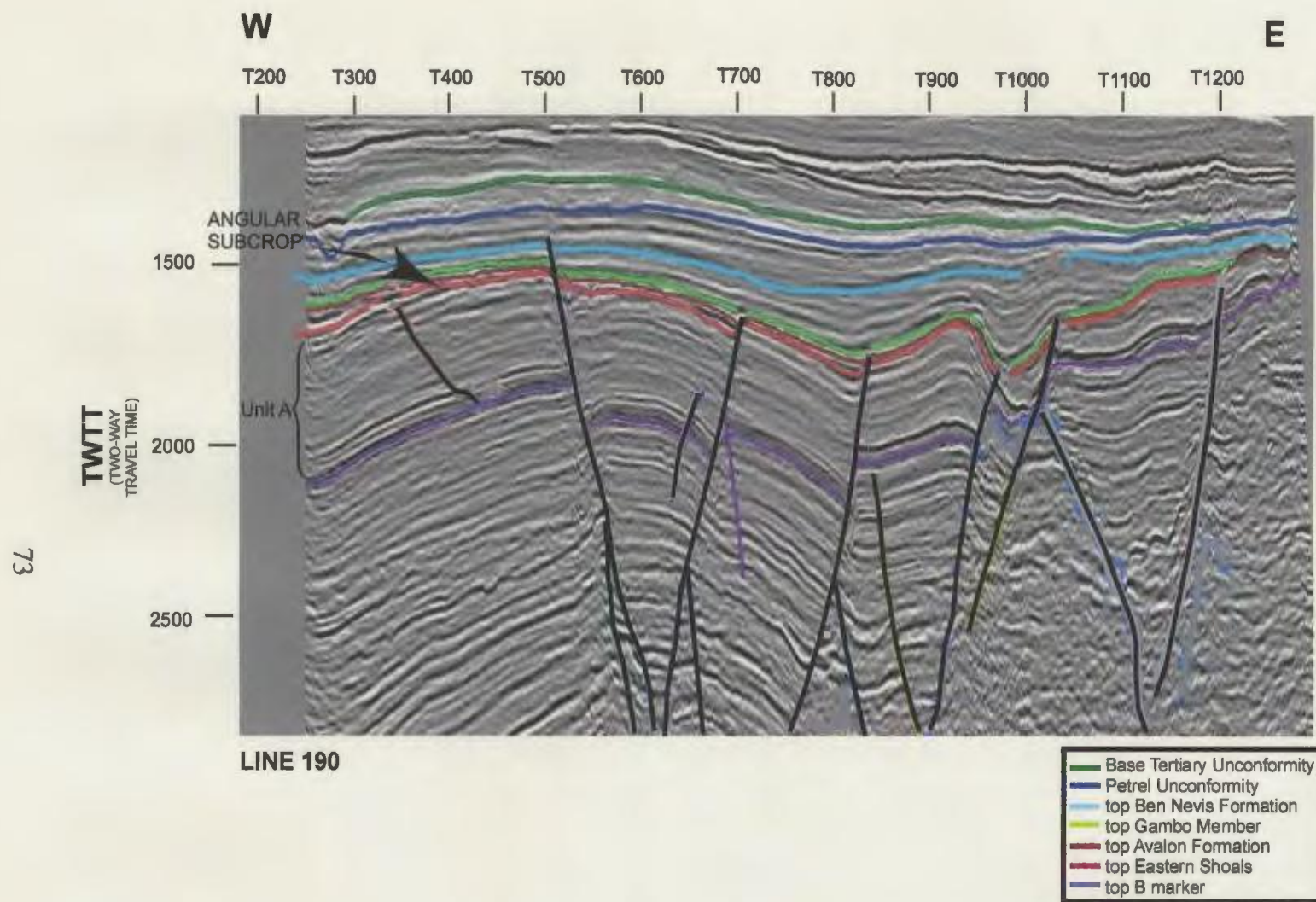


Figure 3.10 Interpreted line showing angular subcrop of seismic reflections below the Barremian unconformity (top Eastern Shoals Formation) and minor thinning in the upper portions of Unit A. See Figure 3.1 for location of seismic line.

(top of the event defining the top of the Avalon Formation). A time-structure map of this horizon is illustrated in Figure 3.11. This marker corresponds to a major angular unconformity that is present throughout the basin. The unconformity is recognizable on several data sets, including wireline logs, lithostratigraphic correlations, and seismic and core data. The seismic character of the upper boundary degrades in amplitude to the north (Figure 3.12), and becomes a “doublet” near the centre of the field. In the study area, Unit B comprises the Avalon Formation, which is a seismic onlap-fill sequence that overlies the Barremian unconformity and is truncated by the mid-Aptian unconformity.

Lithologically, the Avalon Formation is an upward coarsening sandstone- and mudstone-dominated sequence overlying the Eastern Shoals Formation and underlying the Ben Nevis Formation (Figure 3.13). Locally, two subdivisions can be identified within the Avalon sequence: an interbedded sandstone and shale sequence, overlain by a subtly upward-coarsening sandstone-dominated unit. The upper boundary of the Avalon Formation (and hence Unit B) is placed at the top of the upward coarsening sandstone sequence. This contact is sharp and unconformable over most of the Terra Nova field area and is clearly marked on gamma-ray and sonic log profiles, where the upward fining character of the overlying Ben Nevis Formation sharply contrasts with the upward coarsening trend of the Avalon Formation (Figure 3.14). Two seismic lines in the study area show onlap onto the mid-Aptian unconformity, the upper contact of Unit B (Figures 3.15 and 3.16).

The thickness of the Avalon Formation (and hence Unit B) in the study area ranges from 27 – 81 m (from wireline logs), with an average thickness of 55 m. Three

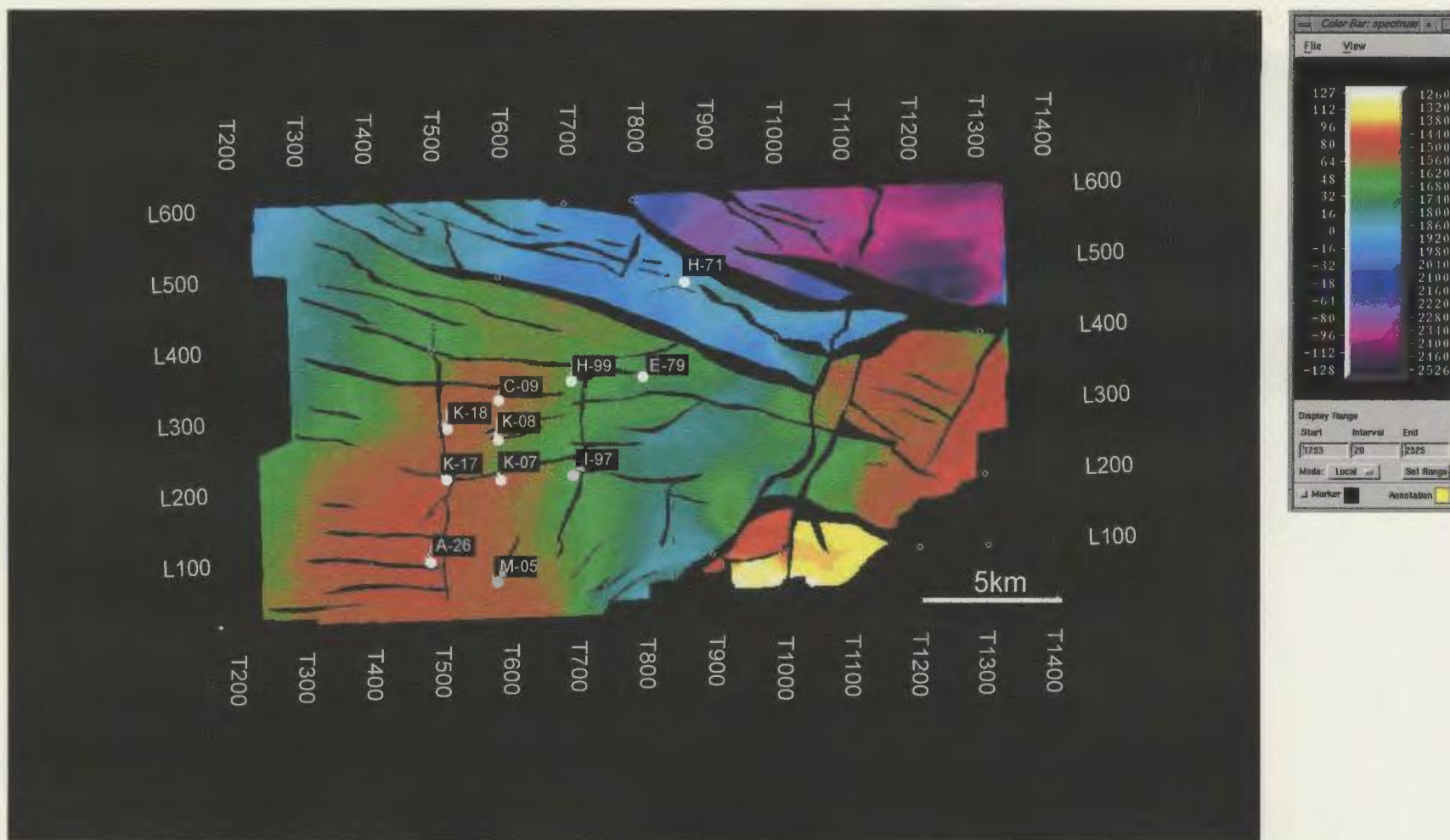


Figure 3.11 Time-structure map of the event defining the top of the Avalon Formation, Terra Nova oil field

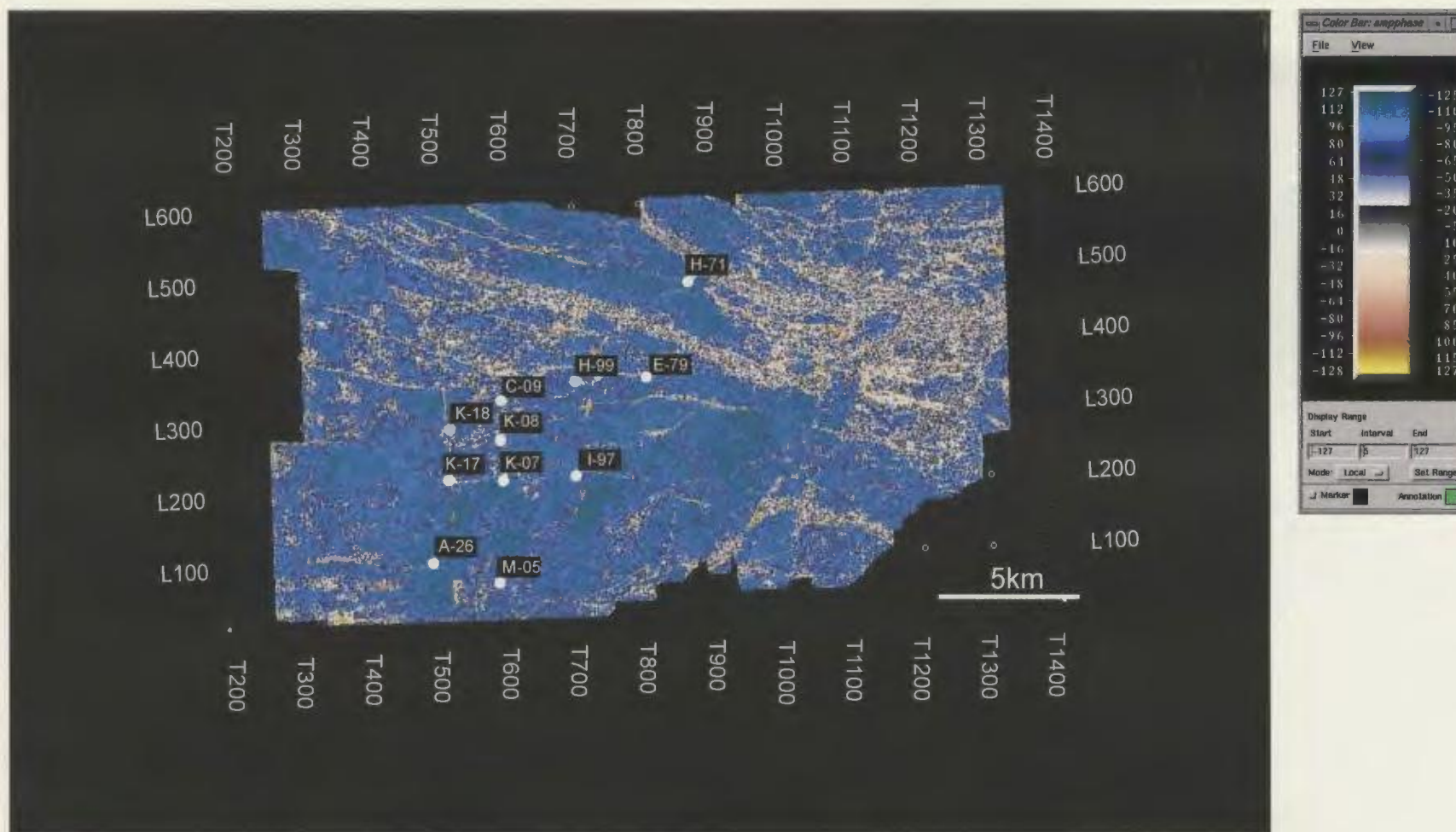


Figure 3.12 Amplitude map of the event defining the top of the Avalon Formation, Terra Nova oil field. The color bar indicates that Avalon marker is a coherent marker over most of the field area, and is characterized by a negative impedance contrast. Zones of low amplitude are lightly colored.

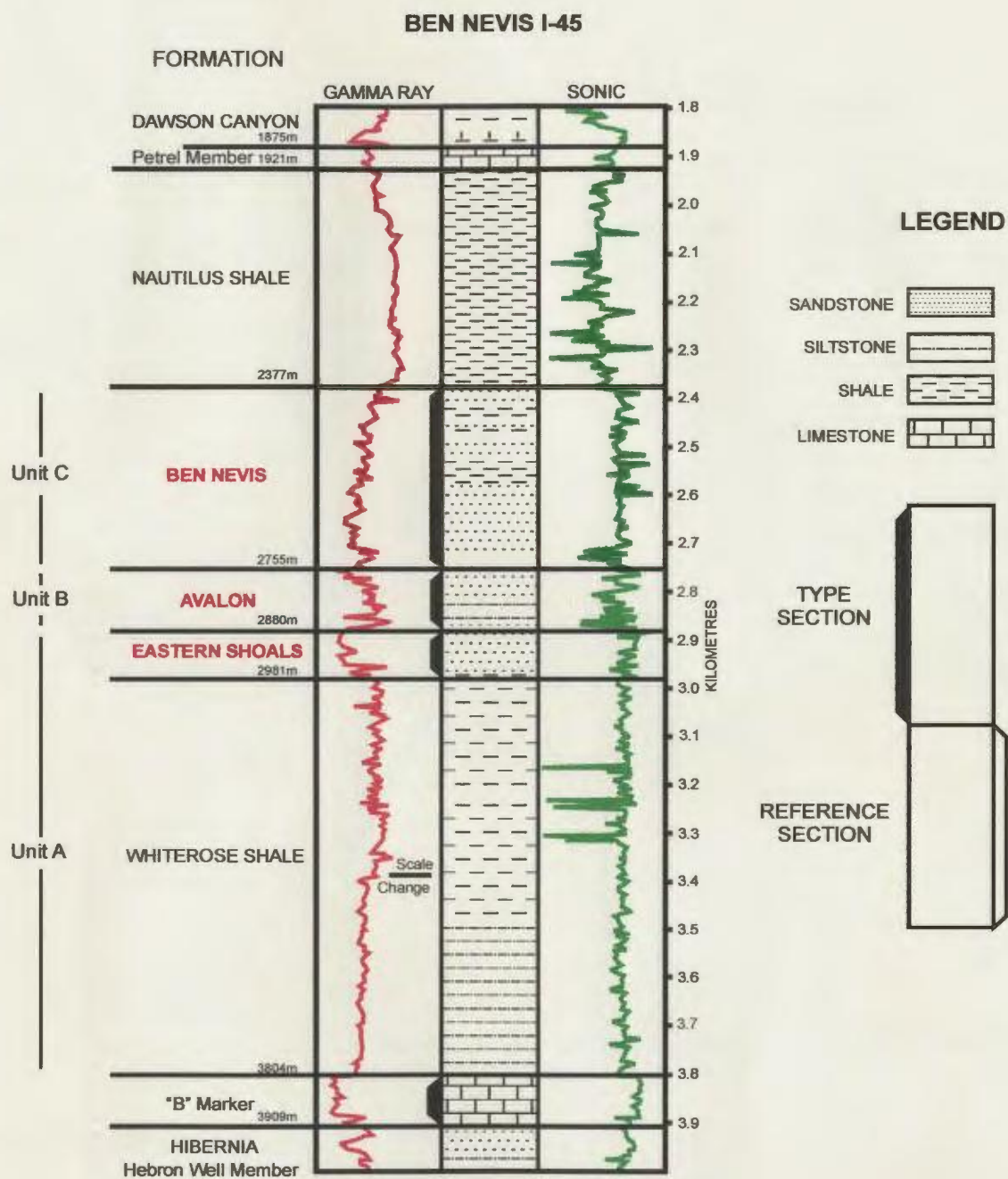


Figure 3.13 Gamma-ray/sonic log and lithostratigraphy of the Ben Nevis I-45 well. This is the type section for the Ben Nevis, Avalon, and Eastern Shoals formations, Jeanne d'Arc Basin (after McAlpine, 1990). There were no cores cut in this well. See Figure 1.4 for well location.

TERRA NOVA H-99

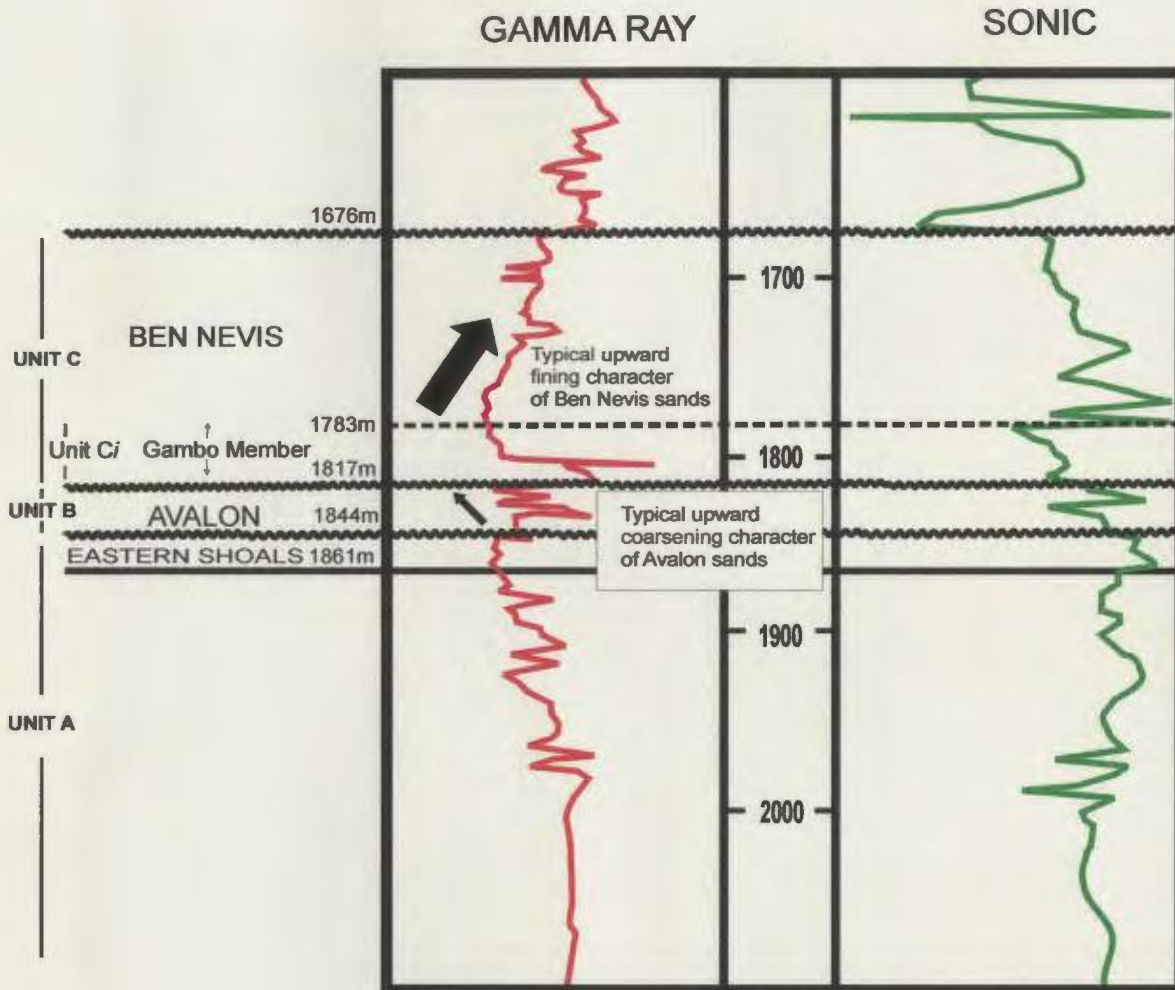


Figure 3.14 Gamma ray/sonic log for the Terra Nova H-99 well. The upper boundary of the Avalon Formation forms a distinct break on the log profiles, where the typically upward fining Ben Nevis Formation contrasts sharply with the upward coarsening Avalon Formation. This boundary is known as the mid-Aptian Unconformity. See Figure 1.8 for well location.

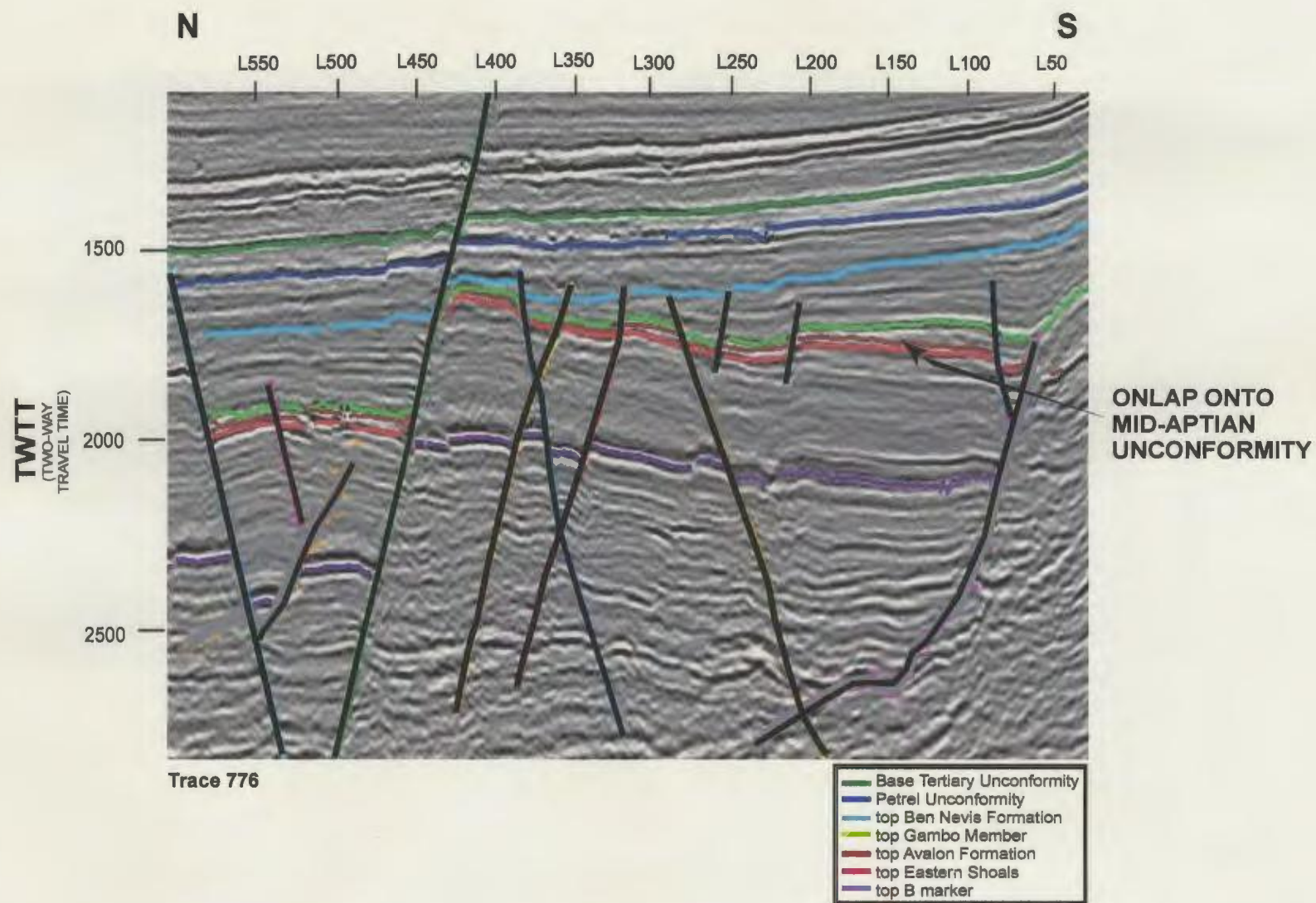


Figure 3.15 Interpreted trace showing onlap onto the mid-Aptian unconformity (top Avalon Formation). See Figure 3.1 for location of seismic trace.

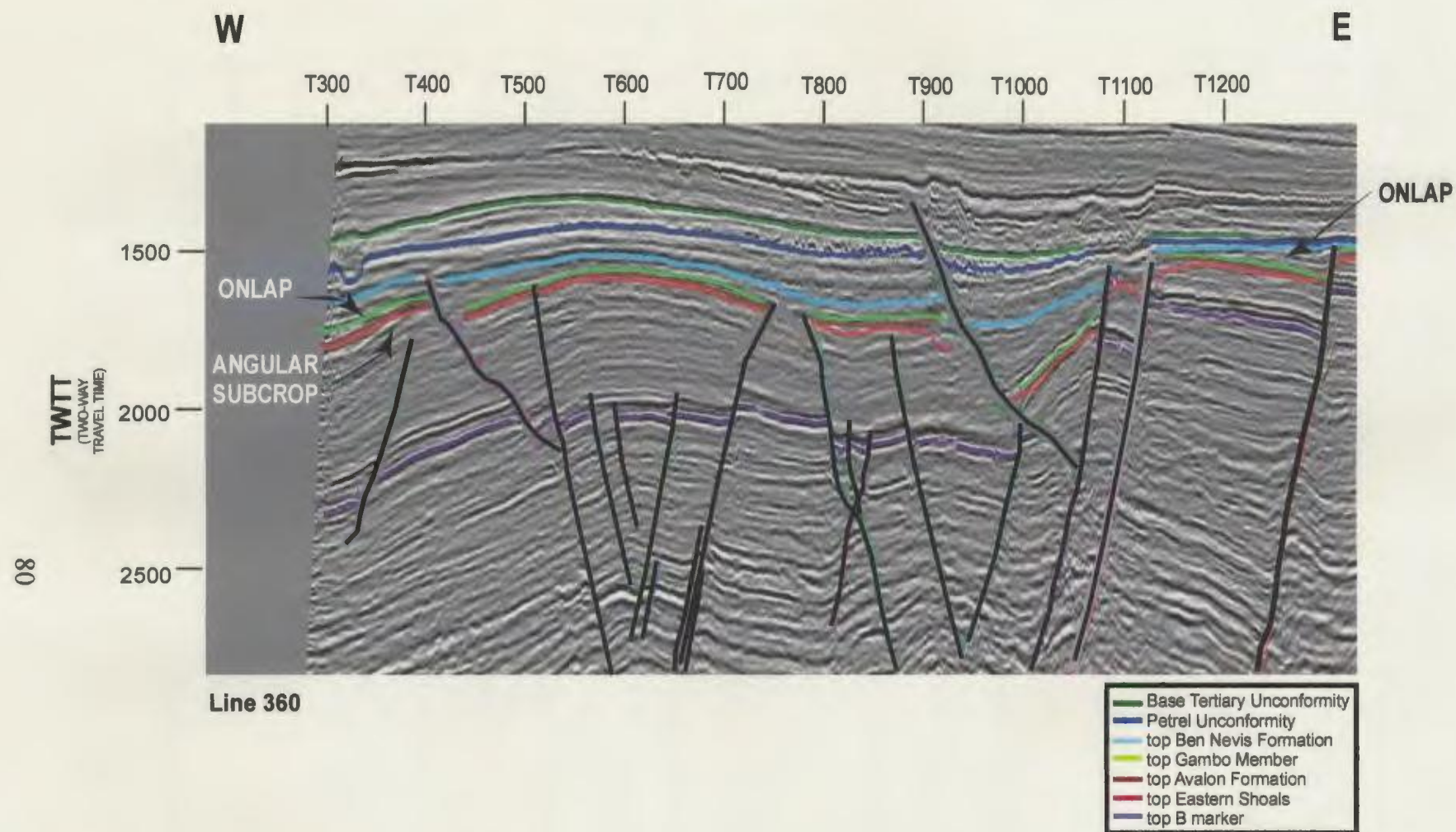


Figure 3.16 Interpreted line showing onlap onto the mid-Aptian unconformity (top Avalon Formation) and subcrop of lower Cretaceous strata beneath the unconformity. See Figure 3.1 for location of seismic line.

wells in the study area (Terra Nova K-17, North Trinity H-71 (Figure 3.17), and King's Cove A-26) show that the mid-Aptian unconformity locally eroded through Avalon Formation sediments, leaving strata of the Ben Nevis Formation superimposed directly on sandstones and limestones of the Eastern Shoals Formation; the North Trinity well is shown in Figure 3.17.

3.3.3 Unit C

Seismically, Unit C consists of lower amplitude internal reflections than the underlying Unit B. The lateral continuity of the internal reflections is fair to poor, making it difficult to determine the internal characteristics of the unit. The package is bounded at its base by the event defining the top of the Avalon Formation (mid-Aptian unconformity) and at its top by an acoustically moderate reflector (Figure 3.2), corresponding to the Albian unconformity. A time-structure map of the event marking the top of the Ben Nevis Formation is shown in Figure 3.18. A dip-azimuth map (Figure 3.19) shows the structural framework in the field area for the event marking the top of the Ben Nevis Formation, as well as a “pop-up feature” in southeastern part of the field. This feature is not present in either of the individual dip or azimuth maps for the same horizon; it is discussed in detail in Section 4.3.4. An amplitude map (Figure 3.20) of the event marking the top of the Ben Nevis Formation (Albian unconformity) shows that it is generally weak over most of the field area. In the study area, Unit C comprises the Ben Nevis Formation, including the Gambo Member (discussed in Section 3.3.4 – Unit C_i).

The Ben Nevis Formation is the first, upward fining sequence immediately above

NORTH TRINITY H-71

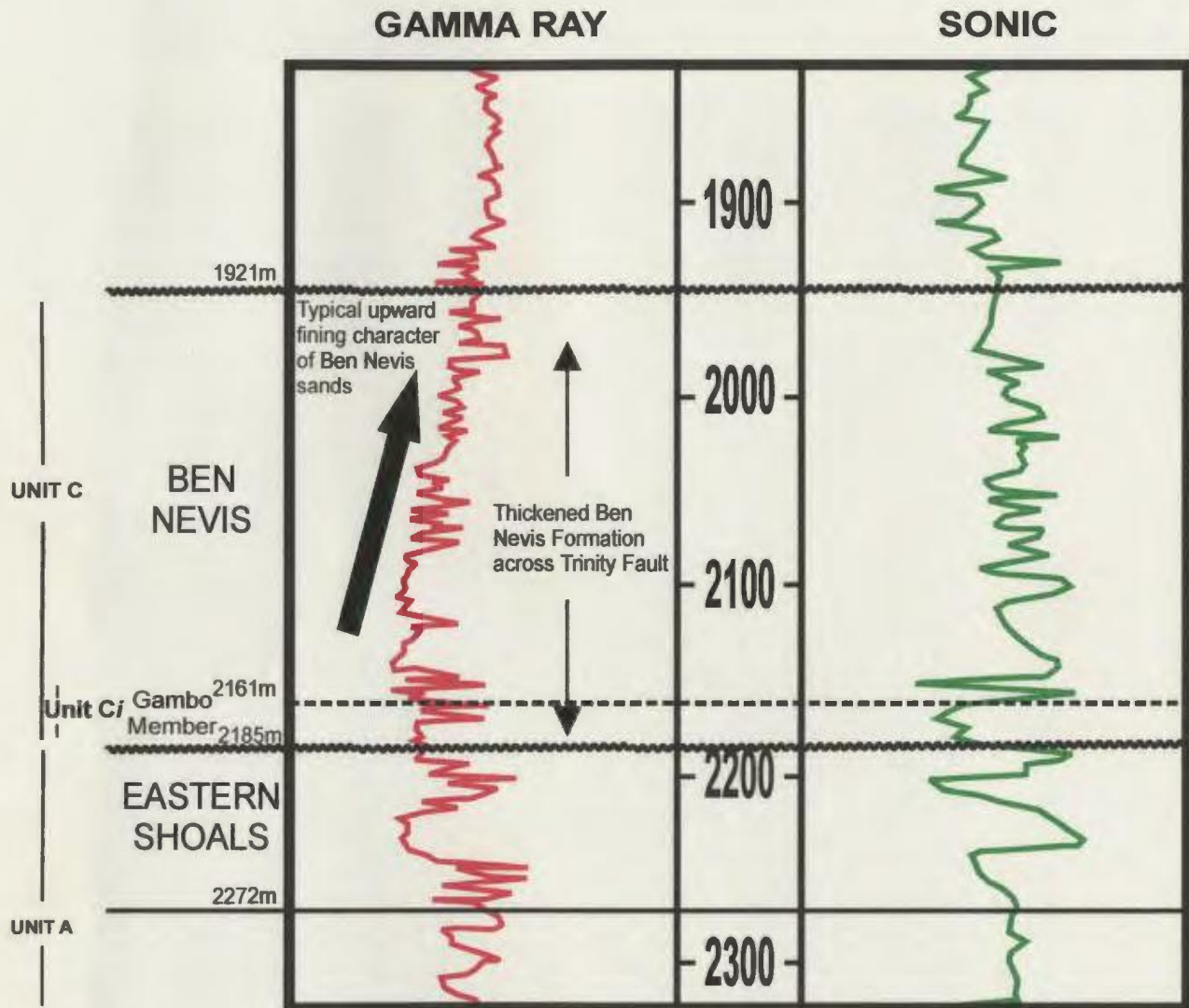


Figure 3.17 Gamma ray/sonic log of the North Trinity H-71 well. This well shows a thickened Ben Nevis section compared to those in the Terra Nova wells, thus demonstrating a northward-thickening wedge of lower Cretaceous sediments across the Trinity Fault, which is located immediately south of the North Trinity H-71 well (see Figure 1.8 for well and fault locations). The Gambo section has relatively the same thickness as in most of the Terra Nova wells. The mid-Aptian unconformity has eroded through the Avalon Formation at this location, so that the Gambo Member (Ben Nevis Formation) lies directly above the Eastern Shoals Formation.

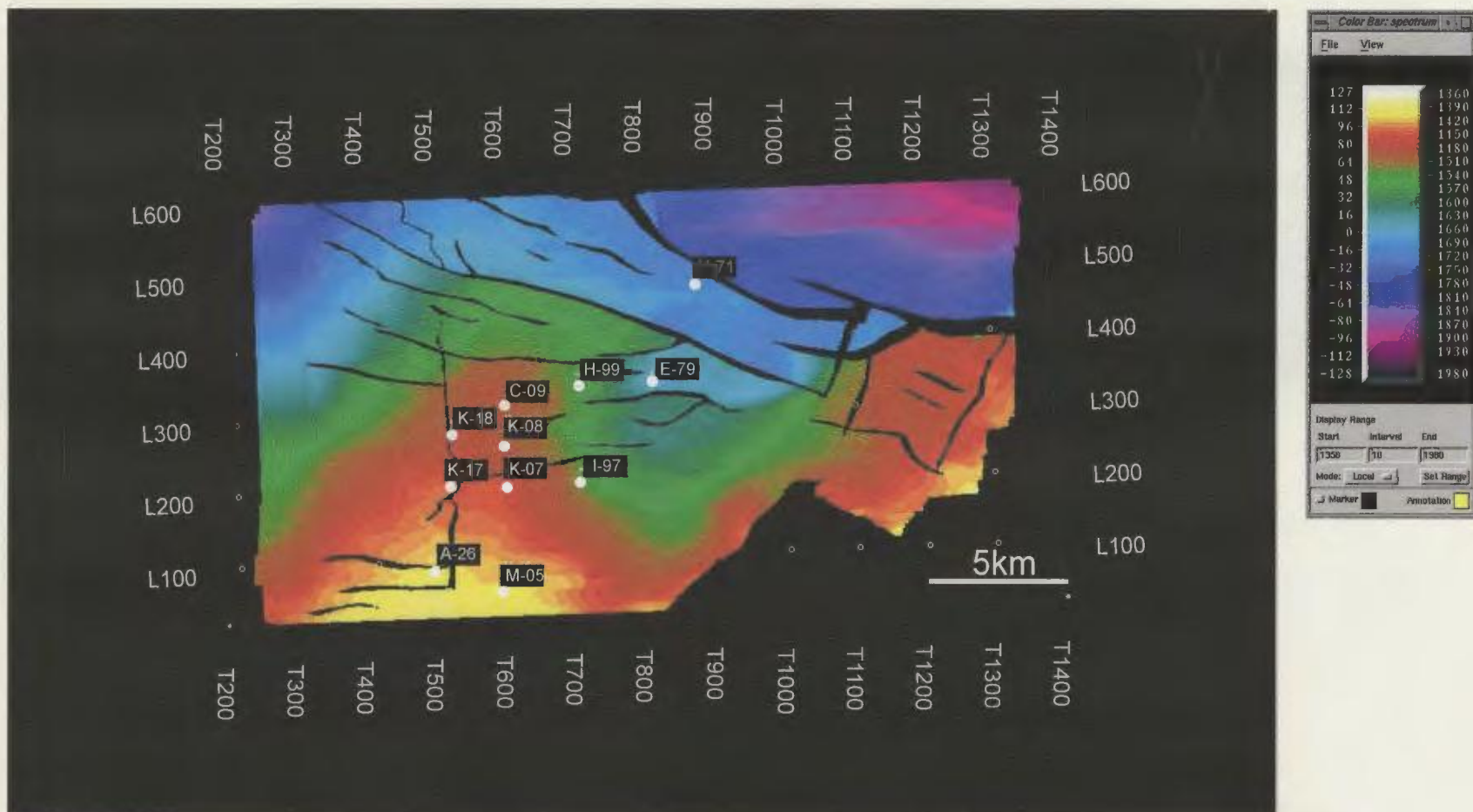


Figure 3.18 Time-structure map of the event defining the top of the Ben Nevis Formation, Terra Nova oil field

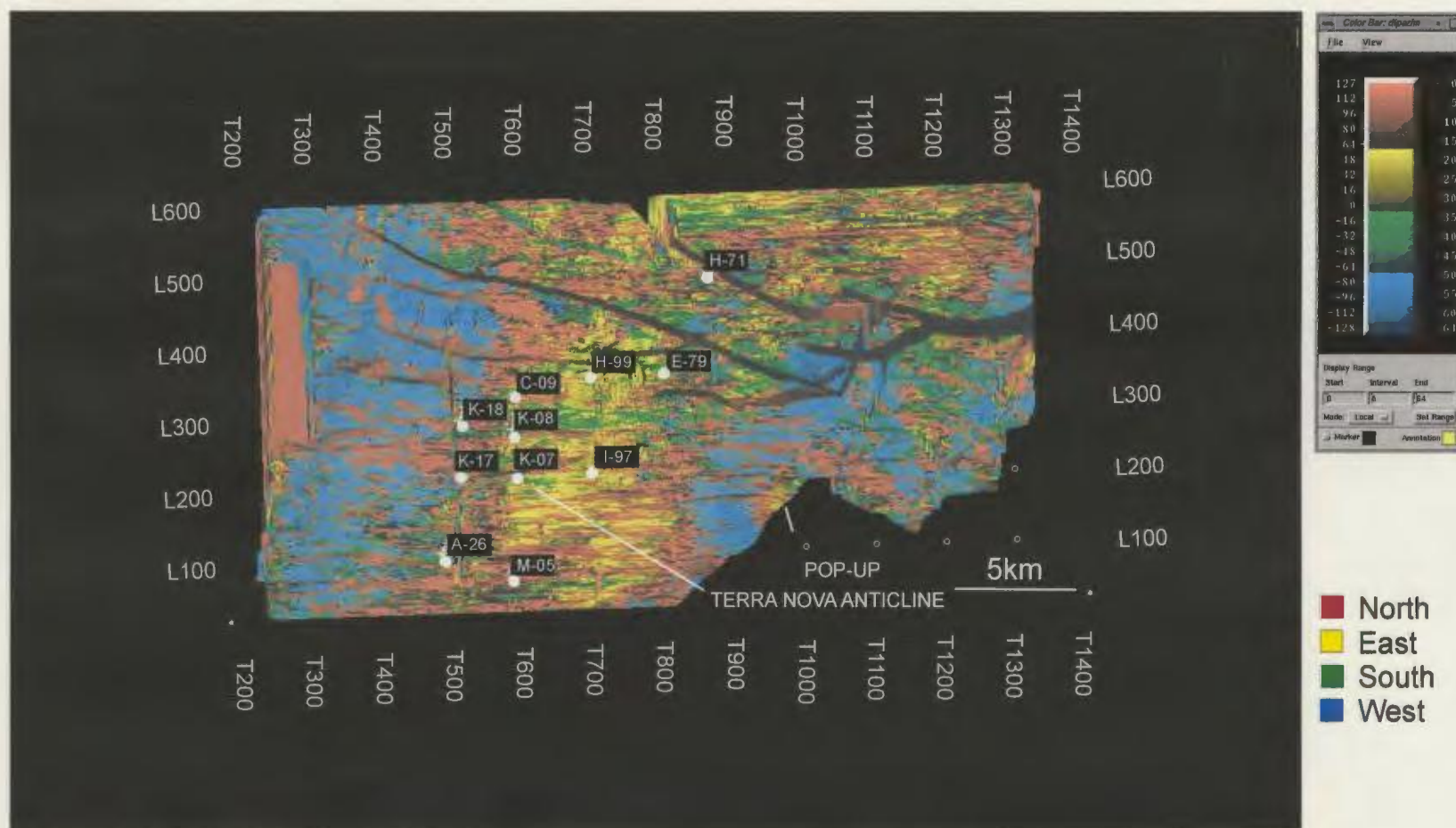


Figure 3.19 Combined dip/azimuth map of the event defining the top of the Ben Nevis Formation, Terra Nova field area. The hue of the colour indicates the azimuth (i.e. north, south, east, or west), whereas the colour intensity indicates the dip angle. The pale colours represent shallow dips and the darker colours represent steep dip.

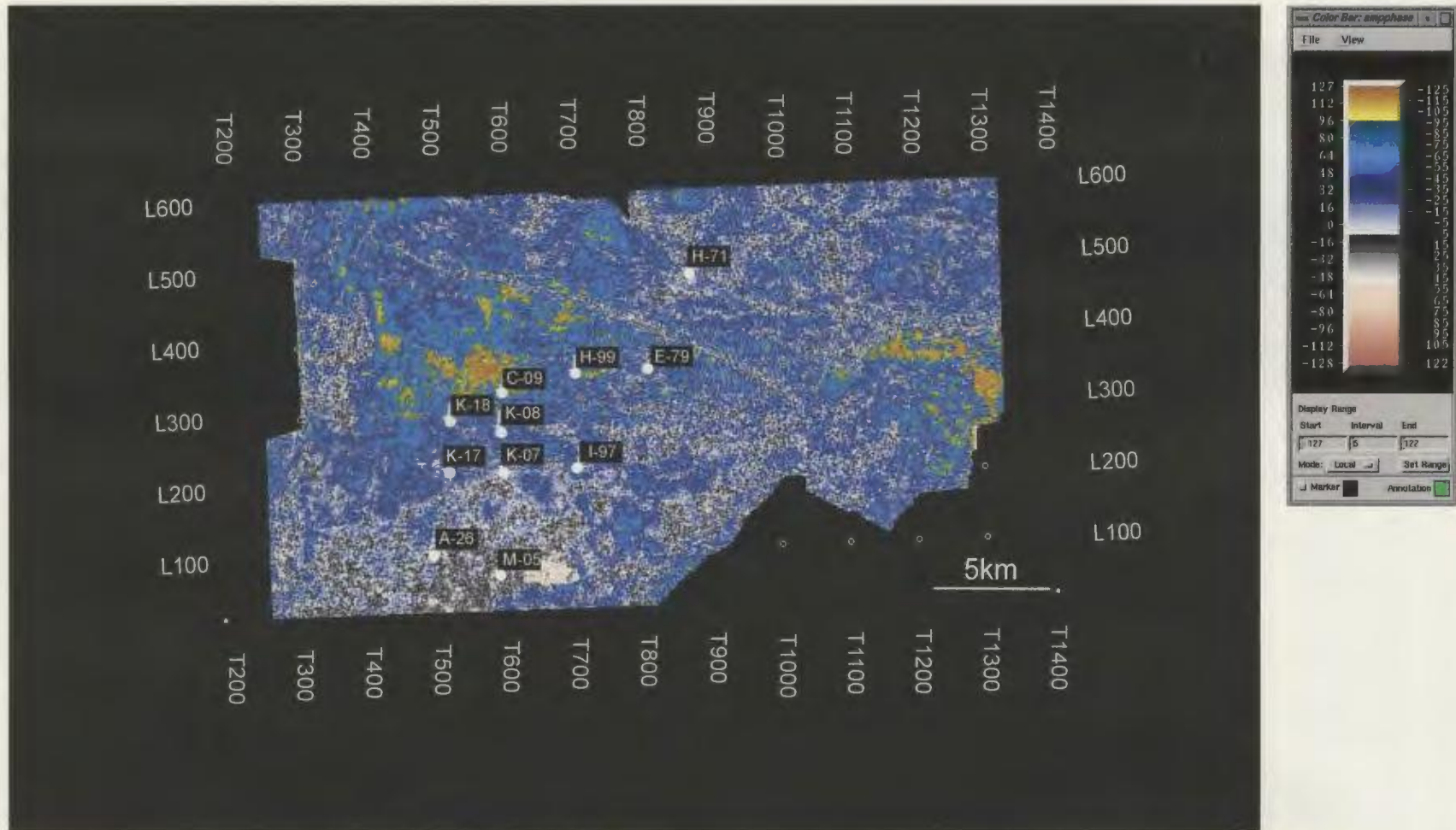


Figure 3.20 Amplitude map of the event defining the top of the Ben Nevis Formation, Terra Nova oil field. This horizon is generally weak over most of the field area, with some locally increased areas of coherence (in the Terra Nova Anticline region and in eastern parts of the field, colored in yellow). The color bar indicates that this horizon is characterized by a negative impedance contrast and is defined by a negative peak on a seismic section.

the Avalon Formation (Figure 3.14). Lithologically, it consists of an upward fining sequence of sandstone with common interbeds of limestone and very minor shale. In the study area, there is a lower subunit (Unit Ci, Gambo Member), which is a sandstone unit with thin interbeds of claystone, siltstone, and limestone. Within Unit C, there is excellent porosity in the sandstone and some in the limestone (from sidewall core data), but no hydrocarbon shows were observed (except in the North Trinity H-71 well) and the zone is considered non-productive and is water-saturated.

The upward fining sequence within Unit C was extensively cored in North Trinity H-71 (cores 1-4). Core 4 was cut from quartzose sandstones, which characterize the base of the upper portion of the Ben Nevis Formation. These sandstones are fine- to medium-grained, non-argillaceous and contain bioclastic and carbonaceous debris as well as glauconite (Petro-Canada, 1986b). These sandstones grade upward in cores 1-3 into thin interbeds of: a) clean sandstones; b) highly burrowed, argillaceous sandstone and siltstones and; c) shales and limestones. The thin interbeds of the upper portion of the Ben Nevis Formation are fine- to very fine-grained sandstone and commonly contain glauconite and abundant shell debris.

The upper boundary of the Ben Nevis Formation (and hence Unit C) is defined as the contact with the overlying Nautilus Formation, which is sharply defined by a return to a sandstone lithology. This contact is abrupt and forms a noticeable shoulder on gamma-ray and sonic logs.

Seismically, the upper contact is unconformable to disconformable near the margins of the basin and over major structures, such as the Terra Nova Anticline (Figure

3.21A), and in other areas of the Terra Nova field, such as near the Trinity Fault (Figure 3.21B). The unconformity is indicated by either an angular subcrop of seismic reflections below this surface (Figure 3.21A) or onlap of the overlying beds onto the unconformity (Figure 3.21B). Both the angular subcrop and the seismic onlap (onto both the upper and lower boundaries of the unit) contribute to the convergence of internal reflections within Unit C. The convergence is also a consequence of depositional thinning toward the basin margins and over positive structures, such as the Terra Nova Anticline (Figure 3.22).

The thickness of the Ben Nevis Formation (Unit C) ranges from 112 – 264 m (from wireline logs), with an average of 166 m. Syndepositional growth of basin structures and faults results in significant thickness fluctuations within Unit C, for example northward across the Trinity Fault (Figures 3.9, 3.17 and 3.23). On a regional scale, the thickest accumulations occur on the eastern side of the basin and in the basin axis.

3.3.4 Unit Ci

Unit Ci corresponds to the Gambo Member of the Ben Nevis Formation. Characterization of the upper boundary of this subunit is accomplished by integrating well log data with seismic profiles in the study area. The upper contact with the rest of the Ben Nevis Formation is generally not well defined regionally, but on a local scale the boundary can be seen as a noticeable shoulder on both the gamma-ray and sonic logs (Figures 3.7 and 3.17). Wireline logs for wells that intersected this upper contact were

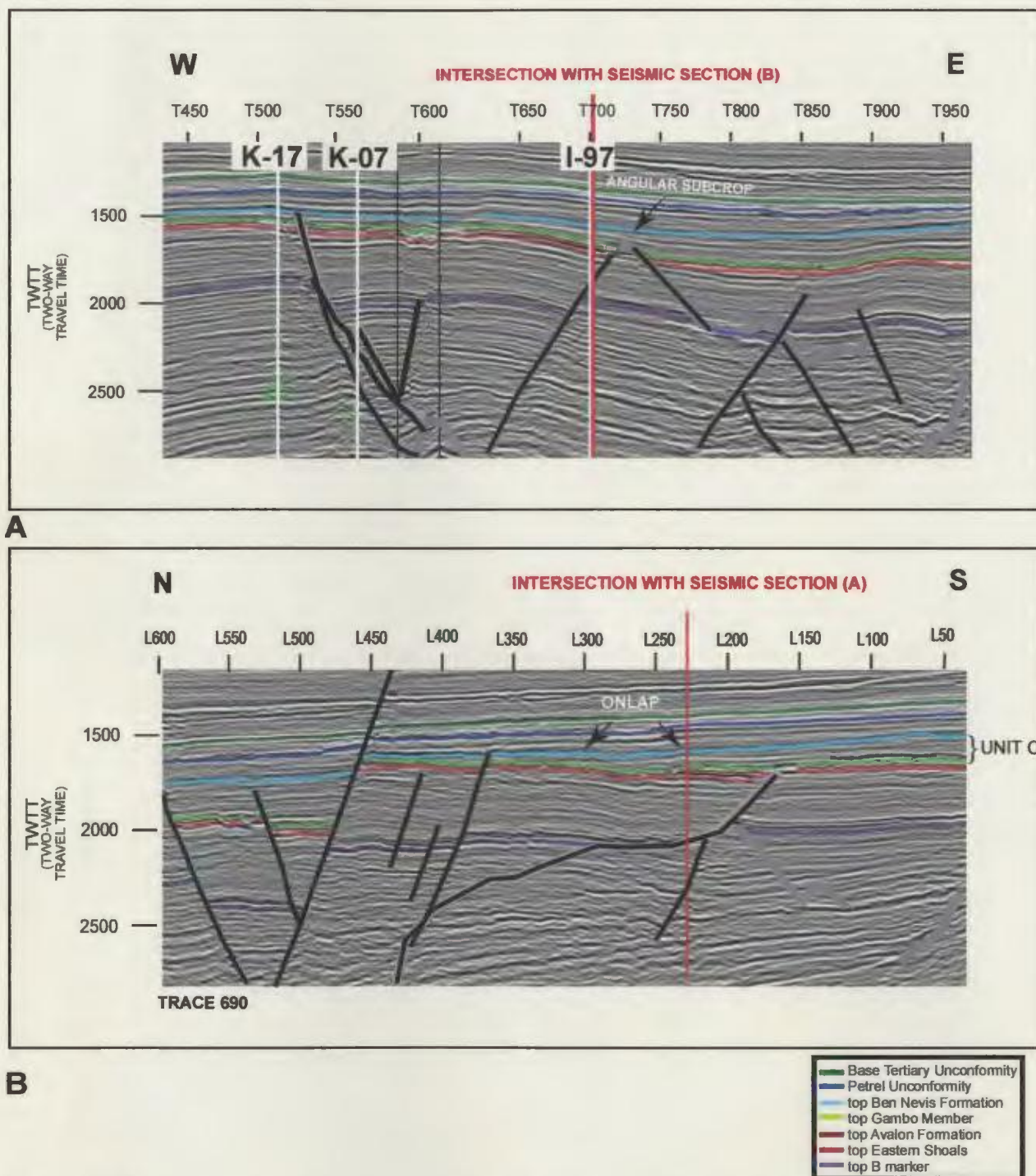


Figure 3.21 Interpreted seismic sections showing: (A) angular subcrop of seismic reflections beneath the Albian unconformity (top Ben Nevis Formation; Unit C) and (B) onlap onto the Albian unconformity. (A) also shows the Terra Nova wells K-17, K-07, and I-97 (in white). The intersection points of the two seismic sections are shown in red. The black vertical lines just before and just after T600 in profile (A) mark the locations of jogs (turning points) in a non-linear “point-to-point” traverse between the end points of the profile. See Figure 3.1 for well and seismic line locations.

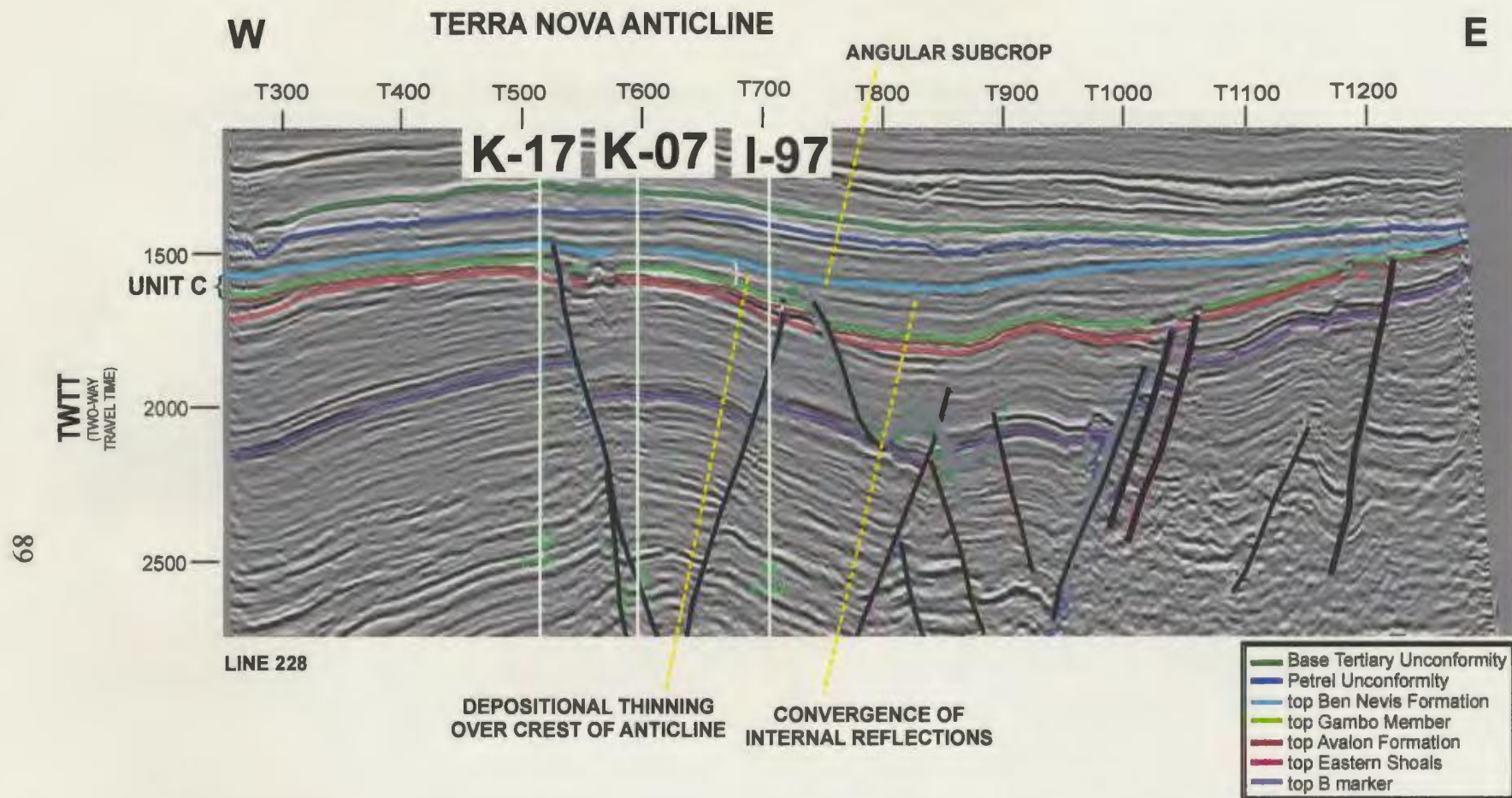


Figure 3.22 Interpreted seismic section showing the structure of the Terra Nova Anticline. This figure shows depositional thinning within the Ben Nevis Formation (Unit C) over the Terra Nova Anticline, due to onlap onto the mid-Aptian unconformity (basal boundary of Unit C) and the angular subcrop of seismic reflections below the Albian unconformity (upper boundary of Unit C). This contributes to the convergence of internal reflections within Unit C. Wellbores are represented by white vertical lines. See Figure 3.1 for well and seismic line locations.

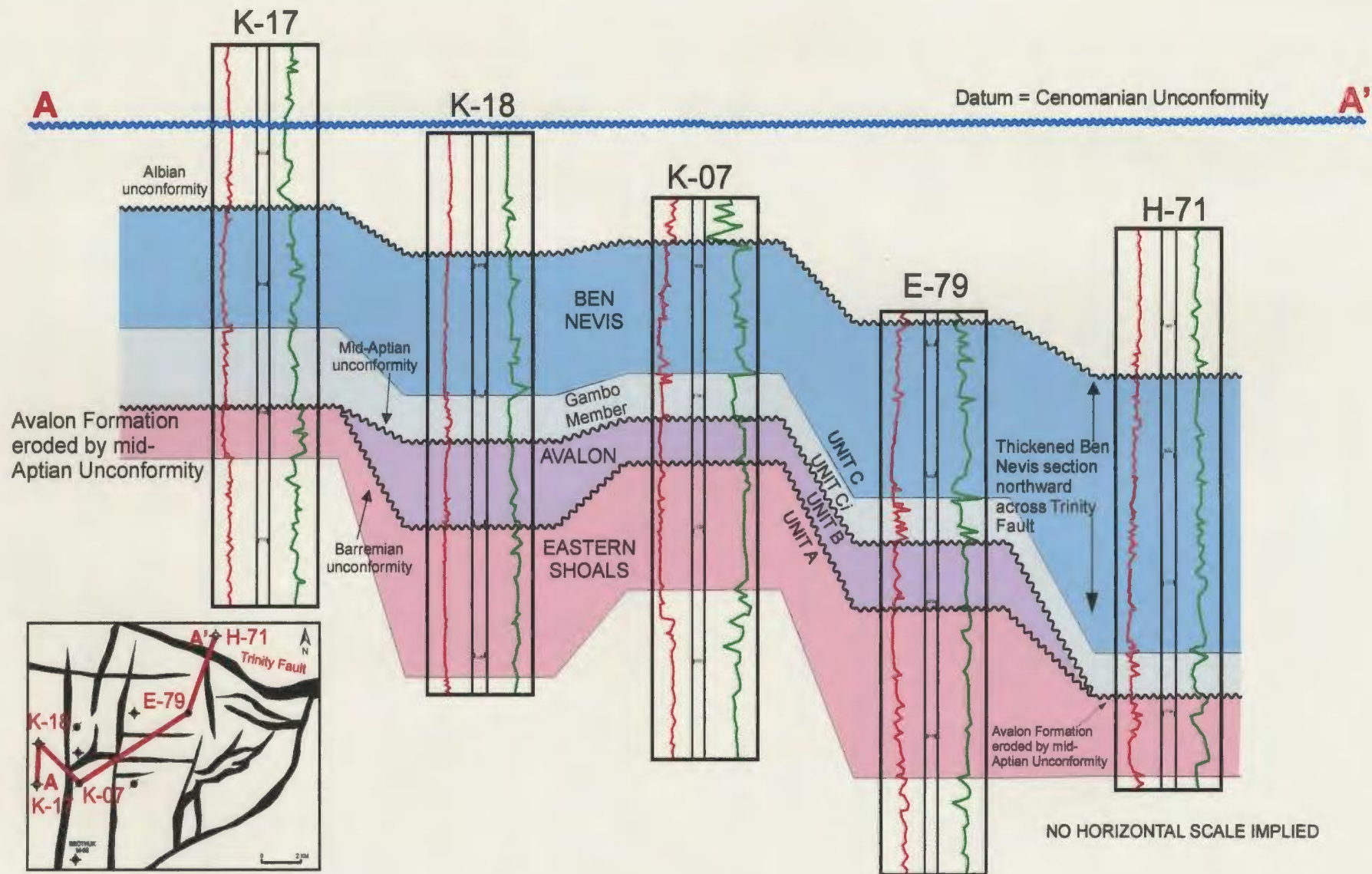


Figure 3.23 Schematic stratigraphic cross-section from Terra Nova K-17 to North Trinity H-71, showing a thickened Ben Nevis Formation northward across the Trinity Fault and Avalon Formation that have been eroded by the mid-Aptian unconformity. The wells show gamma ray logs and sonic logs in red and green, respectively. Location of the cross-section is shown in red on the map.

superimposed onto the seismic data in order to identify the seismic marker closest to the contact. This contact is a moderately reflective marker that can be mapped over most of the study area (Figure 3.2). Lithologically, the contact is defined as the top of interbedded shale and sandstone lithofacies where they underlie relatively clean, stacked sandstones of the upper portion of the Ben Nevis Formation.

The basal contact of Unit *Ci* is the mid-Aptian unconformity. The expression of this contact is highly variable on a regional scale across the Jeanne d'Arc Basin. In areas where the Gambo Member is developed and preserved above the mid-Aptian unconformity, as in the Terra Nova field area, massive, clean sandstones of the Gambo Member are underlain by fine-grained, variably burrowed sandstones of the Avalon Formation.

The Gambo Member was cored at North Trinity H-71 (core 5, 2164.7 – 2168.9 m). According to the Petro-Canada Well History Report for this well (1986b), the core revealed a massive sandstone section, which is white, fine- to medium-grained with occasional coarse grains. The sand is well rounded to subangular and moderately sorted with a porosity of 16-20%. It is poorly cemented in parts, but well cemented in other sections. The shale is light grey, firm and silty. There are thin coal beds and laminae throughout the sandstone section.

Locally, the mid-Aptian unconformity eroded through the Avalon Formation, juxtaposing sediments of the Gambo Member above calcareous, oolitic, bioclastic sandstones of the Eastern Shoals Formation (Figure 3.17 and 3.24). Examples are surrounding the wells Terra Nova K-17, North Trinity H-71, and King's Cove A-26.

Unit *Ci* consists of moderate amplitude reflections with fair to poor continuity. The Gambo Member is widely distributed regionally and is highly variable in thickness. Wireline logs in the Terra Nova field area indicate that the thickness of the Gambo Member ranges from 9 – 65 m, with an average thickness of 34 m. The thickness can vary across very short distances due to variable preservation in areas of erosional topography on the mid-Aptian unconformity (Figures 3.17, 3.23, and 3.24); for example, in regions where a paleovalley was incised into the mid-Aptian unconformity (Figure 3.25 A and B).

3.4 Synthetics

A synthetic seismogram can be generated on a workstation or computer to simulate seismic data acquisition. It is the result of one of many forms of forward modeling to predict the seismic response of the Earth, and is a direct one-dimensional model of acoustic energy traveling through the layers of the Earth. The synthetic is generated by convolving the reflectivity (derived from the acoustic and density logs) with the wavelet derived from the seismic data. Seismic data interpretation can be improved by comparing correlation points picked from a synthetic trace based on well data with major reflections on the seismic section.

The quality of the match between a synthetic seismogram and the seismic data depends on a number of factors, including well log quality, seismic data processing quality, and the ability to extract a representative wavelet from the seismic data. Synthetics usually need to be stretched or squeezed to fit data because of an inadequate

TERRA NOVA K-17

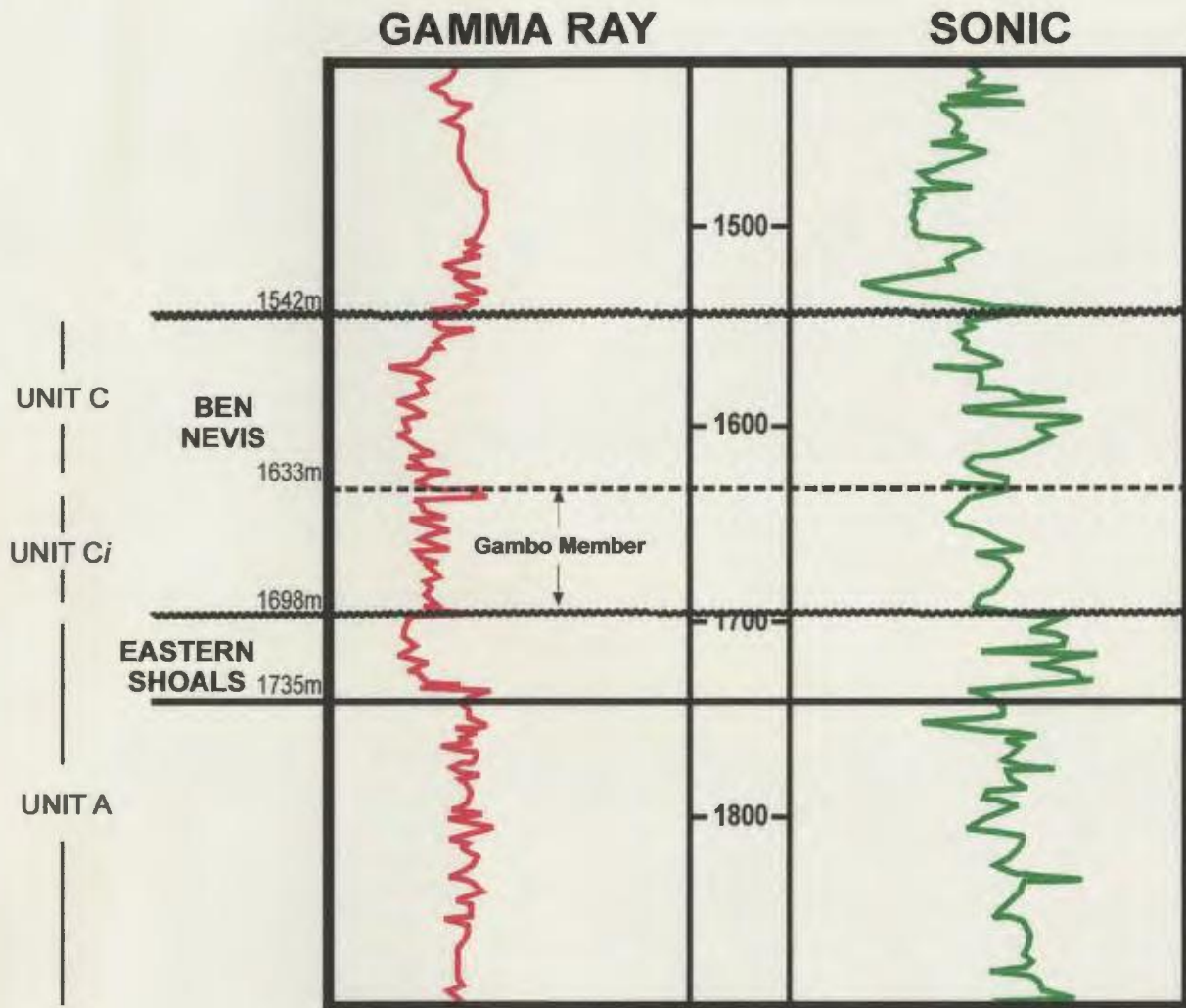
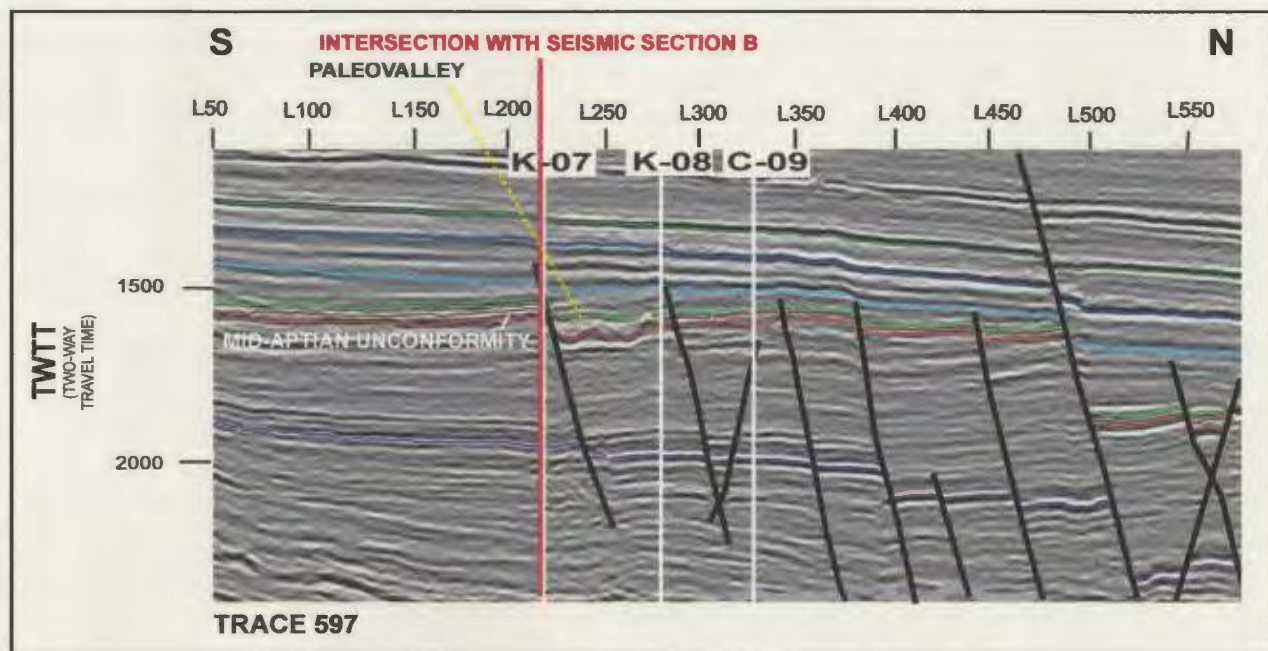
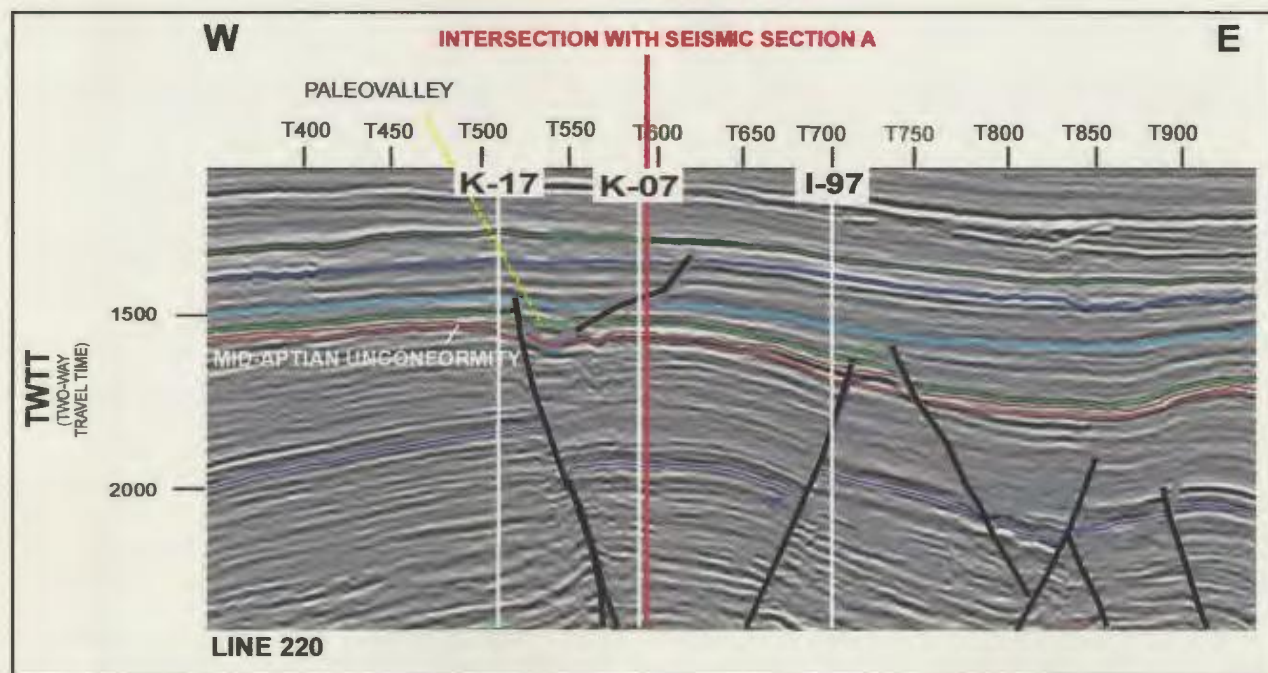


Figure 3.24 Gamma ray/sonic log of the Terra Nova K-17 well. This well shows the mid-Aptian unconformity located at the base of the Ben Nevis Formation. At this location (as well as at the North Trinity H-71 and King's Cove A-26 well locations), the mid-Aptian unconformity has eroded through the Avalon Formation so that the Gambo Member (Ben Nevis Formation) sits directly on calcareous sandstones and oolitic limestones of the Eastern Shoals Formation. Also, this well section shows an anomalous thickness of only 37 m for the Eastern Shoals Formation; in the Terra Nova field area, the thickness of this formation ranges from 37 m to 130 m, with an average thickness of 106 m. See Figure 1.8 for well locations.



A



B

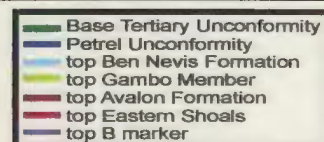


Figure 3.25 Interpreted seismic sections showing the paleovalley incised on the mid-Aptian unconformity, yielding locally thickened Gambo Member. The intersection points of the two seismic sections are shown in red and the wellbores in white. See Figure 3.1 for well and seismic section locations.

measurement of the velocities in the wellbore. The best solution to this problem is to use checkshot information. Vertical Seismic Profile (VSP) surveys are “super-checkshots”. VSPs also provide a direct look at the near-wellbore reflectors at the frequency band of real seismic experiments. Generally, the acoustic log is calibrated with checkshot or VSP information before combining it with the density log to determine acoustic impedance.

In this study, synthetics were generated and checkshot-corrected based on vertical seismic profiles (VSPs) for all wells in the survey area. Both density and sonic logs were used in synthetic generation. Most of the wells in the survey area, with the exception of the Terra Nova C-09 well, have inaccurate density logs as a result of the highly sensitive nature of the density response to poor borehole conditions (N. Carter, pers. comm., 2002). In cases where the density logs produced substandard synthetics, sonic logs were used in combination with the Gardner Equation (Gardner et al., 1974; Sheriff, 1991) to create the synthetic seismograms.

The synthetics for the Terra Nova C-09 and North Trinity H-71 wells (Figures 3.26 and 3.27) show good correlation between the well-log picks and the corresponding seismic events defining the tops of the Ben Nevis Formation, Gambo Member, and Avalon and Eastern Shoals formations. The synthetic for the C-09 well had to be time-shifted in SynTool by -27 ms, and the North Trinity H-71 by -15 ms, enabling a better correlation among lithologic picks (a negative time shift indicates an increase in time and depth). The seismic event for the Eastern Shoals Formation in C-09 and H-71 is a “doublet” in the synthetic.

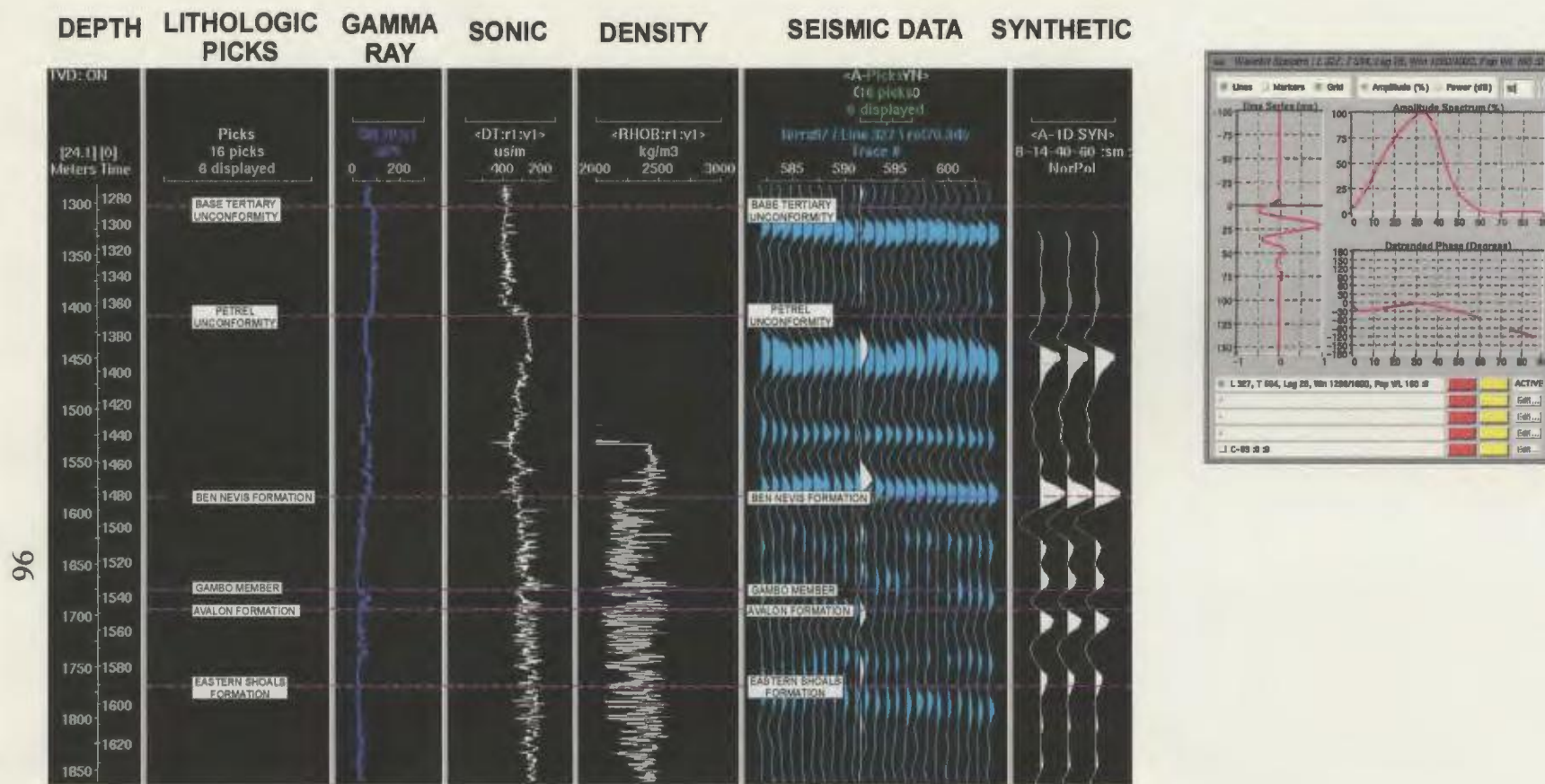


Figure 3.26 Synthetic seismogram and extracted wavelet for Terra Nova C-09. After a -27ms time shift (that is, an increase in time and depth), this seismogram shows a good match for the top of the events defining the tops of the Ben Nevis Formation, Gambo Member, and the Avalon and Eastern Shoals formations. Notice that the marker for the top of the Eastern Shoals Formation is a “doublet” in this region, which is defined by two closely spaced, high-amplitude events. See Figure 1.8 for well location.

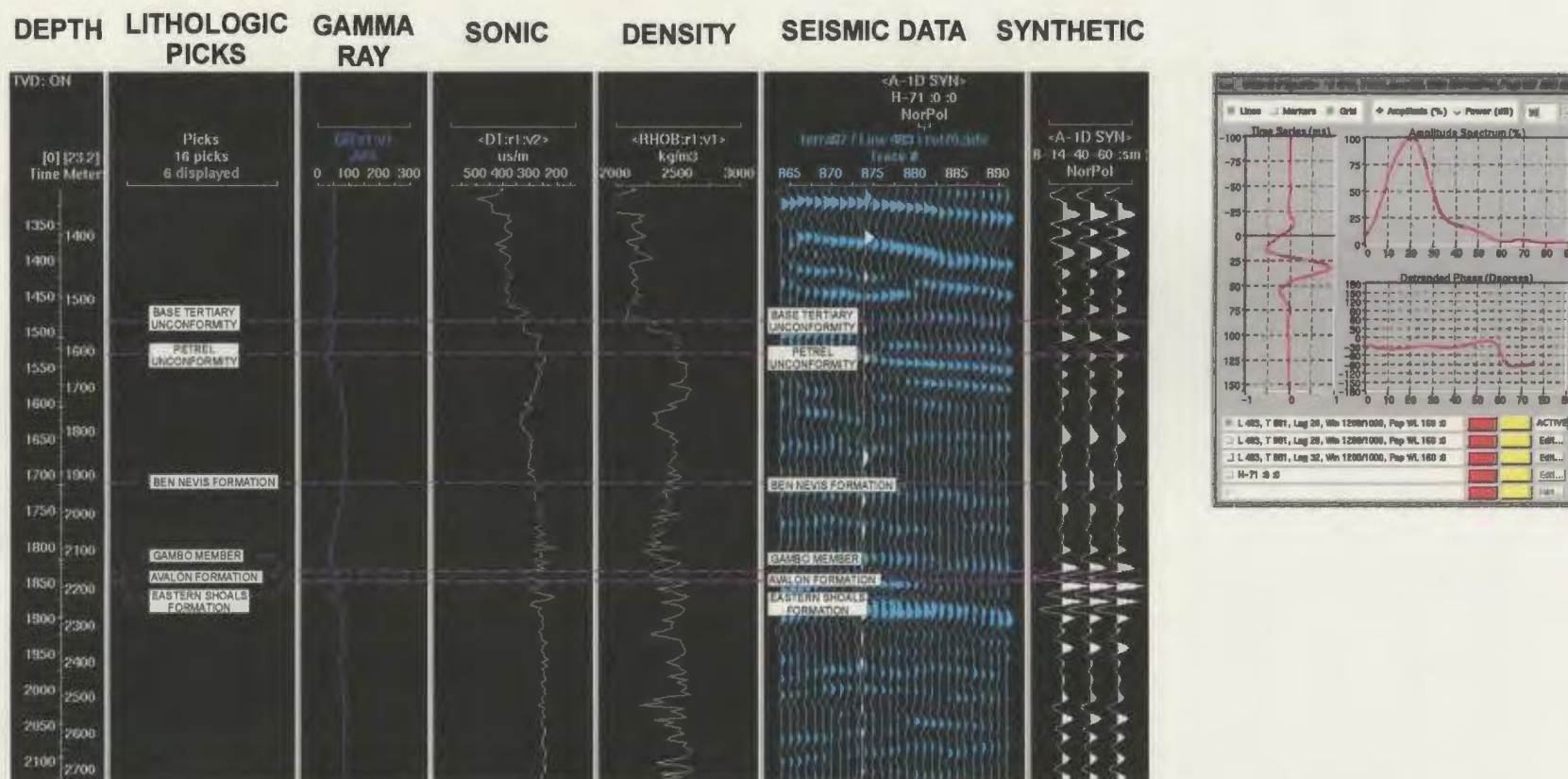


Figure 3.27 Synthetic seismogram and extracted wavelet for North Trinity H-71. After a -15ms time shift (that is, an increase in time and depth), this seismogram shows a good match for the top of the events defining the tops of the Ben Nevis Formation, Gambo Member, and the Avalon and Eastern Shoals formations (the slight offset is due to the highly faulted nature of this area). Note that the marker for the top of the Eastern Shoals Formation occurs as a synthetic “doublet”, which is defined by two closely spaced, high-amplitude events. See Figure 1.8 for well location.

CHAPTER FOUR: DISCUSSION

This section reviews the control of tectonism on the sedimentation of the lower Cretaceous succession in the Terra Nova oil field, consisting of the Eastern Shoals, Avalon, and Ben Nevis formations, based on an interpretation of new results from this thesis and a review of published ideas. Each formation occurs within a distinct sedimentary sequence. The development of these sequences was controlled by an interplay of sediment input, changes in sea level (including changes in rate of sea-level rise or fall), tectonism, accommodation space, and climate. Tectonics and sea-level change control the accommodation space; whereas tectonics, sea-level change and climate interact to control the terrigenous influx and how much of the accommodation is filled.

Because several factors contributed to the formation of the unconformities in the area, a primary objective of this thesis is to decide which geometries in the seismic data have a local tectonic origin and which are controlled by global eustatic sea-level variations. This discussion incorporates a review of the architecture of the depositional sequences and a description of their bounding surfaces. It includes an analysis of the processes that controlled the formation of the sequences and their boundaries, focusing on tectonic controls, eustatic sea-level variations, and salt tectonism.

4.1 Overview of Stratal Architecture and Structure

Each of the lower Cretaceous seismic sequences in the Terra Nova area, roughly corresponding to the Eastern Shoals, Avalon, and Ben Nevis formations, is bounded by

distinct unconformities (Figures 3.2 and 4.1). The lowermost sequence in the study area is seismic Unit A, which includes the Eastern Shoals Formation. It is bounded abruptly at its top by the Barremian unconformity ("A-seismic marker"), which is recognized in wells in the study area and regionally in the Jeanne d'Arc Basin. There is progressive angular subcrop of seismic reflections immediately below this unconformity (Figure 3.10). The Eastern Shoals Formation is an upper Barremian to lower Aptian succession consisting dominantly of interbedded sandstones, shales, and limestones, deposited in a shallow- to marginal-marine environment. The base of seismic Unit A is the B-marker limestone. Seismic sections in the study area reveal minor erosion (i.e. an unconformity) at the top of the B-marker (D. Noseworthy, pers. comm., 2002).

Unit A consists of laterally continuous reflections. Stratal patterns within the Eastern Shoals Formation in the Terra Nova field area indicate that the thickness of the unit does not vary significantly over the Terra Nova Anticline (Figure 3.8). However, there are noticeable thickness variations within the formation northward across the E-W-oriented faults in the field area, including the Trinity Fault (Figure 3.9).

Unit B, which incorporates the Avalon Formation, overlies the Eastern Shoals Formation in the study area (Figures 3.2 and 4.1). It consists mainly of sandstones and mudstones that can be divided into two main lithofacies: an interbedded sandstone and shale sequence, overlain by a subtly upward coarsening sandstone-dominated unit. The generally upward coarsening sandstones of the Avalon Formation represent a regressive phase of basin infilling which contrasts sharply with overlying depositional patterns. A shallow-marine environment is inferred for the sandstones of the Avalon Formation,

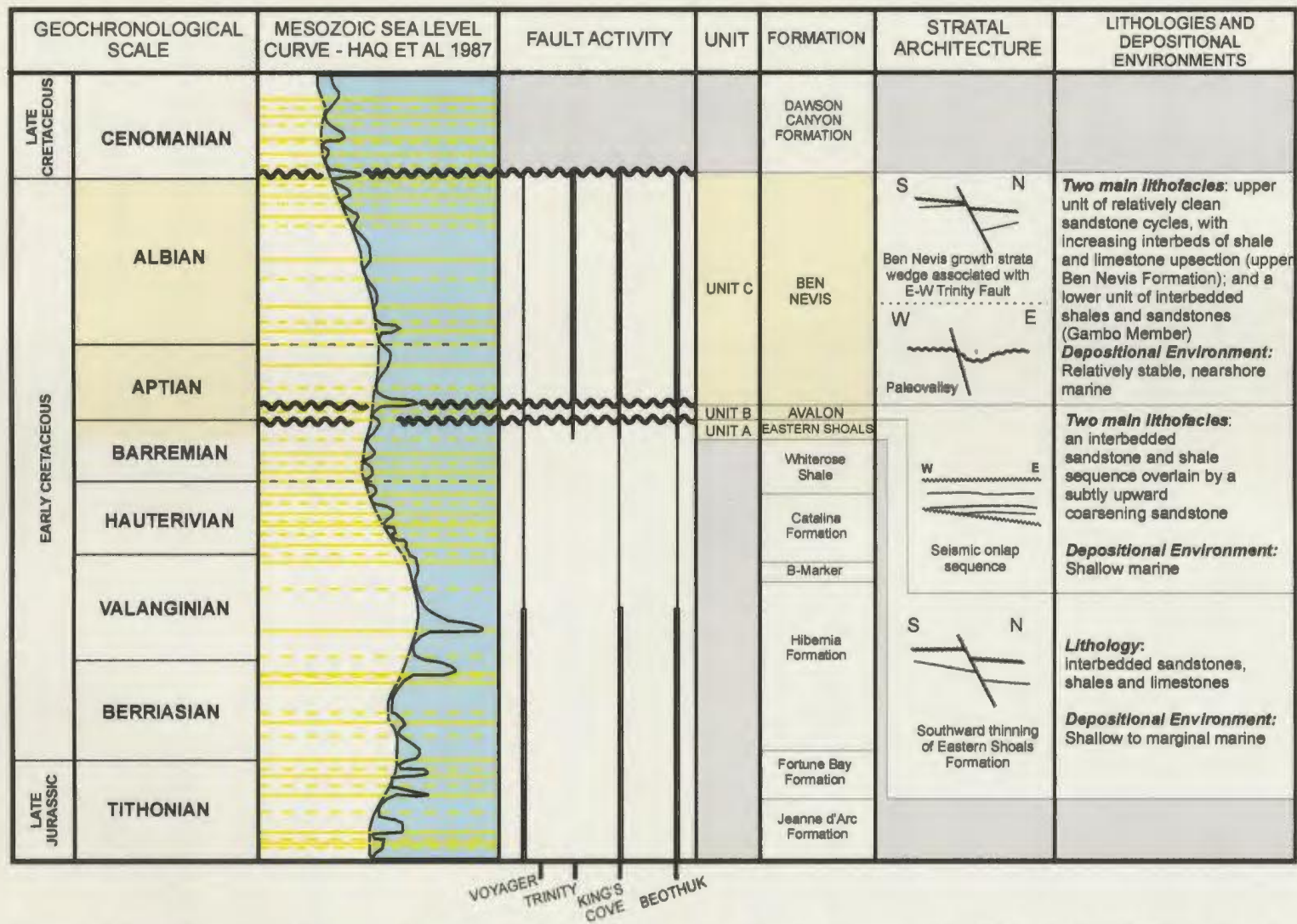


Figure 4.1 Summary diagram showing the Mesozoic sea-level curve proposed by Haq et al. (1987), inferred times of activity of the major faults in the Terra Nova field area, and the stratal architecture of depositional sequences. Fault activity is a bold line for times when significant growth is evident, and a thin line if younger rocks are cut by the fault but with limited or no growth. Units and formations considered in this thesis are shaded in light yellow; formations not considered in this thesis are shaded in grey.

confirmed by the presence of numerous foraminifera, ostracods, bivalves, gastropods, echinoderm debris, and glauconite (Petro-Canada 1985, 1986c).

The top of Unit B is the mid-Aptian unconformity, which marks the end of regression represented by the sandstones of the Avalon Formation. Seismic markers in older deposits (including seismic Unit B) subcrop at this unconformity (Figures 3.15 and 3.16). Thus, the mid-Aptian unconformity is angular in nature and cannot be explained by the preceding regression (infilling) alone; it also owes its origin to the tilting of fault blocks and erosion near the end of the deposition of the Avalon Formation. Unit B consists of moderately strong acoustic reflections which display good lateral continuity. The unit is a seismic onlap-fill sequence that overlies the Barremian unconformity and is truncated by the mid-Aptian unconformity.

The Avalon Formation is missing or is stratigraphically thinner at the eastern and southern margins of the Terra Nova field. This is partially due to depositional thinning onto the structural highs in the area. There was more erosion on the highs than in depressions where sediments of the Avalon Formation are more thickly preserved. Thickness variations are also due to erosion of the sandstones of the Avalon Formation by the mid-Aptian unconformity. This erosion was promoted by the combined actions of fault-block rotation and sea-level fall, resulting in varying erosional cuts at the top of the succession in the Avalon Formation. Erosion on the mid-Aptian unconformity, adjacent to an active fault, is also responsible for a paleovalley (Figures 3.25, 4.1, and 4.2), to the west of the Terra Nova Anticline.

Unit C includes the Ben Nevis Formation (and its Gambo Member) in the Terra

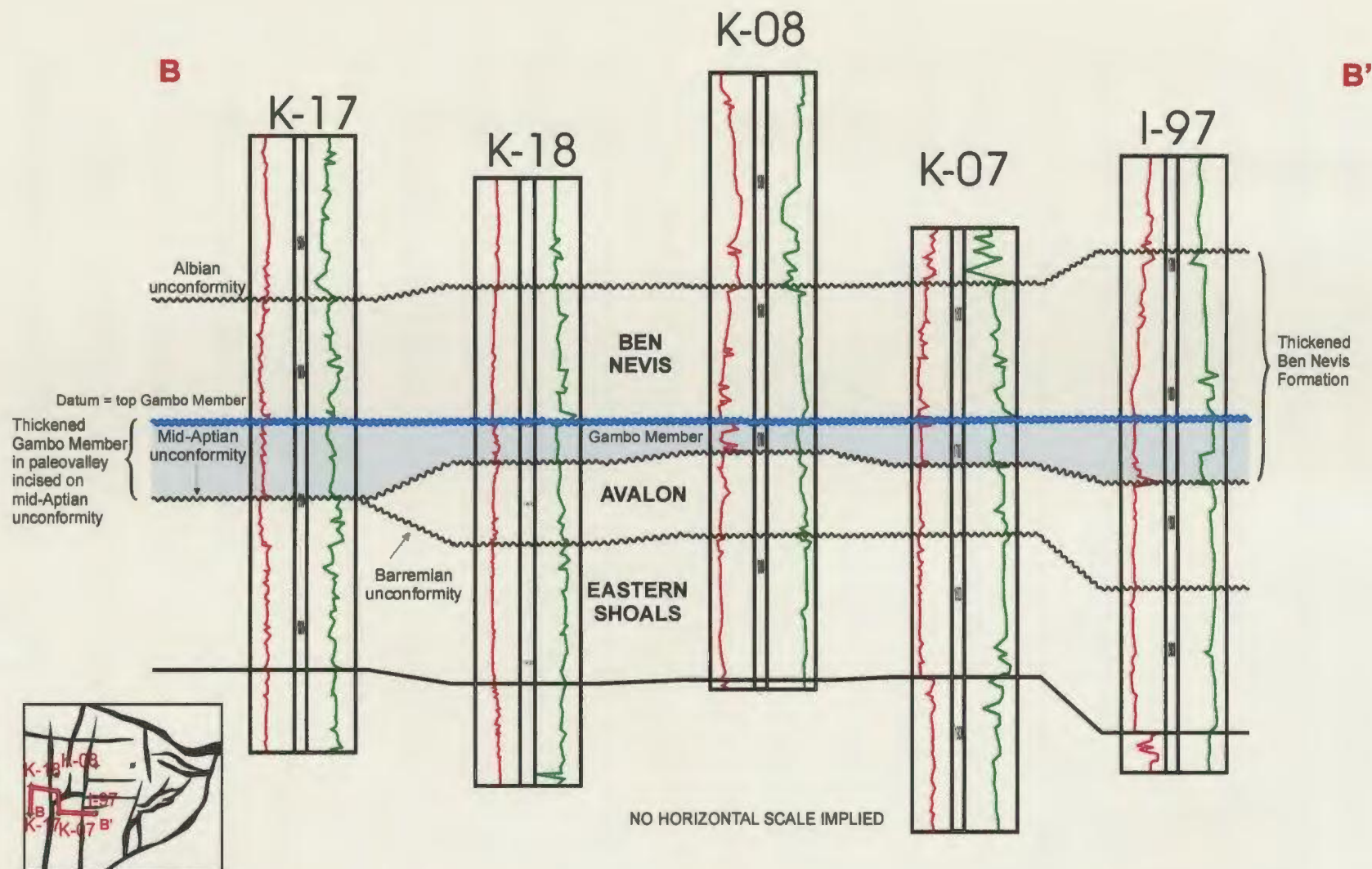


Figure 4.2 Schematic stratigraphic cross-section from Terra Nova K-17 to I-97. The wells show gamma-ray and sonic logs in red and green, respectively. This cross-section shows a thickened Gambo Member in K-17, where it filled a paleovalley incised on the mid-Aptian unconformity. The Ben Nevis Formation (including the Gambo Member) is thicker at I-97, where subsidence was accentuated during the deposition of the Ben Nevis Formation, allowing for a thickened accumulation of sediments. Location of the cross-section is shown in red on the map.

Nova field area (Figures 3.2 and 4.1). Lithologically, it consists of two main facies: an upper unit of relatively clean, stacked sandstone cycles, with increasing interbeds of shale and limestone upsection (upper Ben Nevis Formation) and a lower unit of interbedded shales and sandstones (Gambo Member). While a number of shorter cycles may be present, the overall trend is one of marine transgression. The interpreted depositional environment is a relatively stable, nearshore-marine setting (Petro-Canada, 1996). In the North Trinity H-71 well (Petro-Canada, 1986b), ball and pillow structures, as well as slump features, were noted in core 3, which suggest that at times deposition was very rapid.

Correlations among the Terra Nova I-97, K-07, and K-08 wells (Figure 4.2) indicate that the Ben Nevis Formation is thicker at the I-97 location (181 m versus 134 m and 135 m at K-07 and K-08, respectively; Table 1.2). In the absence of channelling, areas where the Ben Nevis Formation is thicker must have subsided at a faster rate during deposition of the Ben Nevis Formation, allowing for a more substantial sandstone accumulation. The Ben Nevis Formation is of intermediate thickness (approximately 145 – 160 m) at the crest of the Terra Nova Anticline (near the Terra Nova K-17 and K-18 wells). This can be attributed to deeper erosion at the mid-Aptian unconformity, so that some or all of the Avalon Formation was removed, allowing for a thicker infill of clastics of the Ben Nevis Formation. Seismically, Unit C consists of lower amplitude internal reflections than the underlying Unit B, with fair to poor lateral continuity.

The upper boundary of Unit C is unconformable to disconformable near the margins of the basin and over major structures (e.g. the Terra Nova Anticline). The

unconformity is indicated by either an angular subcrop of seismic reflections below this surface or onlap of the overlying beds onto the unconformity (Figure 3.21). The angular subcrop and seismic onlap geometries contribute to the convergence of internal reflections within Unit C. The convergence is also due to thinning over major structures, such as the Terra Nova Anticline (Figure 3.22).

Unit Ci (Gambo Member) consists of moderate amplitude reflections with fair to poor continuity. A paleovalley, which was incised on the mid-Aptian unconformity surface, was subsequently filled with sediments of the Gambo Member, as documented by the Terra Nova K-07 and K-17 wells. The Gambo Member at K-17 shows an anomalous thickness of 65 m, compared with an average thickness of 34 m for the rest of the Terra Nova field area (Figure 4.2). While this valley is difficult to trace laterally, its presence locally indicates that intense erosion took place along this unconformity surface. This erosion was at least partly induced by fault block uplift and tilting during deposition of the Gambo Member; sea-level variations possibly contributed as well. Following deposition of sediments of the Gambo Member, the paleovalley was blanketed by shoreface sediments of the upper Ben Nevis Formation and ultimately open-marine strata of the Nautilus Formation.

4.2 Origin of Unconformities

4.2.1 Tectonic controls on stratigraphic sequence development

The stratigraphic response to extensional tectonics can be determined using seismic reflection and exploratory well data and incorporating the principles of seismic

sequence stratigraphy. Seismic sequence stratigraphy allows the determination of where and when accommodation space is created and how sediments fill that accommodation. Key indicators are the stratal patterns and lithofacies preserved in the basin. Consequently, the timing of tectonic activity within a basin can be revealed and the stratigraphic response to that extension can be studied. In particular, this thesis focuses on the Early Cretaceous tectonic controls on stratigraphic sequence development.

Prior to Barremian time, during the Valanginian to Hauterivian, there was a thermal subsidence phase following the second episode of rifting in the Jeanne d'Arc Basin (Enachescu, 1986 and 1987; Sinclair, 1988). Subsequently, Barremian to late Albian times are marked by significant changes in both uplift and subsidence patterns. Unit A shows thickness increases northward across the E-W-trending fault system in the Terra Nova field area (Figure 3.9). This wedge-shaped geometry is also reflected in strata of the Avalon Formation (Unit B), where the unit thins to the south. This can be attributed to a combination of (a) increasing uplift and erosion southward toward the Avalon Uplift with (b) subsidence of the basin to the north during the late Barremian to early Aptian (Sinclair, 1993). Driscoll et al. (1995) also argue that subsidence increased from south to north, tilting the entire basin to the northeast during the deposition of both Units A and B. This is further substantiated by Sinclair (1988), who states that the Avalon Uplift was formed during two distinct phases of uplift, erosion, and non-deposition: first, during the Tithonian to early Valanginian; and second, during Barremian to Albian. The latter deformation phase is responsible for the wedge-shaped geometry.

The deposition of both the Eastern Shoals Formation (upper portions of Unit A) and the Avalon Formation (Unit B) is correlated with the “onset warp” phase of the third rifting episode in the Jeanne d’Arc Basin, which is interpreted as representing a phase of differential subsidence in the basin without significant faulting (Sinclair, 1988; Figure 4.1). Toplap (or angular subcrop) geometry, as observed at the top of Unit A, can develop in subsiding basins with falling base level, where rates of subsidence equal rates of sea-level fall (T. Calon, pers. comm., 2002).

The tilting of fault blocks during NE-SW-oriented extension, synchronous with the onset of subsidence, possibly formed the prominent angular unconformity known as the mid-Aptian unconformity. Located at the top of Unit B, the unconformity displays well-developed angularity regionally near basin margins and over major structures (McAlpine, 1990). Angular unconformities are indicative of renewed tectonic activity in any basin. The mid-Aptian unconformity indicates that parts of the basin underwent uplift and erosion immediately preceding rifting in the mid-Aptian to Albian (Sinclair, 1995). Uplift of the flanks of the basin might cause progradation because of increased sediment supply, as evidence by progradational parasequence sets of the Avalon Formation (Unit B). The large-scale erosion and tilting indicate that this unconformity is tectonically-induced. Coincidentally, Haq et al. (1987) proposed a rapid global fall in sea level at this time. If their eustatic change is truly global, rather than due to tectonic stresses (cf. Cloetingh, 1986), then the coincidence of tilting and a sea-level fall would account for the profound unconformity.

A large paleovalley was incised on the mid-Aptian unconformity and is located

adjacent to the graben-bounding N-S-trending King's Cove Fault (Figure 3.25). Relief produced by displacement during the renewed tectonic activity, combined with simultaneous erosion on the mid-Aptian unconformity, may have affected the location of the paleovalley.

Rapid thickness changes across the NW-SE-oriented faults in the basin (E-W-oriented faults at Terra Nova) are indicative of fault growth during the deposition of the Ben Nevis Formation, subsequent to formation of the mid-Aptian unconformity (Figures 3.9 and 4.1). Thus, the Ben Nevis Formation (Unit C) represents syn-tectonic deposits related to this period of basin development. In particular, these thickness trends strongly reflect tectonically induced (fault-controlled) basinal subsidence, previously noted by Sinclair (1988) and Enachescu (1986, 1987). A regional transgression was initiated at this time, which controlled the facies in the Ben Nevis Formation. The thick accumulations of transgressive strata of the Ben Nevis Formation are attributed to high sedimentation rates that kept pace with subsidence during transgression. Sediment was likely supplied from the uplifted margins of the basin (such as the Central Ridge) and down the axis of the basin. The NW-SE-trending faults in the basin (E-W-trending in the Terra Nova field area) were not active during the second rifting episode, as demonstrated by the lack of thickening of the Tithonian to mid-Hauterivian sequence toward these faults (Sinclair, 1988; Petro-Canada, 1996).

Thickness variations within the Ben Nevis Formation (Unit C) are more pronounced than those in Units A and B, indicating slower rates of faulting before deposition of the Ben Nevis Formation. The intense period of fault-induced subsidence

during this interval caused a landward retreat of the shoreline, despite massive sediment supply from the uplifted margins. The interaction between subsidence and sediment influx resulted in the deposition of a very thick Ben Nevis Formation.

Salt movement appears to have occurred during the final episode of fault growth in the Jeanne d'Arc Basin. Salt evacuation is potentially responsible for thickened Ben Nevis Formation, causing depressions (e.g. above the salt diapir; see Section 4.3.4), which rapidly filled with clastics, and growth strata wedges (e.g. to the east of the Terra Nova Anticline). Salt movement related to the lower Cretaceous succession at Terra Nova is discussed in detail in Section 4.3.4.

The Albian unconformity, which overlies the Ben Nevis Formation, was less erosive than the underlying mid-Aptian unconformity. However, the Albian unconformity is abrupt to unconformable in places, as evidenced by seismic onlap onto units below the unconformity (Figure 3.21). Thermal subsidence was initiated in the latest Albian or early Cenomanian (Hubbard et al., 1985; Hubbard, 1988; Sinclair, 1988), contributing to onlap onto the Albian unconformity.

Angular subcrop geometries at the Albian unconformity were not observed in the study area. McAlpine (1990) states that angularity is observed at the unconformity only over the most prominent regional structures and at the basin margins. McAlpine (1990) also says that the unconformity represents a base-level surface, caused by an interplay of syntectonic infill and bevelling of the Albian-age structures. Seismic onlap above this surface, regionally in the Jeanne d'Arc Basin and locally in the Terra Nova field area, indicates that the basin was eventually subsiding faster than sediment was infilling it.

Shales of the Nautilus Formation, which overlie the Albian unconformity, represent accumulation during the thermal phase of subsidence associated with the last episode of rifting on the Grand Banks.

A “break-up unconformity” has been defined by Falvey (1974) as the unconformity that is approximately time-equivalent with the onset of seafloor spreading along many passive continental margins. The age of a true break-up unconformity should coincide with the time when rifting stopped and seafloor spreading began (Falvey, 1974; Hubbard et al., 1985; Tankard and Welsink, 1987; Boillot and Winterer, 1988; Meador and Austin, 1988; Meador et al., 1988; Austin et al., 1989; Tankard et al., 1989; Tucholke et al., 1989; Embry and Dixon, 1990). This unconformity separates syn-rift from post-rift (drift) strata. However, in some cases, the age of the last major unconformity before the drift phase is younger than the onset of seafloor spreading in a region (Falvey, 1974; Tankard et al., 1989). This might be because the unconformity represents the final episode of brittle deformation within an extensional setting, instead of the onset of seafloor spreading (Karner et al., 1993; Driscoll and Hogg, 1994). Thus, determining the exact timing of the onset of seafloor spreading remains problematic in many basins, including the Jeanne d’Arc Basin. In terms of basin tectonics, however, the “break-up unconformity” can still be used to resolve the end of rifting in the basin. Most researchers interpret the end of active rifting in the Jeanne d’Arc Basin to have occurred in the latest Albian (Hubbard et al., 1985; Hubbard, 1988; Enachescu, 1986 and 1987; Sinclair, 1988, 1993 and 1995; Hiscott et al., 1990; and McAlpine, 1990). Thus, the cessation of rifting in the Jeanne d’Arc Basin is marked by the Albian unconformity.

4.2.2 Eustatic controls on stratigraphic sequence development

There is close correspondence between the sequence boundaries (unconformities) seen at the Terra Nova field and the eustatic sea-level lows recognized by Haq et al. (1987). In particular, the mid-Aptian and Albian unconformities and their correlative conformities show good correlation with the eustatic sea-level falls which Haq et al. (1987) identify as 112 Ma and 98 Ma second-order sequence boundaries, respectively (Figure 4.1). The Barremian unconformity could be correlated with the sea-level fall that Haq et al. (1987) propose as a 113 Ma second-order sequence boundary; however, this is a less-pronounced fall on the sea-level chart than those interpreted for the mid-Aptian and Albian unconformities. Haq et al. (1987) also interpret a period of long-term eustatic sea-level rise from the mid-Aptian to late Albian, which corresponds to a regional transgression in the Jeanne d'Arc Basin that deposited the Ben Nevis Formation. The Avalon Formation was deposited during the final stages of a proposed global sea-level fall, corresponding to a regressive period in the Jeanne d'Arc Basin.

There is no doubt that depositional systems and their seismic expression are strongly affected by eustatic fluctuations that occur during basin formation. However, these fluctuations will not necessarily dominate or obscure tectonic effects. This is especially so in areas most affected by tectonic processes, for example close to active faults. In an actively rifting half-graben, it is unlikely that eustasy is the overriding control over aggradation, progradation, and retrogradation (Cloetingh, 1986; Prosser, 1993). Hiscott et al. (1990) state that rapid eustatic fluctuations are difficult to explain for this part of the Mesozoic, when there were no large ice caps to drive glacio-eustatic

fluctuations.

Assuming the eustatic fluctuations proposed by Haq et al. (1987) are accurate (for an example of a contrary view, see Miall, 1994), it remains questionable that such variations could explain the characteristics of the Early Cretaceous unconformities and the architecture of the sequences at the Terra Nova area. As pointed out by Sinclair (1993), the 112 Ma sequence boundary (mid-Aptian) of Haq et al. (1987) has been ascribed to a 75 m drop in sea level, occurring in less than one million years. The amount of erosion evident at this unconformity in the study area (e.g. the paleovalley incised on the unconformity and the missing Avalon sections in the King's Cove A-26, Terra Nova K-17, and North Trinity H-71 wells) cannot be accounted for solely by a eustatic sea-level fall. Tectonism must account for the uneven spatial distribution of this erosion on adjacent fault blocks that were simultaneously rising and subsiding (Sinclair, 1993).

In addition, eustatic sea-level variations alone cannot adequately account for the extremely thick accumulations of syn-rift sediments of the Ben Nevis Formation deposited throughout the Jeanne d'Arc Basin and locally in the hangingwall of the E-W-trending fault system in the Terra Nova field. During the mid-Aptian to late Albian period, Haq et al. (1987) propose a sea-level rise of about 75 m over 14 million years, which cannot explain the large amount of accommodation space required to deposit the large sediment thicknesses in the Ben Nevis Formation (264 m at the North Trinity H-71 well, which is located in the hangingwall of the Trinity Fault, versus 141 m and 153 m in the Terra Nova H-99 and E-79 wells, respectively, both located south of the Trinity Fault; Table 1.2). Tectonism (i.e. fault block subsidence and rotation) must therefore be the

principal cause for the differential and thick deposition. Hiscott et al. (1990) claim that the widespread mid-Aptian unconformity coincides with the separation of the Grand Banks from Iberia and the first formation of oceanic crust in the North Atlantic. The large-scale erosion and tilting at this time clearly point to a tectonically-induced unconformity, although Haq et al. (1987) interpret a rapid global fall in sea level at this time (Hiscott et al., 1990).

Tectonism was also the dominant factor controlling the formation of the Albian unconformity. Changes in depositional styles across the unconformity, from the Ben Nevis Formation to the overlying Nautilus Formation, cannot be accounted for solely by a continued rise of eustatic sea-level into the Cenomanian (Sinclair, 1993). Although a eustatic rise could explain flooding of the eroded basin margins, it cannot account for the end of fault-controlled subsidence and rotation (Sinclair, 1993). If subsidence had persisted and eustatic sea level had risen, there would be evidence of sediment thickening into the subsiding basin or condensed sections in a deep-water basin. None of these features are seen in the Jeanne d'Arc Basin. Instead, the end of faulting and the flooding of the basin margins is interpreted to indicate the onset of post-rift regional subsidence (Sinclair, 1993).

Another concern is the age of the unconformities as determined from biostratigraphy. Only vague biostratigraphic reports are available for the sedimentary successions in this study; in fact, no data are available at all for the Avalon Formation in the Terra Nova area. Therefore, determining the exact ages of the successions and their bounding unconformities based on microfossil occurrences remains difficult. As a

consequence, correlation of the Barremian, mid-Aptian, and Albian unconformities in the study area, as determined from well and seismic data, to the sequence boundaries of Haq et al. (1987), remains imprecise and potentially circumstantial.

4.3 Development of Structures in the Terra Nova Field Area

4.3.1 Fault systems

Faults in the study area are generally well defined down to the Hibernia Formation, where the fault geometries start to become complex as faults that are older than the Hibernia Formation begin to merge at depth. The timing of fault movement was determined using thickness variations between prominent sequence boundaries.

The faults in the Terra Nova field area (and in the Jeanne d'Arc Basin overall) belong to two associated and intersecting extensional fault systems (N-S- and E-W-trending) that fragment the Jeanne d'Arc Basin. The main antithetic to the Murre Fault is the large NE-SW-trending Voyager Fault, which marks the eastern limit of the field area. In the study area, the faults trending approximately north—south are antithetic and synthetic to this major fault. The E-W-trending faults are generally minor faults with smaller throws, except the Trinity Fault, which records a large throw in the lower Cretaceous strata.

Faults in the N-S system are roughly parallel to the basin-bounding Murre and Voyager Faults. The faults have dips of 40 – 60° and consist of two sets: an easterly-dipping set and a westerly-dipping set. The King's Cove and Beothuk Faults bound the western and eastern flanks of the keystone graben at the top of the Terra Nova Anticline,

and are the main N-S-trending faults in the study area. Salt is interpreted to sit immediately below the footwall of the graben, resting against the Beothuk Fault (Petro-Canada, 1996).

Extension and salt migration also promoted uplift west of the King's Cove Fault (Petro-Canada, 1996). As this N-S-trending fault system was reactivated in the mid-Aptian to Albian (Figure 4.1), extension and salt movement caused the cover rocks in the region to detach, resulting in an uplifted area surrounding Terra Nova wells K-17 and K-18 (that is, the West Flank).

The thickness variations (fault growth strata) within the Tithonian to mid-Valanginian (in particular the top Hibernia to top Rankin formations) indicate that the N-S-trending fault system was active during this period of deposition (Petro-Canada, 1996; Figure 4.1). Angular subcrop and the amount of thinning by erosion below the top of the marker defining the top of the Eastern Shoals Formation suggests that growth was accentuated during the deposition of the upper part of Unit A. The King's Cove and Beothuk Faults were initiated during the second rifting episode, but were reactivated in the mid-Aptian to early Albian (Figure 4.1), during the formation of the Terra Nova Anticline (see Section 4.3.2), as shown by the offset of seismic reflections within Eastern Shoals and Avalon formations. They remained active during the deposition of the Ben Nevis Formation, as evidenced by growth strata associated with the formation of the Terra Nova Anticline.

The NE-SW-trending fault system in the Jeanne d'Arc Basin swings to a E-W-trending fault system at Terra Nova (Sinclair, 1995). Most of the E-W-trending faults in

the Terra Nova field area are minor and have small throws, with the exception of the Trinity Fault. There is significant growth northward across the Trinity Fault within Unit C (Ben Nevis Formation). Seismic data convincingly show the mid-Aptian to Albian sedimentary sequence thickens to the north. The fault was therefore active from at least mid-Aptian to Albian time (Figure 4.1). The Avalon Formation (Unit B) is eroded northward across the Trinity Fault and is not present in the North Trinity H-71 well, where the Gambo Member of the Ben Nevis Formation lies directly above the Eastern Shoals Formation. Thus, the mid-Aptian unconformity was quite erosive in the region north of the Trinity Fault.

The Eastern Shoals Formation shows thickness increases northward across the E-W-trending fault system in the study area. This system was previously interpreted to have formed during the mid-Aptian to Albian during NE-SW-oriented extension (Enachescu, 1986 and 1987; Sinclair, 1988). However, growth strata patterns within the Eastern Shoals Formation suggest instead that the E-W-trending fault system at Terra Nova was initiated by at least the late Barremian. This fault system terminates upwards against the Albian unconformity, when active rifting in the Jeanne d'Arc Basin is interpreted to have ceased.

4.3.2 Terra Nova Anticline

The Terra Nova field area is located in a restraining bend of the Voyager Fault (Sinclair, 1993; Enachescu et al., 1997). The Voyager Fault is a large, listric, west-dipping extensional fault with an associated rollover anticline in the hangingwall. This

large rollover anticline, located to the west of the Voyager Fault, is called the Terra Nova Anticline (Figure 3.22) and formed in response to mid-Cretaceous, NE-oriented tensional stresses and associated deep-seated salt migration (Petro-Canada, 1996). The structure is interpreted to be salt-cored (Sinclair, 1993). The salt rests against the west-dipping Beothuk Fault and contributed to the irregular relief on the anticline (Petro-Canada, 1996). The anticlinal structure is complicated by a keystone graben located at its crest, commonly referred to as a crestal collapse graben (cf. McClay and Ellis, 1987). A crestal collapse graben is bounded by planar antithetic and synthetic faults that form during extension (McClay and Ellis, 1987). Such graben are produced by extension of the developing rollover anticline above a listric ramp/flat geometry. The architecture of the Terra Nova Anticline was further accentuated by subsequent subsidence and salt migration (Petro-Canada, 1996).

The keystone graben in the study has a funnel-shaped geometry in map view and strikes NE-SW. Its width varies from approximately 2 km in the south to 5 km in the north; along strike, it extends approximately 15 km (Petro-Canada, 1996). It is likely that the graben extends further to the south, but its extension is unknown because of limited seismic coverage in the area. It is bounded to the west by the east-dipping King's Cove Fault and to the east by the west-dipping Beothuk Fault. There are several other subsidiary high-angle faults present in the area of the graben, which are similar in orientation to the graben-bounding faults. Thus, a conjugate system of high-angle normal faults dominates the structure around the crest, and east in the flank of the anticline.

The strata in the study area can be used to determine the age of formation of the

Terra Nova Anticline. Interpreted pre-growth strata (Avalon Formation) are present in the hangingwall of the Voyager Fault, but are truncated by an unconformity (the mid-Aptian unconformity), which is also folded. The mid-Aptian unconformity records a major fall in base level in the basin or a significant increase in the rate of uplift relative to sedimentation (at fixed base level) during the formation of the Terra Nova Anticline (T. Calon, pers. comm., 2002). Syn-growth strata, represented by the Ben Nevis Formation, are present in the asymmetric half-graben (Figure 4.3). Part of this fill is attributed to the rise of the anticline and part is associated with the emplacement of salt in the area (discussed in Section 4.3.4).

The timing of the formation of the Terra Nova Anticline remains difficult to constrain because most of the strata that have been interpreted as pre-growth have been eroded beneath the mid-Aptian unconformity. Since the unconformity is folded over the anticline, one would assume that the unconformity pre-dates the formation of the anticline. It is also possible that part of the growth of the anticline pre-dates the unconformity, but the erosion of the upper portion of the Avalon Formation that might have recorded such growth makes this impossible to establish.

A small growth strata wedge within the Avalon Formation (below the unconformity) in the western part of the field (Figure 4.3), where there is onlap onto the Barremian unconformity, might indicate that sediments of the Avalon Formation were being deposited during the rise of the anticline. However, the upper portions of this wedge are also eroded by the mid-Aptian unconformity and the wedge extends beyond the western limits of the seismic survey block. With the presently available data, the

anticline can be estimated to have formed sometime in the late Barremian to Aptian. The evidence for this timing is: (a) folding of sediments that are older than late Barremian (and have uniform thickness) over the anticline; and (b) the termination of growth faulting associated with formation of the anticline at the base of the Ben Nevis Formation.

4.3.3 Transpressional structures

Transpressional stresses have been interpreted to have caused numerous structures in the Jeanne d'Arc Basin. Sinclair (1995) suggested that the anomalous E-W-oriented faults in the Terra Nova area were caused by the rotation of NE-SW-directed extension found elsewhere in the Jeanne d'Arc Basin to N-S-directed extension in the Terra Nova area. This hypothesis was used by Sinclair (1995) to explain the formation of local structural inversion elements in the basin, including the Terra Nova Anticline and the "pop-up" feature located immediately to the west of the Voyager Fault. These inversion structures were thus interpreted to have been controlled by induced oblique-slip transpression (Sinclair, 1995). This explanation is an alternative to the hypothesis that salt movements controlled the development of these structures in the study area, as discussed later in Section 4.3.4.

Stratal patterns within Cretaceous sediments indicate that the NW-SE-trending fault system (in the Jeanne d'Arc Basin) and the E-W-trending faults (in the Terra Nova field) were active during the third rifting episode to have affected the basin, in the mid-Aptian to late Albian (under dominantly NE-SW-oriented extensional stresses). Sinclair

(1995) has interpreted the NE-SW-oriented faults (initiated during the first rifting episode) to have been conveniently oriented for strike-slip reactivation under the new NE-SW-directed extensional stress regime of the third rifting episode. The association of sinistral faults, to accommodate strike-slip motion, created a series of restraining and releasing bend pairs (Sinclair, 1995; Woodcock and Fisher, 1986). Partial inversion of an extensional structure by later oblique-slip at a restraining bend could account for pop-up features (Sinclair, 1995), such as the one seen in the study area.

Both the Terra Nova Anticline and the “pop-up” feature in the study area are located in a restraining bend of the Voyager Fault (Sinclair, 1993; Enachescu et al., 1997), which was active during the third rifting episode. According to Sinclair (1995), the N-S-orientation of the anticline, as well as the pop-up, is compatible with the development of transpressional folds oblique to the Voyager Fault during NE-SW-oriented extension, in the mid-Aptian to late Albian.

4.3.4 Salt structures

A complex extensional tectonic history is recorded in strata of the Jeanne d’Arc Basin. Existing structural styles were modified, and new structural styles were created, by subsequent salt mobilization (Jansa et al., 1980; Grant et al., 1986). Salt in the Jeanne d’Arc Basin is provided by the Argo Formation, which was deposited during the Late Triassic to Early Jurassic stage of rifting in an epicontinental sea (McAlpine, 1990). In the study area, the main elements linked to salt tectonics include: an active salt diapir in the footwall of the Voyager Fault; associated growth strata wedges, recording growth and

movement of the diapir; and a “pop-up” feature and graben (at the crest of the salt diapir), both related to the later stages of salt movement in the footwall of the Voyager Fault (Figures 4.3 and 4.4).

There is a strong suggestion, based on the model of Jackson and Vendeville (1992 and 1994) that a large salt diapir lies in the footwall of the Voyager Fault (T. Calon, pers. comm., 2002). This creates a noticeable contrast in the geometry and structural style between the two domains west and east of this large diapir (Figure 4.3 and 4.4). To the west, a large rollover (Terra Nova Anticline) and a keystone graben are present in the hangingwall of the Voyager Fault. A “pop-up” feature is located immediately to the west of the Voyager Fault. To the east, the geometry is structurally complex with numerous faults. There is a large salt diapir sitting in the footwall of the basin-bounding fault, with a graben sitting at its crest (Figure 4.4B).

Jackson and Vendeville (1994) compellingly argue that salt diapirism is facilitated by regional tectonic extension of the overburden¹, leading to the development of so-called *reactive diapirs*. Comparison with the Jackson and Vendeville model (1992 and 1994) suggests that the footwall diapir seen in the Terra Nova area evolved rapidly from a reactive to an active structure (T. Calon, pers. comm., 2002). The hangingwall strata record the evolution of a late rollover anticline (Terra Nova Anticline) and were folded and deformed during this active phase of diapirism. Similarly, the footwall strata are deformed and cut by several faults to the east of the Voyager Fault. Consequently, the active diapir has inflicted serious distortion on the pre-growth strata in both the

¹ Overburden consists of strata which is younger than the salt source layer. It is generally used as a stratigraphic term rather than as a structural term (Jackson and Talbot, 1991)

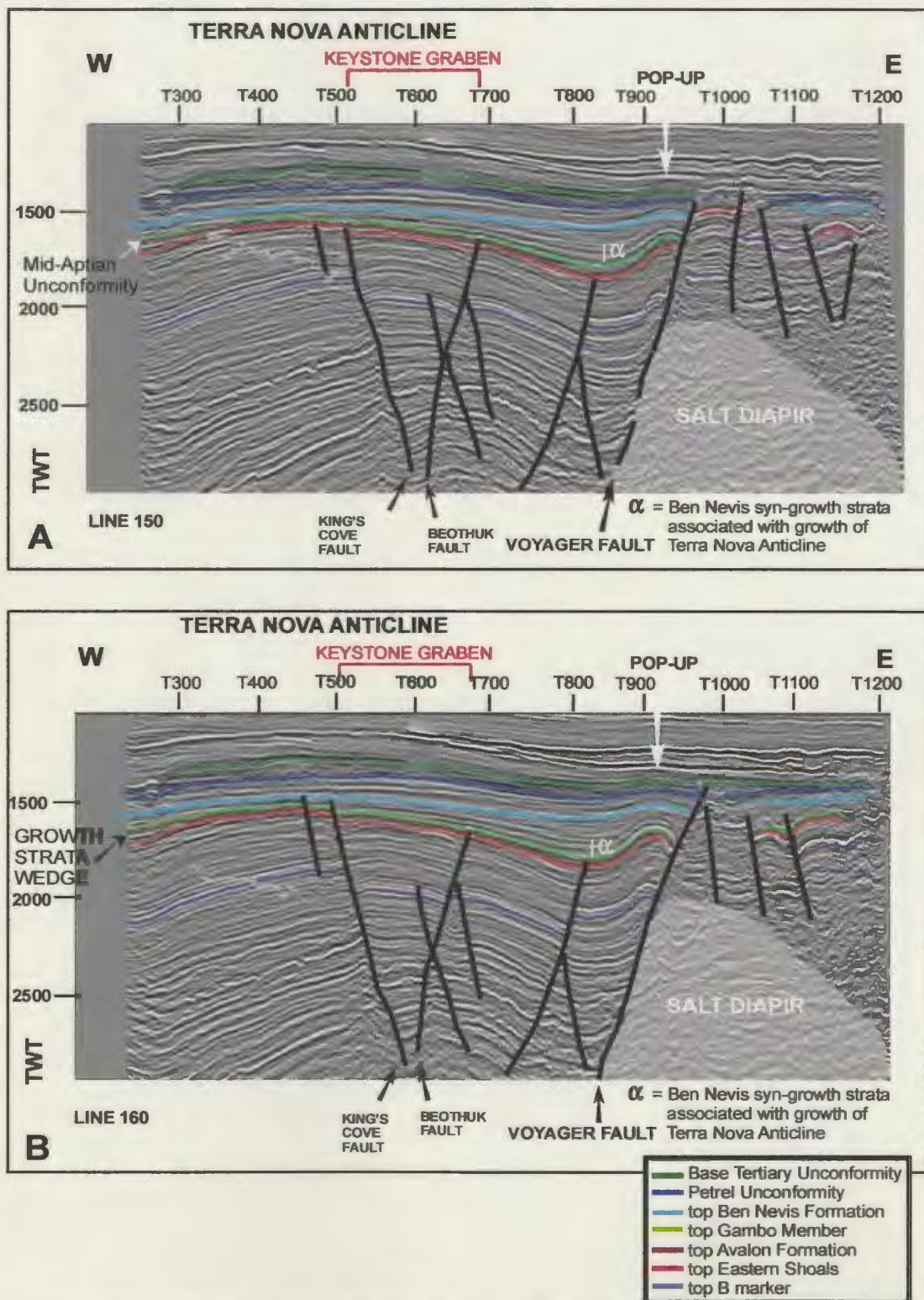


Figure 4.3 Lines 150 (A) and 160 (B) showing the location of the Terra Nova Anticline and the keystone graben. Syn-growth strata within the Ben Nevis Formation are related to the formation of the anticline and are shown in (A). A small growth strata wedge within the Avalon Formation is illustrated in (B). The location of a large salt diapir and associated “pop-up” feature are also illustrated. See Figure 3.1 for seismic line locations.

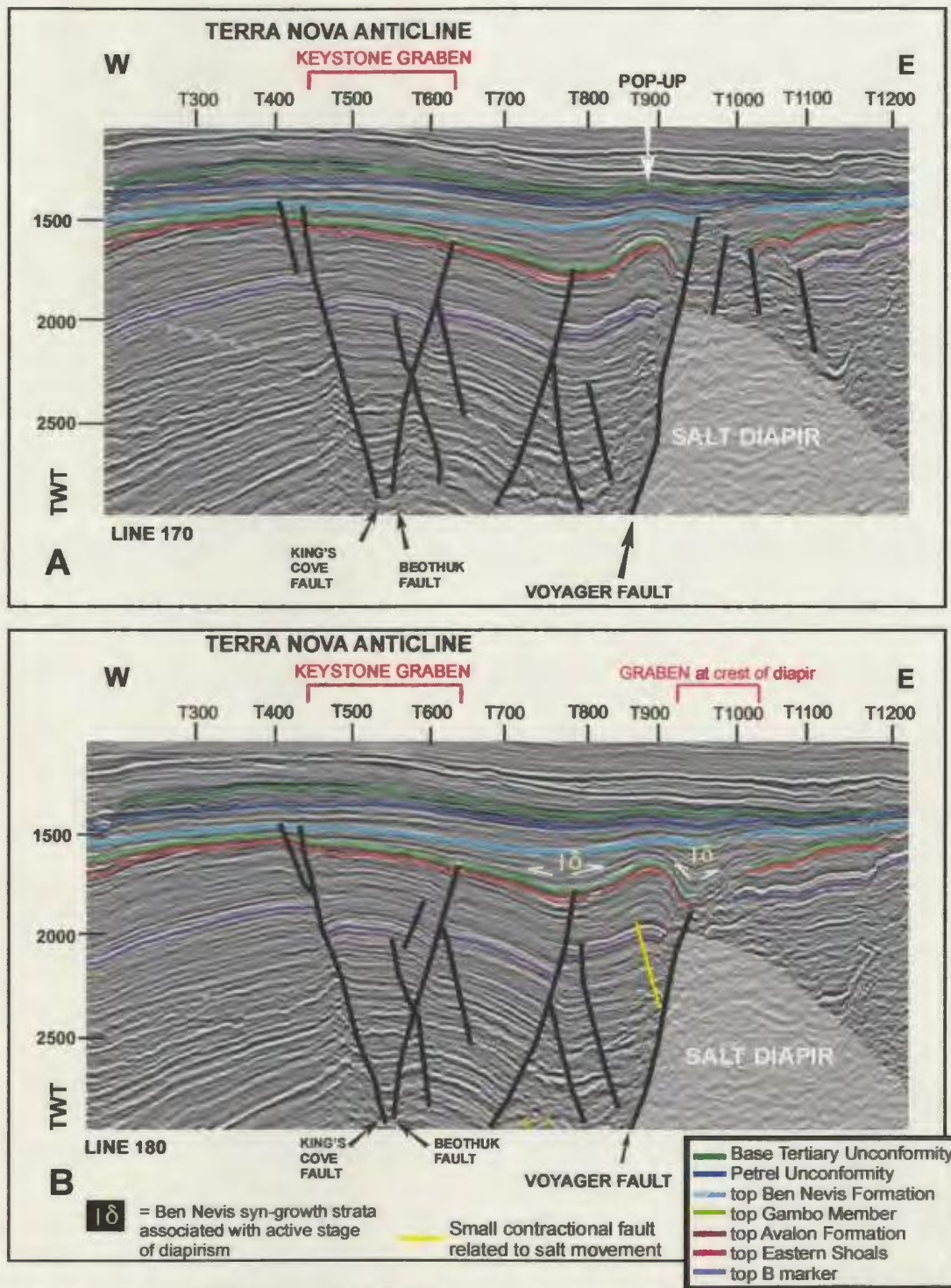


Figure 4.4 Lines 170 (A) and 180 (B) showing the approximate outline of a salt diapir. The locations of the “pop-up” feature and graben associated with the movement of the diapir are also noted. The small contractional fault indicated in (B) is related to the late stage of plugging and uprising of the diapir. Onlap geometry (white arrows in B) in the lower portions of the upper Ben Nevis Formation, and growth strata wedges in the upper portions of the Ben Nevis Formation (indicated in B), document the active stage of diapirism. See Figure 3.1 for seismic line locations.

hangingwall and footwall domains to the west and east of the fault, respectively. Both the “pop-up” and the graben that sits at the crest of the diapir are interpreted as subsidiary structures related to the later stages of salt movement in the footwall of the eastern basin-bounding fault.

The “pop-up” to the west of the Voyager Fault can be interpreted as a localized contractional feature related to diapirism (T. Calon, pers. comm., 2002). It formed either simultaneously with, or just after, the formation of the Terra Nova Anticline. The pop-up shows arching of Eastern Shoals, Avalon, and Ben Nevis formations (only the Gambo Member), indicating that it post-dates the deposition of these successions. There is onlap geometry seen in the lower parts of the upper Aptian to Albian Ben Nevis Formation, just above the Gambo Member (Figure 4.4 B). Thus, the pop-up must have formed during the deposition of these sediments, in the late Aptian or early Albian. Growth strata wedges within the upper portion of the Ben Nevis Formation, to the west of the pop-up and to the east in the graben that sits at the crest of the diapir, document this active stage of diapirism (Figure 4.4 B).

The graben at the crest of the diapir to the east of the Voyager Fault is also related to salt movement in the footwall. However, it is difficult to determine whether the graben is a “withdrawal graben”, attributed to the fall of the footwall diapir, or whether it is related to the formation of the pop-up feature seen to the west, which formed during salt emplacement.

4.4 Implications for Hydrocarbon Occurrences

The Avalon and Ben Nevis formations together form one of the most important petroleum systems in the Jeanne d'Arc Basin. They are the main reservoir rocks at such fields as Hibernia, White Rose, and the Ben Nevis/West Ben Nevis Complex. At Terra Nova, although they consist of excellent reservoir rocks, these formations are mostly water-saturated and hence do not contain hydrocarbons. In particular, wells to the west of the N-S-trending King's Cove Fault tend to contain only minor hydrocarbon shows within both the Ben Nevis and Avalon formations and older successions. This fault was initiated during the second rifting episode in the Jeanne d'Arc Basin (Tithonian to Valanginian), but was re-activated during Aptian to Albian (Sinclair, 1995). The Terra Nova Anticline developed during the Aptian. There is a heavy oil accumulation within the Ben Nevis Formation, which has an average porosity of 24%, in the Terra Nova K-17 well, located to the west of the fault (RFS #1 and DST #2, Table 2.3). Wells to the east of the King's Cove Fault contain more significant volumes of oil and oil inclusions² in the Jeanne d'Arc, Ben Nevis, Avalon, and Dawson Canyon formations (e.g., Parnell et al., 2001). Possible explanations for hydrocarbon charge within the lower Cretaceous succession at Terra Nova and the contrasting hydrocarbon presence in wells to the east and west of the King's Cove Fault are provided below. The aim is to clarify why the Ben Nevis and Avalon formations are water-saturated in the Terra Nova field area.

The fact that the Ben Nevis and Avalon formations are generally water-saturated

² Fluid inclusions are micro-scale, fluid-filled isolated cavities in or between crystals in rock material. They form during subsurface diagenetic processes in which cement is added to intergranular pore space or microfractures. They track the movement of aqueous and petroleum fluids (Fluid Inclusion Technologies Inc., 2002)

instead of hydrocarbon-bearing in the Terra Nova field area implies that: (a) reservoirs were charged at some point but were subsequently breached (particularly to the west of the King's Cove Fault), allowing oil to be flushed out of the traps; (b) there was not an effective seal formed in certain areas of the field (in particular, to the west of the King's Cove Fault) or there was no effective up-dip termination of the reservoir facies; (c) oil migration followed an alternative pathway, thus no oil and/or gas entered the reservoir; or (d) the local trap formed too late; that is, after the movement of oil and gas through the reservoir rock (Levorsen, 1967; Parnell et al., 2001).

The stratigraphy of the Jeanne d'Arc Basin, the age of source, reservoir and seal rocks, the timing of trap formation, and the timing of generation, migration, and accumulation of hydrocarbons in the basin are presented in Figure 4.5. This diagram indicates that trap formation took place during the last two rifting episodes in the Jeanne d'Arc Basin: first, during the Tithonian to Valanginian; and second, during late Barremian to Albian. Figure 4.5 clearly shows that oil migration took place either during or subsequent to trap formation (cf. Creaney and Allison, 1987; von der Dick et al., 1989; Williamson, 1992; Fowler and McAlpine, 1994; Parnell et al., 2001), thus ruling out option (d) above. Also, data from Parnell et al. (2001) indicate that there are oil inclusions within the now-barren Ben Nevis and Avalon formations in the Terra Nova field area, indicating that these formations once acted as reservoirs, thus also ruling out option (c). To support this idea, Parnell et al. (2001) point out that although fluid inclusion studies are not normally performed to distinguish between rocks that have acted as hydrocarbon reservoirs and those which are merely migration pathways, areas where

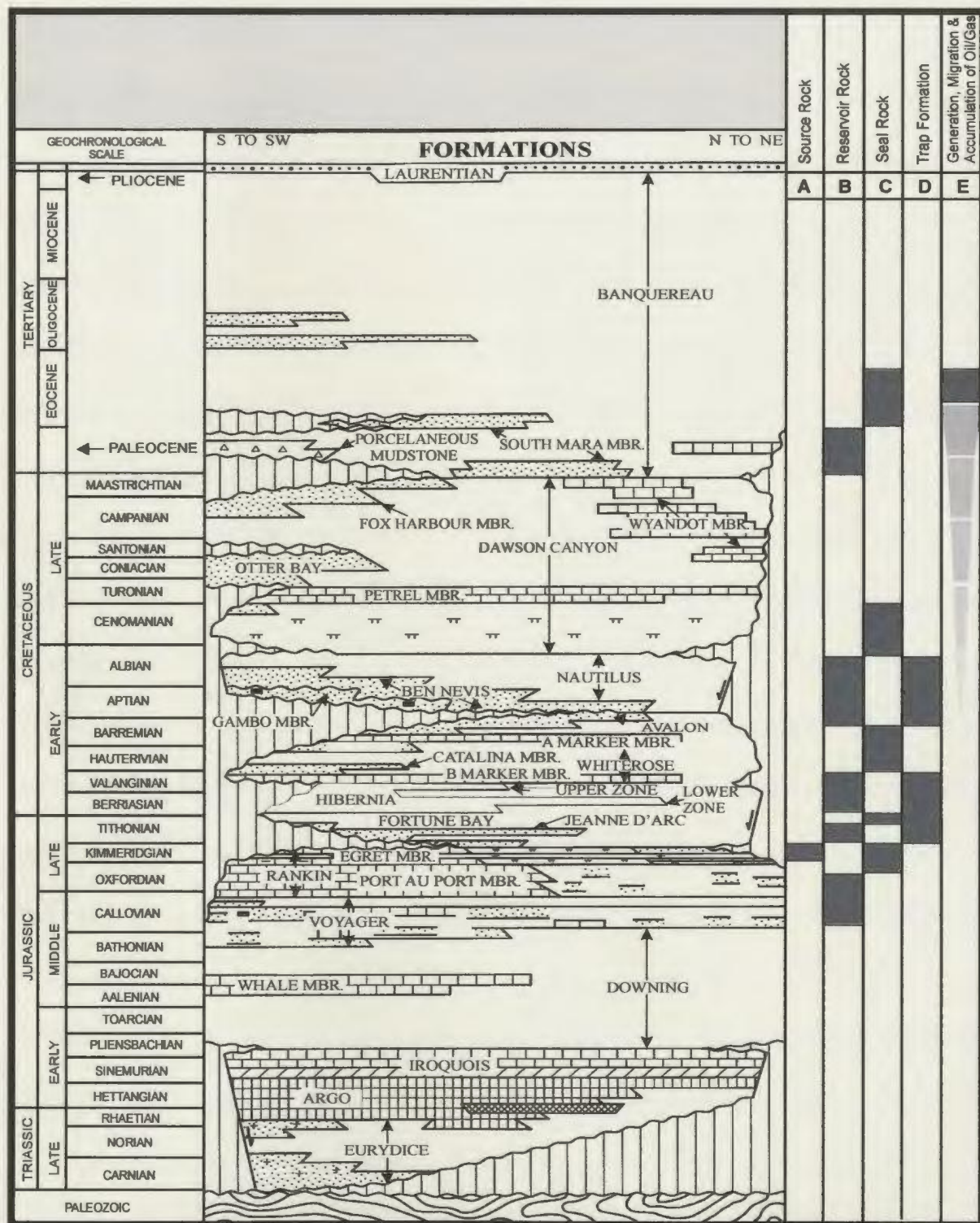


Figure 4.5 Petroleum Systems Events Chart (modified from De Silva, 1999, and Parnell et al., 2001), showing the lithostratigraphy of the Jeanne d'Arc Basin, along with: the temporal distribution of source (A), reservoir (B), and seal (C) rocks; the timing of trap formation (D); and the timing of generation, migration, and accumulation of hydrocarbons (E). The heavily highlighted section in Column E indicates late oil migration; however, fluid inclusion stratigraphy (FIS) studies by Parnell et al. (2001) show an earlier (Cretaceous) oil charge (gradually darkening and widening pattern in Column E).

oil inclusions are abundant in cements as opposed to microfractures are indicative of reservoir conditions. Also, where aqueous and oil inclusions are both present, the system was probably water-wet and acted as a migration pathway. Since there are abundant oil inclusions, and an absence of coeval aqueous inclusions, Parnell et al. (2001) conclude that these formations acted as reservoirs, not migration pathways. Therefore, the remaining plausible explanations for the water-wet Ben Nevis and Avalon formation in the study area is option (a); options (b), (c), and (d) are all eliminated.

Parnell et al. (2001) support the hypothesis that the Barremian to Albian succession west of the King's Cove fault, now barren of oil, were once oil-charged (and acted as reservoirs) but have since been breached. This is based on the presence of oil inclusions and fluid inclusion stratigraphy³ (FIS) results (Parnell et al., 2001), and is further substantiated by Levorsen (1967), who states that oil showings and oil-stained reservoir facies suggest that the oil was once present but has since moved out. According to Parnell et al. (2001), oil inclusions in Terra Nova K-18 prove that the porous Ben Nevis and Avalon formations in this well once acted as reservoirs. They also demonstrate that wells to the east and west of the King's Cove Fault show very similar values for bulk volatile analysis³, despite the fact that only wells east of the fault presently contain oil. If oil had migrated into the eastern wells first, higher hydrocarbon responses (based on bulk volatile chemistry) would be expected; however, since the volatile chemistry is the same, both the eastern and western wells probably shared a

³ Fluid inclusion stratigraphy (FIS) is the stratigraphic mapping of paleofluid chemistries through bulk mass spectrometric analysis of fluid inclusion volatile species, inorganics and organics to C13 (Fluid Inclusion Technologies Inc., 2002)

related charge history (Parnell et al., 2001). The similar hydrocarbon responses further support the suggestion that the sandstones west of the fault once acted as reservoirs, not simply transient migration pathways (Parnell et al., 2001).

There is an exception to the hypothesis that the sandstones to the west of the King's Cove Fault once acted as reservoirs but have subsequently been breached; that is, an oil accumulation in the Ben Nevis Formation at the K-17 well site (Table 2.3). Breaching likely occurred along particular faults, so depending on reservoir geometry could not be expected to drain all the oil present in the reservoir. It is believed that the oil at K-17 remained because it was updip from the drainage point in that part of the reservoir, but drained at all other locations. Also, the hydrocarbon accumulation at K-17 consists of heavy, biodegraded⁴ oil, which now makes the hydrocarbons more viscous and prevents their easy escape from the reservoir. Thus, at the K-17 well location, it is hypothesized that breaching of the trap did not allow hydrocarbons to escape, unlike at other areas in the Terra Nova field area where there are presently no hydrocarbons. Flexing and bending of strata to the immediate west of the King's Cove Fault, adjacent to the K-17 well (as evidenced on seismic) could have provided the remaining closure updip of the fault; this flexing is not present at the K-18 site, thus no fault existed to prevent drainage.

⁴ Biodegradation is defined as the destruction of petroleum and related bitumen by bacteria (Hunt, 1996) and is one of the primary processes responsible for the degradation of petroleum in the Jeanne d'Arc Basin (Williamson et al., 1995).

CHAPTER FIVE: CONCLUSIONS

The study of the lower Cretaceous succession at Terra Nova, incorporating the Eastern Shoals, Avalon, and Ben Nevis formations, reveals the following significant conclusions:

- 1 The formation of the sequences and their bounding unconformities at Terra Nova was controlled by an interplay of tectonism, sediment input, changes in sea level, accommodation space, and climate. However, the large-scale erosion and tilting of fault blocks, along with the differential and thick deposition during the mid-Aptian to Albian (Ben Nevis Formation), indicate that tectonism (i.e., fault-block subsidence and rotation) must be the principal cause of sequence development in the Terra Nova field.
- 2 The E-W-trending fault system in the Terra Nova field was previously interpreted to have formed during the final rifting episode to have affected the Jeanne d'Arc Basin, during the mid-Aptian to Albian (Enachescu 1986, 1987; Sinclair, 1988). However, growth strata within the Eastern Shoals Formation indicate that this fault system was initiated by at least the late Barremian. Most of the faults in the Terra Nova field area terminate upward against the Albian unconformity. Therefore, active rifting in the Terra Nova area is interpreted to have ended by the late Albian.
- 3 The "pop-up" structure to the immediate west of the Voyager Fault in the Terra Nova field area has been interpreted by Sinclair (1995) as a

transpressional inversion feature, controlled by oblique-slip movement.

However, there is a strong suggestion, based on the application of the model of Jackson and Vendeville (1992 and 1994) that a large salt diapir lies in the footwall of the Voyager Fault. Therefore, the “pop-up” can be interpreted instead as a contractional feature related to diapirism. Other methods, such as examining geophysical gravity surveys over the “pop-up”, could be taken into consideration, in order to confirm this interpretation and distinguish it from Sinclair’s explanation.

- 4 The Ben Nevis and Avalon formations are water-saturated in the Terra Nova field area, but contain fluid inclusions of hydrocarbons (Parnell et al., 2001). These inclusions imply that the reservoir facies were oil-charged at some point but were subsequently breached, allowing oil to be flushed out of the traps. A heavy oil accumulation at the Terra Nova K-17 site at first seems inconsistent with this hypothesis. However, breaching could not be expected to drain all the oil present in the reservoir. Specifically, the oil at K-17 is believed to have remained because it was updip from the drainage point in that part of the reservoir. The bending of strata to the immediate west of the King’s Cove Fault (near the K-17 site) could have provided the remaining closure updip of the inferred breaching fault. In addition, biodegradation made the hydrocarbons that remain more viscous and therefore prevented the oil from escaping easily from the reservoir. Thus, it is hypothesized that, at

K-17, breaching of the trap did not allow hydrocarbons to escape, unlike at other locations in the Terra Nova field area.

REFERENCES

- Arthur, K.R., Cole, D.R., Henderson, G.G.L., and Kushnir, D.W. 1982. Geology of the Hibernia Discovery. *In*: Halbouty, M.T. (ed.), *The Deliberate Search for the Subtle Trap*. American Association of Petroleum Geologists Memoir 32, pp. 181-195.
- Ascoli, P. 1990. Foraminiferal, ostracode and calpionellid zonation and correlation of 42 selected wells from the north Atlantic margin of North America. *Bulletin of Canadian Petroleum Geology*, v. 38, no. 4, pp. 485-492.
- Ascoli, P. 1976. Foraminiferal and ostracod biostratigraphy of the Mesozoic-Cenozoic, Scotian Shelf, Atlantic Canada. *In*: *First International Symposium on Benthonic Foraminifera of Continental Margins, Part B, Paleoecology and Biostratigraphy, Maritime Sediments Special Publication 1*, pp. 653-771.
- Austin Jr., J.A., Tucholke, B.E., and Uchupi, E. 1989. Upper Triassic—Lower Jurassic salt basin southeast of Grand Banks. *Earth and Planetary Science Letters*, v. 92, pp. 357-370.
- Awai-Thorne, B., Malott, M.L., and Wall, D. 1986. The micropaleontology and palynology of the interval 670 m – 3550 m (T.D.), Terra Nova K-07 well, offshore Eastern Canada. Robertson Research Canada Limited, Calgary, AB for Petro-Canada Exploration Inc., pp. 1-32.
- Bartenstein, H. and Bettenstaedt, F. 1962. Marine Unterkreide (Boreal and Tethys). *In*: Simon, W. and Bartenstein, H. (eds.), *Leitfossilien der Mikropaläontologic*, Gebrüder Borntraeger, Berlin, pp. 225-298.
- Boillot, G. and Winterer, E.L. 1988. Drilling on the Galicia margin: retrospect and prospect. *In*: Boillot, G., Winterer, E.L., Meyer, A.W. et al. (eds.), *Proceedings of the Ocean Drilling Program, Scientific Results*, 103, College Station, TX, pp. 809-828.
- Brown, A.R. 1996. Seismic attributes and their classification. *The Leading Edge*, p. 1090.
- Bujak, J.P. and Williams, G.L. 1978. Cretaceous playnostratigraphy of offshore southeastern Canada. *Bulletin of the Geological Survey of Canada*, v. 297, 13 pp.
- Canadian Hydrographic Services. 1990. Newfoundland shelf bathymetry (cartographic material). Bathymetric contours interpreted by Warren, J.S., Pantalone, D.J., and Prest, C.A. Scale 1:1 000 000. Lambert conformal projection, standard parallels

43°00' N – 49°00' N; (W 57°00' – W 43°00' / N 50°30' – N 41°30'). Geoscience Section of the Canadian Hydrographic Service, Department of Fisheries and Oceans, Ottawa, ON. Map 802A.

Canadian-Newfoundland Offshore Petroleum Board (C-NOPB). 2002a. Schedule of Wells, Newfoundland Offshore Area. Updated in June 2002.

Canadian-Newfoundland Offshore Petroleum Board (C-NOPB). 2002 b. C-NOPB Website. www.cnopb.nfnet.com

Canterra Energy. 1987. Canterra PCI et al. Terra Nova K-17, Well History Report. Canadian-Newfoundland Offshore Petroleum Board, St. John's, NL. Prepared by N.R.C van Regen.

Canterra Energy. 1985. Canterra PCI et al. Beothuk M-05, Well History Report. Canadian-Newfoundland Offshore Petroleum Board, St. John's, NL.

Cloetingh, S. 1986. Tectonics of passive continental margins: implications for the stratigraphic record. *Geologie en Mijnbouw*, v. 65, pp. 103-117.

Creaney, S. and Allison, B.H. 1987. An organic geochemical model of oil generation in the Avalon/Flemish Pass sub-basins. *Bulletin of Canadian Petroleum Geology*, 35, pp. 12-23.

Davey R.J. 1979. The stratigraphic distribution of dinocysts in the Portlandian (latest Jurassic) to Barremian (Early Cretaceous) of northwest Europe. *In: American Association of Stratigraphic Palynologists Foundation, Contributions of Stratigraphic Palynology (with emphasis on North America)*, v. 2, Mesozoic Palynology, pp. 49-81.

Davey, R.J. 1974. Dinoflagellate cysts from the Barremian of the Speeton Clay, England. *In: Sah, S.C.D. and Cross, A.T. (eds.), Symposium on Stratigraphical Palynology*, Birbal Sahni Institute of Palaeobotany Special Publication 3, pp. 41-75.

Davey, R.J. and Williams, G.L. 1966. The genus *Hystrichosphaeridium* and its allies, Studies on Mesozoic and Cainozoic dinoflagellate cysts. *Bulletin of the British Museum of Natural History (Geology)*, v. 3, pp. 53-106.

Department of Mines and Energy, Energy Branch, Newfoundland and Labrador. 2000. Sedimentary Basin and Hydrocarbon Potential of Newfoundland and Labrador. 71 pp.

- DeSilva, N.R. 1999. Sedimentary basins and petroleum systems offshore Newfoundland and Labrador. *In: Fleet, A.J. and Boldy, S.A.R. (eds.), Petroleum Geology of Northwest Europe: Proceedings of the 5th Conference, Geologic Society of London*, pp. 501-515.
- Driscoll, N.W. 1992. Tectonic and depositional processes inferred from stratal relationships. Ph.D. thesis, Columbia University, New York, 464 pp.
- Driscoll, N.W. and Hogg, J.R. 1995. Stratigraphic response to basin formation: Jeanne d'Arc Basin, offshore Newfoundland. *In: Lambiase, J.J. (ed.), Hydrocarbon Habitat in Rift Basins. Geological Society Special Publication 80*, pp. 145-163.
- Driscoll, N.W., Hogg, J.R., Christie-Blick, N., and Karner, G.D. 1995. Extensional tectonics in the Jeanne d'Arc Basin, offshore Newfoundland: implications for the timing of break-up between Grand Banks and Iberia. *In: Scrutton, R.A., Stoker, M.S., Shimmield, G.B. and Tudhope, A.W. (eds.), The Tectonics, Sedimentation and Palaeoceanography of the North Atlantic Region. Geological Society Special Publication 90*, pp. 1-28.
- Driscoll, N.W., Karner, G.D., and Christie-Blick, N. 1990. Strategic evidence from Jeanne d'Arc Basin for the timing of break-up between Grand Banks and Iberia. *EOS Abstracts*, 71, p. 1563.
- Duxbury, S. 1978. Early Cretaceous dinoflagellate cysts. *In: Thusu, B. (ed.), Distribution of biostratigraphically diagnostic dinoflagellate cysts and miospores from the Northwest European continental shelf and adjacent areas. Continental Shelf Institute Publication 100*, pp. 19-29.
- Embry, A.F. and Dixon, J. 1990. The break-up unconformity of the Amerasia basin, Arctic Ocean: evidence from Arctic Canada. *Geological Society of America Bulletin*, 102, pp. 1526-1534.
- Emery, D. and Myers, K. 1996. *Sequence Stratigraphy*, Blackwell Science, 297 pp.
- Enachescu, M.E. 1993. North Grand Banks Basin, offshore Newfoundland: a sedimentary epeiric basin west of the Murre-Mercury detachment fault. *Marine and Petroleum Geology*, 10, no. 5, pp. 439-449.
- Enachescu, M.E. 1988. Extended basement beneath the intracratonic rifted basins of the Grand Banks of Newfoundland. *Canadian Journal of Exploration Geophysics*, v. 24, pp. 48-65.
- Enachescu, M.E. 1987. Tectonic and structural framework of the northeast

- Newfoundland continental margin. *In*: Beaumont, C. and Tankard, A.J. (eds.), *Sedimentary Basins and Basin Formation Mechanisms*. Canadian Society of Petroleum Geologists Memoir 12, pp. 117-146.
- Enachescu, M.E. 1986. Integrated geophysical study of Newfoundland continental margin (east coast Canada). Expanded Abstracts, Society of Exploration Geophysicists Annual International Meeting 56, Houston, 2-6 November 1986, pp. 488-492.
- Enachescu, M.E. and Dunning, G. 1994. Basin Monitor: Grand Banks Basin, Canada. Petroconsultants International Energy Services, Switzerland.
- Enachescu, M.E., Harding, S.C., Smee, G.R., Briscoe, R.G., Emery, D.J., Hallstrom, S.K. 1997. Structural, tectonic and seismo-stratigraphic study of the Terra Nova oil field, Jeanne d'Arc Basin, offshore Newfoundland. *Atlantic Geology*, 33, no. 2, pp. 170-171.
- Falvey, D.A. 1974. The development of continental margins in plate tectonic theory. *Association of Petroleum and Explosives Administration Journal*, 14, pp. 95-106.
- Fluid Inclusion Technologies Incorporated. 2002. Website: <http://www.fittulsa.com>
- Fowler, M.G. and McAlpine, K.D. 1994. The Egret member, a prolific Kimmeridgian source rock from offshore eastern Canada. *In*: Katz, B.J. (ed.), *Source rock case studies*, pp. 111-130.
- Gradstein, F.M. and Sheridan, R.E. 1983. On the Jurassic Atlantic Ocean and synthesis of results of Deep Sea Drilling Project Leg 76. *In*: Sheridan R.E., Gradstein R.M. et al. (eds.), *Initial Reports of the Deep Sea Drilling Project*, v. 76, pp. 913-943.
- Grant and McAlpine, 1990. Chapter 6: The Continental Margin Around Newfoundland. *In*: Keen, M.J. and Williams, G.L. (eds.), *Geology of the Continental Margin of Eastern Canada*. Geological Survey of Canada, *Geology of Canada*, no. 2, pp. 238-292.
- Grant, A.C., McAlpine, K.D., and Wade, J.A. 1986. The continental margin of eastern Canada – geological framework and petroleum potential. *In*: Halbouty, M.T. (ed.), *Future Petroleum Provinces of the World*, American Association of Petroleum Geologists Memoir 40, pp. 177-205.
- Gardner, G.H.F., Gardner L.W., and Gregory, A.R. 1974. Formation velocity and density, the diagnostic basics for stratigraphic traps. *Geophysics*, v. 39, pp. 770-780.

- Haq, B.U., Hardenbol, J., and Vail, P.R. 1987. Chronology of fluctuating sea levels since the Triassic. *Science*, v. 235, pp. 1156-1167.
- Harrison, J.C. and Bally, A.W. 1988. Cross section of the Parry Islands fold belt on Melville Island, Canadian Arctic Islands: implications for the timing and kinematic history of some thin-skinned décollement systems. *Canadian Petroleum Geology Bulletin*, v. 36, p. 311-332.
- Hart, B.S. 1999. Geology plays key role in seismic attribute studies. *Oil and Gas Journal*, July 12th, pp. 76-80.
- Hassan, S. 1990. Sequence stratigraphy, Depositional Facies and Reservoir Continuity of a Storm-Wave and Tide-Dominated Delta: An Example from the Lower Cretaceous Ben Nevis and Avalon Formation, Jeanne d'Arc Basin, Grand Banks, Canada. *AAPG Bulletin*, 74, 5, p. 754.
- Hiscott, R.N., Wilson, R.C.L., Gradstein, F.M., Pujalte, V., García-Mondéjar, J., Boudreau, R.R. and Wishart, H.A. 1990. Comparative stratigraphy and subsidence history of Mesozoic rift basins of North Atlantic. *American Association of Petroleum Geologists Bulletin* 74, pp. 60-76.
- Hiscott, R.N. and Wilson, R.C.L. 1987. Final Report: Comparison of Late Jurassic and Early Cretaceous Stratigraphy, Tectonics, and Paleogeography of the Iberian and European Shelf Basins with that of the Jeanne d'Arc Basin of the Grand Banks of Newfoundland. Memorial University (Centre for Earth Resources Research) and The Open University (U.K.), pp. 46-120. UNPUBLISHED
- Hubbard, R.J. 1988. Age and significance of sequence boundaries on Jurassic and Early Cretaceous rifted continental margins. *Bulletin of the American Association of Petroleum Geologists*, v. 72, pp. 49-72.
- Hubbard, R.J., Pape, J., and Roberts, D.G. 1985. Depositional sequence mapping to illustrate the evolution of a passive continental margin. *In*: Berg, O.R. and Wollverton, D. (eds.), *Seismic Stratigraphy II*. American Association of Petroleum Geologists Memoir 39, pp. 93-115.
- Hunt, J.M. 1996. *Petroleum Geochemistry and Geology*. 2nd Edition. W.H. Freeman and company, 734 pp.
- Jackson, M.P.A. and Talbot, C.J. 1991. A Glossary of Salt Tectonics. Geological Circular 91-4, Bureau of Economic Geology, University of Texas at Austin. 44 pp.

- Jackson, M.P.A. and Vendeville, B.C. 1994. Regional extension as a geologic trigger for diapirism. *Geological Society of America Bulletin*, v. 106, pp. 57-73.
- Jackson, M.P.A. and Vendeville, B.C. 1992. The rise of diapirism during thin-skinned extension. *Marine and Petroleum Geology*, v. 9, pp. 331-353.
- Jansa, L.F. and Wade, J.A. 1975. Geology of the continental margin off Nova Scotia and Newfoundland. *In*: van der Linden, W.J.M. and Wade, J.A. (eds.), *Offshore Geology of Eastern Canada*. Geological Survey of Canada Paper 74-30, pp. 51-105.
- Jansa, L.F., Bujak, J.P., and Williams, G.L. 1980. Upper Triassic deposits of the western North Atlantic. *Canadian Journal of Earth Sciences*, v. 17, pp. 547-559.
- Jayashinghe, N.R. 1988. Development of the Ben Nevis Fault Trend, Grand Banks, Newfoundland. *Geological Association of Canada Meeting Abstracts*, p. A61.
- Karner, G.D., Driscoll, N.W., and Weissel, J.K. 1993. Response of the lithosphere to in-plane force variations. *Earth and Planetary Science Letters*, 114, pp. 397-416.
- Keen, C.E., Courtner, R.C., Dehler, S.A., and Williamson, M.C. 1994. Decompression melting at rifted margins: Comparison of model predictions with the distribution of igneous rocks on the eastern Canadian margin. *Earth and Planetary Science Letters*, v. 121, pp. 403-416.
- Keen, C.E., Loncarevic, B.D., Reid, I., Woodside, J., Haworth, R.T., and Williams, H. 1990. Tectonic and geophysical overview; Chapter 2. *In*: Keen, M.J. and Williams, G.L. (eds.), *Geology of the Continental Margin of Eastern Canada*. Geological Survey of Canada, *Geology of Canada*, no. 2, pp. 5-30.
- Keen, C.E., Boutilier, R., de Voogd, B., Mudford, B.S., and Enachescu, M.E. 1987. Crustal geometry and models of the evolution of rift basins on the Grand Banks of eastern Canada: constraints from deep seismic data. *In*: Beaumont, C. and Tankard, A.J. (eds.), *Sedimentary Basins and Basin-Forming Mechanisms*. Canadian Society of Petroleum Geologists Memoir 12, pp. 101-115.
- Kerr and Associates. 1985. *Geology and Petroleum Potential of the Western and Eastern Grand Banks (2 Parts); A Special Report to Industry*. Available at the CNOPB Library, St. John's, NL.
- La Borde, K.T. and de Gasparis, S. 1984. Palynological Biostratigraphy of Terra Nova K-08, Grand Banks. *Petro-Canada Geological Resources and Services*,

- Biostratigraphic Section, Project BIS-147 and Report No. 87-0066.
- Levorsen, A.I. 1967. *Geology of Petroleum*. W.H. Freeman and Company, San Francisco. 724 pp.
- McAlpine, K.D. 1990. Mesozoic Stratigraphy, Sedimentary Evolution, and Petroleum Potential of the Jeanne d'Arc Basin, Grand Banks of Newfoundland. *Geological Survey of Canada Paper* 89-17. 50 pp.
- McClay, K.R. and Ellis, P.G. 1987. Geometries of extensional fault systems developed in model experiments. *Geology*, v. 15, p. 341-344.
- Meador, K.J. and Austin, J.A. 1988. Seismic comparison of the early stratigraphic evolution of conjugate passive continental margins: the Newfoundland/Flemish basin and the eastern Iberian Abyssal plain south of the Galicia Bank. *In*: Boillot, G., Winterer, E.L., Meyer, A.W. et al. (eds.), *Proceedings of the Ocean Drilling Program, Scientific Results*, v. 103, College Station, TX, pp. 777-786.
- Meador, K.J., Austin, J.A., and Dean, D.F. 1988. Shelf to basin correlations in the Newfoundland Basin. *In*: Bally, A.W. (ed.), *Atlas of Seismic Stratigraphy*. American Association of Petroleum Geologists Studies in Geology, v. 27, no. 2, pp. 88-95.
- Miall, A.D. 1994. Sequence stratigraphy and chronostratigraphy: problems of definition and precision in correlation, and their implications for global eustasy. *Geoscience Canada*, v. 21, no. 1, pp. 1-26.
- Millioud, M.E. 1969. Dinoflagellates and acritarchs from some western European Lower Cretaceous type localities. *In*: Bronniman, P. and Renz, H.H. (eds.), *Proceedings of the First International Conference on Planktonic Microfossils*, Geneva, 1967, E.J. Brill, Leiden, v. 2, pp. 420-434.
- Mitchum Jr., R.M. 1977. Seismic stratigraphy and global changes of sea level. Part 2: Glossary of terms used in seismic stratigraphy. *In*: Clayton, C.E. (ed.), *Seismic Stratigraphy*. American Association of Petroleum Geologists Memoir 26, pp. 205-212.
- Mitchum Jr, R.M., Vail, P.R., and Thompson III, S. 1977. Seismic stratigraphy and global changes of seal level, Part 2: The depositional sequence as a basic unit for stratigraphic analysis. *In*: Clayton, C.E. (ed.), *Seismic Stratigraphy*. American Association of Petroleum Geologists Memoir 26, pp. 53-62.
- Myers, K.J. and Milton, N.J. 1996. Concepts and Principles of Sequence Stratigraphy. *In*: Emery, D. and Myers, K.J. (eds.), *Sequence Stratigraphy*. Blackwell Science

- Ltd., London, England, pp. 11-44.
- Parnell, J., Middleton, D., Hongan, C., and Hall, D. 2001. The use of integrated fluid inclusion studies in constraining oil charge history and reservoir compartmentalization: examples from the Jeanne d'Arc Basin, offshore Newfoundland. *Marine and Petroleum Geology*, v. 18, pp. 535-549.
- Petro-Canada. 1996. Development Application - Terra Nova Development, Part 1. Prepared by Petro-Canada on behalf of the Terra Nova Proponents — Petro-Canada, Mobil Oil Canada Properties, Husky Oil Operations Limited, Murphy Oil Company Limited, and Mosbacher Operating Limited.
- Petro-Canada. 1990. Petro-Canada et al. King's Cove A-26, Well History Report. Canadian-Newfoundland Offshore Petroleum Board, St. John's, NL. Prepared by J.L. Cotterill.
- Petro-Canada. 1988a. Petro-Canada et al. Terra Nova C-09, Well History Report. Canadian-Newfoundland Offshore Petroleum Board, St. John's, NL. Prepared by J.L. Cotterill.
- Petro-Canada. 1988b. Petro-Canada et al. Terra Nova E-79, Well History Report. Canadian-Newfoundland Offshore Petroleum Board, St. John's, NL. Prepared by J.L. Cotterill.
- Petro-Canada. 1988c. Petro-Canada et al. Terra Nova H-99, Well History Report. Canadian-Newfoundland Offshore Petroleum Board, St. John's, NL. Prepared by J.L. Cotterill.
- Petro-Canada. 1986a. Petro-Canada et al. Terra Nova I-97, Well History Report. Canadian-Newfoundland Offshore Petroleum Board, St. John's, NL. Prepared by W.L. Grieve.
- Petro-Canada. 1986b. Petro-Canada et al. North Trinity H-71, Well History Report. Canadian-Newfoundland Offshore Petroleum Board, St. John's, NL. Prepared by G.B. Steeves.
- Petro-Canada. 1986c. Petro-Canada et al. Terra Nova K-07, Well History Report. Canadian-Newfoundland Offshore Petroleum Board, St. John's, NL. Prepared by G.B. Steeves.
- Petro-Canada. 1985. Petro-Canada et al. Terra Nova K-18, Well History Report. Canadian-Newfoundland Offshore Petroleum Board, St. John's, NL. Prepared by G.B. Steeves.

- Petro-Canada. 1984. Petro-Canada et al. Terra Nova K-08, Well History Report. Canadian-Newfoundland Offshore Petroleum Board, St. John's, NL. Prepared by G.B. Steeves.
- Posamentier, H.W., Jervey, M.T. and Vail, P.R. 1988. Eustatic controls on clastic deposition I. *In*: Wilgus, C.K., Hastings, B.S., Kendall, C.G., Posamentier, H.W., Ross, C.A., and Van Wagoner, J.C. (eds.), *Sea Level Changes: An Integrated Approach*. Society of Economic Paleontologists and Mineralogists Special Publication 42, pp. 109-124.
- Powell, T.G. 1985. Paleogeographic implications for the distribution of Upper Jurassic source beds, offshore Eastern Canada. *Bulletin of Canadian Petroleum Geology*, v. 30, pp. 167-179.
- Prosser, S. 1993. Rift-related linked depositional systems and their seismic expression. *In*: Williams, G.D. and Dobb, A. (eds.), *Tectonics and Seismic Sequence Stratigraphy*. Geological Society Special Publication 71, pp. 35-66.
- Sargeant, W.A.S. 1966. Further dinoflagellate cysts from Speeton Clay (Lower Cretaceous), Studies on Mesozoic and Cainozoic dinoflagellate cysts. *Bulletin of the British Museum of Natural History (Geology)*, v. 3, pp. 199-213.
- Sheriff, R.E. 1991. *Encyclopedic Dictionary of Exploration Geophysics*. Society of Exploration Geophysicists Geophysical Reference. Tulsa, Oklahoma. 376 pp.
- Sinclair, I.K. 1995. Transpressional inversion due to episodic rotation of extensional stresses in Jeanne d'Arc Basin, offshore Newfoundland. *In*: Buchanan, J.G. and Buchanan, P.G. (eds.), *Basin Inversion*. Geological Society of London Special Publication 88, pp. 249 – 271.
- Sinclair, I.K. 1994. *Tectonism and Sedimentation in the Jeanne d'Arc Basin, Grand Banks of Newfoundland*. PhD Thesis, University of Aberdeen. 248 pp. plus appendices and enclosures.
- Sinclair, I.K. 1993. Tectonism: the dominant factor in mid-Cretaceous deposition in the Jeanne d'Arc Basin, Grand Banks. *Marine and Petroleum Geology*, v. 10, pp. 530-549.
- Sinclair, I.K. 1988. Evolution of Mesozoic-Cenozoic sedimentary basins in the Grand Banks area of Newfoundland and comparison with Falvey's (1974) rift model. *Bulletin of Canadian Petroleum Geology*, v. 36, pp. 255-273.

- Sinclair, I.K., McAlpine, K.D., Sherwin, D.F. and McMillan, N.J. 1992. Petroleum Resources of the Jeanne d'Arc Basin and Environs, Grand Banks, Newfoundland. Geological Survey of Canada Paper 92-8, 48 pp.
- Srivastava, S.P. 1978. Evolution of the Labrador Sea and its bearing on the early evolution of the North Atlantic. *Geophysical Journal of the Royal Astronomical Society*, v. 52, pp. 313-357.
- Stamp, L.D. 1921. On cycles of sedimentation in the Eocene strata of the Anglo-France—Belgium Basin. *Sedimentary Geology*, v. 14, pp. 1-43.
- Sullivan, K.D. and Keen, C.E. 1978. On the nature of the crust in the vicinity of the Newfoundland Ridge. *Canadian Journal of Earth Sciences*, v. 15, pp. 1462-1471.
- Swift, D.J.P. 1975. Barrier island genesis: evidence from the Middle Atlantic shelf of North America. *Sedimentary Geology*, v. 14, pp. 1-43.
- Swift, D.J.P., Stanley, D.J., and Curray, J.R. 1971. Relict sediments on continental shelves: a reconsideration. *Journal of Geology*, v. 79, pp. 322-349.
- Swift, J.H. and Williams, J.A. 1980. Petroleum source rocks, Grand Banks area. *In*: Miall, A.D. (ed.), *Facts and Principles of World Petroleum Occurrences*. Canadian Society of Petroleum Geologists Memoir 6, pp. 567-588.
- Tankard, A.J. and Welsink, H.J. 1989. Mesozoic extension and styles of basin formation in Atlantic Canada. *In*: Tankard, A.J. and Balkwill, H.R. (eds.), *Extensional Tectonics and Stratigraphy of the North Atlantic Margins*. American Association of Petroleum Geologists Memoir 46, pp. 175-195.
- Tankard, A.J. and Welsink, H.J. 1988. Extensional tectonics and stratigraphy of the Mesozoic Grand Banks of Newfoundland. *In*: Manspeizer, W. (ed.), *Triassic-Jurassic Rifting: Continental Breakup and the Origin of the Atlantic Ocean and Passive Margins, Part A*. Development in Geotectonics, v. 22, Amsterdam, pp. 129-165.
- Tankard, A.J. and Welsink, H.J. 1987. Extensional tectonics and stratigraphy of Hibernia oilfield, Grand Banks, Newfoundland. *American Association of Petroleum Geologists Bulletin*, v. 71, pp. 1210-1232.
- Tankard, A.J., Welsink, H.J., and Jenkins, W.A.M. 1989. Structural styles and stratigraphy of the Jeanne d'Arc Basin, Grand Banks of Newfoundland. *In*: Tankard, A.J. and Balkwill, H.R. (eds.), *Extensional Tectonics and Stratigraphy of the North Atlantic Margins*. American Association of Petroleum Geologists

Memoir 46, pp. 265-282.

- Todd, B.J. and Keen, C.E. 1989. Temperature effects and their geological consequences at transform margins. *Canadian Journal of Earth Sciences*, v. 26, pp. 2591-2603.
- Tucholke, B.E., Austin, J.A. Jr., and Uchupi, E. 1989. Crustal structure and rift-drift evolution of the Newfoundland Basin. *In*: Tankard, A.J. and Balkwill, H.R. (eds.), *Extensional Tectonics and Stratigraphy of the North Atlantic Margins*. American Association of Petroleum Geologists Memoir 46, pp. 247-264.
- Vail, P.R. 1987. Seismic stratigraphy interpretation and utilizing sequence stratigraphy. *In*: Bally, A.W. (ed.), *Atlas of Seismic Stratigraphy*. American Association of Petroleum Geologists Studies in Geology, v. 27-1, pp. 1-10.
- Vail, P.R. and Mitchum Jr., R.M. 1977. Seismic stratigraphy and global changes of sea level, Part 1: Overview. *In*: Clayton, C.E. (ed.), *Seismic Stratigraphy*. American Association of Petroleum Geologists Memoir 26, pp. 51-52.
- Vail, P.R., Mitchum Jr., R.M., Rodd, R.G., Widmier, J.M., Thompson III, S., Sangree, J.B., Bubbs, J.N. and Hatelid, W.G. 1977. Seismic stratigraphy and global changes of sea level. *In*: Clayton, C.E. (ed.), *Seismic Stratigraphy*. American Association of Petroleum Geologists Memoir 26, pp. 49-212.
- Van Wagoner, J.C., Posamentier, H.W., Mitchum Jr, R.M., Vail, P.R., Sarg, J.F., Louitt, T.S. and Hardenbol, J. 1988. An overview of the fundamentals of sequence stratigraphy and key definitions. *In*: Wilgus, C.K., Hastings, B.S., Kendall, C.G., Posamentier, H.W., Ross, C.A., and Van Wagoner, J.C. (eds.), *Sea Level Changes: An Integrated Approach*. Society of Economical Paleontologists and Mineralogists Special Publication 42, pp. 39-45.
- von de Dick, H., Meloche, J.D., Dwyer, J., and Gunther, P. 1989. Source-rock geochemistry and hydrocarbon generation in the Jeanne d'Arc Basin, Grand Banks, offshore Eastern Canada. *Journal of Petroleum Geology*, v. 12, pp. 51-68.
- Wade, J.A. 1978. The Mesozoic-Cenozoic history of the northeastern margin of North America. *Offshore Technology Conference Proceedings*, v. 3, pp. 1849-1859.
- Welsink, H.J., Srivastava, S.P., and Tankard, A.J. 1989. Basin architecture of the Newfoundland Continental margins and its relationship to ocean crust fabric during extension. *In*: Tankard, A.J. and Balkwill, H.R. (eds.), *Extensional Tectonics and Stratigraphy of the North Atlantic Margins*. American Association of Petroleum Geologists Memoir 46, pp. 197-213.

- Williams, G.L. 1974. Dinoflagellate and spore stratigraphy of the Mesozoic-Cenozoic, offshore eastern Canada. Offshore Geology of Eastern Canada. Geological Survey of Canada Paper 74-30, v. 2, pp. 107-162.
- Williamson, M.A. 1992. The subsidence, compaction, thermal and maturation history of the Egret Member source rock, Jeanne D'Arc Basin, offshore Newfoundland. Bulletin of Canadian Petroleum Geology, v. 40, pp. 136-150.
- Williamson, M.A. 1987. A quantitative foraminiferal biozonation of the Late Jurassic and Early Cretaceous of the East Newfoundland Basin. Micropaleontology, v. 33, no. 1, pp. 37-65.
- Williamson, M.A., Coflin, K.C., Agrawal, A., Huang, A., Dickie, K., and McAlpine, K.D. 1995. The risk of encountering biodegraded crudes in the Jeanne d'Arc Basin. In: Bell, J.S., Bird, T.D., Hillier, T.L., and Greener, P.L. (eds.), Proceedings of the Oil and Gas Forum '95 – Energy from Sediments. Geological Survey of Canada Open File 3058, pp. 313-316.
- Woodcock, N.H. and Fisher, M. 1986. Strike-slip duplexes. Journal of Structural Geology, v. 74, pp. 725-735.

